Heterologous Expression of the Mammalian Microtubule Associated Proteins (MAPs) tau, MAP2c and MAP4 in the fission yeast *Schizosaccharomyces pombe*

Supriya Bezbaruah

A thesis submitted to the University of London for the Degree of Doctor of Philosophy

October 1998

University College London

Gower Street

London

Acknowledgements

My thanks to my supervisor, Jeremy Hyams, for his guidance, support and patience throughout this project. I would also like to thank members of this laboratory, past and present, for their help and encouragement throughout my years there, particularly Vasanti and Thein, and Hazel Williams in the LMCB. I am also grateful to Kat, Nicky, Laura and Saul and everyone else in the fifth floor for all their help and advice. My immense gratitude to Jonathan Nugent for his patience and wise words.

To my many friends in this department, at UCL, and elsewhere, an enormous 'thank you' for making my days at UCL so thoroughly enjoyable and memorable. I am particularly grateful to Chloe, Sandra, Neela, and Carola for their constant support and unwavering faith in me.

Finally, my deep and heartfelt gratitude to my family , my parents and sister, for the strength I derived from their love in spite of the distance.

ABSTRACT

The mammalian microtubule associated proteins (MAPs) tau, MAP2c and MAP4 were subcloned and expressed in the fission yeast *Schizosaccharomyces pombe* using the thiamine repressible pREP1 vector. Tau, MAP2c and MAP4 have similar C-terminal microtubule binding domains, but unique N-terminal projection domains. At the start of this study, there were no known MAPs in *S. pombe* and therefore this appeared to be a unique *in vivo* system to both study the roles of the three mammalian MAPs and to further define the function of microtubules.

All three MAPs inhibited growth of wild type cells at 36^0C over a range of temperatures. However each MAP produced distinct phenotypes in fission yeast, indicating that their effect was specific for that MAP. Tau expression resulted in a weak phenotype of long, multiseptate or branched cells. The MAP2c-induced phenotype was stronger, and resulted in long cells with bulbous ends, whilst MAP4 expression produced bent or hammer shaped cells. The MAPs tau and MAP2c accelerated and slowed entry into mitosis, respectively, of G2-arrested *cdc25.211* cells. Expression of tau and MAP2c in *tea1* cells (which plays a role in directing the cell to grow along a perfectly opposed longitudinal axis) and *tea2* cells (which codes for a kinesin) result in distorted shapes and loss of the original phenotype.

Immunofluorescence studies showed that each MAP had a unique effect not only on the cell phenotype but also on microtubule organisation of the cell. Tau caused microtubule bundling and displacement towards the cell periphery, MAP2c resulted in short microtubules around the nucleus, whilst MAP4 caused total depolymerisation of

interphase microtubules. Both tau and MAP2c appeared to bind to microtubules, but MAP4 was seen distributed throughout the cell. Similarly, MAP2c caused the formation of short microtubules in *tea1* cells, but tau had very little effect. *tea2* control cells have short microtubules, and tau expression resulted in even shorter microtubules near the nucleus. MAP2c expression in *tea2*, however, resulted in microtubule depolymerisation, and assymetrical distribution towards one end of the cell.

Tau and MAP2c also appeared to rescue the combined sensitivity of fission yeast to the cold and the microtubule depolymerisation agent, thiabendazole (TBZ). This observation was used as a strategy to isolate possible *S. pombe* MAPs by expressing an *S. pombe* cDNA library subcloned in pREP. Eight clones were isolated, and sequence analysis of two of those clones revealed that they coded for fatty acid synthetase *(lsd1+)* and the ribosomal protein L19.

CONTENTS

1. Introduction

1.1 The Cytoskeleton

The cytoskeleton consists of protein filaments that define the physical shape of the cell by forming its skeletal backbone. The filaments are highly dynamic and constantly reorganise themselves for various functions - for cell movement, for transport of organelles within the cell, and the segragation of chromosomes at mitosis. Enabling the cytoskeleton to perform these diverse functions are three different types of protein filaments : actin, intermediate filaments and microtubules. This thesis will focus on the last of these, microtubules.

1.2 Microtubules

Microtubules are the major component of the cytoskeleton in all eucaryotic cells. They are long tubular structures composed of heterodimers of two related proteins, the α and β tubulins. These heterodimers form protofilaments, and generally thirteen such protofilaments organise themselves into a tubular structure to form microtubules [reviewed by Downing, 1998 #94, Mandelkow, 1994 #14].

Microtubules play a variety of roles in the cell. First, they maintain cell shape by forming an extensive fibrous network which constitutes the skeletal 'backbone' of the

cell and resists the compressive forces of the actin cytoskeleton. Second, they act as 'railtracks' along which cellular components such as membrane bound organelles, secretory vesicles and macromolecules are transported within the cell. When the cell enters mitosis, the interphase microtubules depolymerise, and the tubulin re-polymerises to form the fibres of the mitotic spindle. The spindle is involved in chromosome segregation to the daughter cells. Microtubules are also involved in cell motility as the major components of the cilia and flagella.(reviewed in Stearns, 1997 #95, Bloom, 1998 #96, Hyman, 1996 #97).

In order to perform such diverse functions, microtubules require to be highly adaptable. *In vivo* and *in vitro* studies have shown that microtubules undergo intermittent periods of growth and shrinkage, allowing the cell to remodel its microtubule array in response to various signals (Mitchison and Kirchner, 1984). However, for some cells, particularly differentiated cells such as neurons, the stabilisation of the microtubule array is essential for their particular specialised roles. Regulating the flexibility of microtubules are a wide array of enzymes, which cause post-translational modification of the polymers, and proteins that bind to them, called microtubule associated proteins (MAPs) (Mandelkow, 1995).

1.2.1 Tubulins and their structure

The basic subunit protein of microtubules is tubulin, a 100 kD dimer composed of two 50 kD polypeptides, α and β tubulin. They are 36-42% homologous to each other, and are found to be highly conserved in most eucaryotes. Comparing known tubulin

sequences from metazoa, plants and algae, and fungi have shown that approximately 41% of the α- and 30% of the β- tubulin residues are totally conserved (reviewed by (Burns and Surridge, 1994)).

Sequence analysis has shown that the most conserved regions are in the N-terminal regions - residues 394-436 in α- and 384-426 in β-tubulin. In addition, the regions 60-69, 142-148, 180-183 and 242-246 in α and 58-67, 140-146, 178-181 and 240-244 in βhave been proposed as GTP-binding sites, on the basis of affinity studies and GTP-binding sites in other proteins. The carboxy terminal regions of both α and β tubulin vary greatly, both among the different organisms and among the various isotypes. These regions are almost always rich in glutamates, indicating that they are highly negatively charged. MAPs appear to interact with these regions. MAPs generally have a stabilising effect on microtubules, and on deleting the C-terminal region, tubulin can polymerise in the absence of MAPs. This suggests that the carboxy terminal regions may be endogenous inhibitors of assembly and this inhibition may be relieved either by deleting this region or by having them interact with MAPs (Luduena, 1992).

In a recent breakthrough, Downing *et al.*(1998) produced a detailed three-dimensional structure of the tubulin dimer that could be resolved to 3.7 angstroms, obtained by electron crystallography of tubulin sheets induced from purified tubulin in the presence of zinc ion. This study shows that in spite of differences in sequence, the three dimensional structures of α- and β- tubulin are very similar. The tubulin monomers are shown as compact structures formed by a core of two β-sheets

surrounded by α-helices. The model of the tubulin dimer revealed a structure consisting of a core of two β-sheets of 6 and 4 strands, flanked by 12 α-helices. The molecule, on the basis of this model, can be divided into three functional domains - the amino-terminal domain containing the nucleotide binding region, an intermediate domain containing the taxol binding site, and the carboxy-terminal domain which is possibly the binding site for MAPs and motor proteins(Downing and Nogales, 1998). The N-terminal domain includes residues 1-205 and forms a structure, called Rossman fold, where parallel β strands alternate with α helices. This is typical of nucleotide-binding proteins . The intermediate domain (residues 206-381) consists of a mixed β sheet and five surrounding helices. The C-terminal domain consists of helices overlaying the other domains, present on the outside of the microtubule, where it can bind to other proteins. the region not shown in this model are the last C-terminal domains, which are hypervariable in sequence and therefore likely to vary in structure.

Both α and β tubulin exist as families of isotypes, differing in their amino-acid sequence mainly around the hypervariable C-terminal end. Isotypes occur in tubulins from plants to mammals (Burns and Surridge, 1970). In mammals there appear to be five isotypes of α and six of β tubulin. (Villasante et. al. 1986; Wang et. al., 1986). It is possible that different isotypes exist in order to perform the different roles of microtubules in the cell. In *Aspergillus*, there are two α tubulin isotypes. Disrupting one of these genes blocks nuclear division, while disrupting the other does not, but leads to abnormal morphology of the cell and nucleus. This suggests that one α tubulin may be involved in cell division, while the other is involved in regulating the

interphase pattern of microtubules (Doshi et al., 1991). The yeasts *Saccharomyces cerevisiae* and *Schizosaccharomyces pombe* also show two α-tubulin isotypes.

1.2.2 Microtubule Assembly

Microtubules have been shown by three dimensional reconstructions to be hollow cylinders of approximately 25nm in diameter, in which tubulin dimers are packed head-to-tail with an 8nm spacing, to form protofilaments running lengthwise along the microtubule wall. The protofilaments fit together laterally so that neighbouring subunits follow shallow-pitch three-start helices. These helices can be of two types - the A-lattice, in which tubulin subunits alternate around the helix, and the B-lattice, in which identical tubulin monomers associate laterally around the helix. The latter model would result in a 'seam' being present within the microtubule where the consistency of the subunit would be lost, and this is the form that microtubules favour when polymerised in vivo. The importance of this lies in the fact that the organisation of the microtubule surface lattice is could influence such events as nucleation and ineteractions between microtubules and microtubule binding proteins (reviewed by Mandelkow et. al, 1995).

The highly ordered structure of microtubules indicate that its assembly does not take place by random polymerisation of tubulin , but is a highly precise and regulated process. Microtubules have intrinsic structural and functional polarity, determined by the orientation of the tubulin dimer in the polymer, and the rate constants of addition

of subunits to the microtubule ends. The plus end of the microtubule grows faster than the minus end. Polarity studies have assigned β-tubulin to the fast-growing end, and α-tubulin at the minus end (Hoenger and Milligan, 1996). Microtubule polarity appears tightly controlled in cells. Microtubules emanate from the cell centre in most cells with uniform polarity and this important for many cellular activities, including chromosome migration, intracellular transport and cell locomotion.

Microtubule assembly can be divided into two phases, nucleation and elongation. In *in vitro* assembly, there is an initial lag period in which a polymer forms in a solution of tubulin under polymerising conditions. This lag is interpreted as a nucleation phase during which stable oligomers form into which subunits can add. This interpretation is supported by the fact that short microtubule segments or 'seeds' eliminate this initial lag phase. Microtubules then elongate by direct addition of subunits to the growing polymer (Johnson and Borisy, 1977). *In vivo*, the 'seed' is provided by the Microtubule Organising Centre (MTOC).

1.2.2.1 The Microtubule Organising Centre (MTOC) and Gamma-Tubulin

MTOCs were initially identified as discrete cellular sites from which microtubules originate. MTOCs 'organise' microtubules by playing a major role in the control of microtubule number, polarity, length and protofilament number, as well as determining the points of microtubule assembly in a cell. Electron microscopy (EM) studies have revealed MTOCs as highly complex and variable structures, and

understanding the details of this structure provide clues to the regulation of microtubule organisation (Tucker, 1992).

The centrosomes of mammalian cells were the first MTOC to be studied in detail. The centrosome consists of a pair of centrioles surrounded by an amorphous pericentriolar material. The centriole itself is a short cylinder of nine triplet microtubules. The pericentriolar material provides the sites of microtubule nucleation, and microtubule number is determined by the number of these sites present. Plant cell MTOCs lack centrioles. The yeast MTOC, called the spindle pole body (SPB), is a disc-shaped structure embedded in the nuclear envelope that organises nuclear microtubules from one face and cytoplasmic microtubules from the other. The SPBs consist of several layers, and like plants, lack centrioles (reviewed by (Schliwa, 1986)).

The belief that the MTOC decided microtubule polarity and specified protofilament number in the cell stemmed from the observations that microtubules in the cell are uniformly polar, and that there were always 13 protofilaments in microtubules assembled in vivo, whilst in vitro the protofilament number was generally 14, occasionally 13 or 15. However direct evidence for structures in MTOC serving as templates for microtubule assembly was lacking till genetic studies in Aspergillus nidulans revealed the existence of γ-tubulin, a novel tubulin which was as homologous to α- and β-tubulin as α- and β-tubulin were to each other (Oakley and Oakley, 1989).

γ-tubulin was found to be conserved in most eucaryotes, indicating that in had a fundamental role to play. A null mutation of γ-tubulin in S. pombe was shown to be lethal (Stearns et al., 1991), but his lethality could be rescued by the human γ-tubulin (Horio, 1994). In all organisms, γ-tubulin did not form any part of the bulk of the microtubule lattice, but was highly concentrated in the MTOC, indicating that it may play a role in microtubule organisation. (Stearns et al., 1991; Zheng et al., 1991). Its role in microtubule organisation was supported by experiments is *Aspergillus nidulans* where depletion of γ-tubulin led to the depletion of microtubules and growth arrest (Oakley et al., 1990; Oakley and Oakley, 1989). Its role in microtubule nucleation was made apparent when microinjection of an antibody against γ-tubulin in mammalian cells disrupted microtubule nucleation in interphase and the morphogenesis of the microtubule spindle in mitosis (Joshi et al., 1992). In vivo overexpression of γ tubulin in mammalian cells results in a major reorganisation of normal radial microtubule architecture as numerous microtubule nucleation sites are formed outside the centrosome in the cytoplasm. Stearns and Kirchner (Stearns and Kirchner, 1994) provided further evidence for the role of γ-tubulin in microtubule nucleation by revealing that the molecule existed as part of a heteromeric protein complex in *Xenopus*, and depletion of this complex from *Xenopus* egg extracts diminished the ability of the extract to support the formation of sperm-mediated microtubule asters. Concurrently, Li and Joshi (Li and Joshi, 1995) provided direct evidence that γ-tubulin interacted with microtubules, showing that γ-tubulin bound to microtubule ends *in vitro* in a minus-end specific manner. This also suggested that γ-tubulin could influence microtubule polarity.

A better idea of how γ-tubulin could nucleate microtubule assembly and fix protofilament number at 13 could be formed when Zheng et al (1995) purified the γ tubulin complex from *Xenopus* in an active form, and found that it has a ring strucure of about the same diameter of a microtubule, and contain 10-13 γ tubulin subunits as well as several other proteins. These rings nucleate microtubule assembly and cap the minus ends of microtubules *in vitro*. Zheng et al (1995) also found that each γ tubulin ring contains one molecule each of α and β tubulin. Moritz et al (1995) confirmed using immuno-electron microscopic tomography that γ tubulin is localised in a ring structure in the pericentriolar material of purified centrosomes without microtubules, and that γ tubulin is located at the minus ends when these centrosomes are used to nucleate microtubules. Based on the evidence above, a model for microtubule nucleation was put forward. In this model, 13 molecules of γ-tubulin are arranged in an open ring structure with overlapping ends, on a helical scaffold provided by the non-tubulin components of the complex. This would provide a template for the B-lattice of microtubules, with the open ring consistent with the 'break' found in the lattice. The α/β tubulin dimer present at the offset in the γ tubulin ring, stabilised the lateral interactions for an exogenous tubulin dimer binding to this region, allowing nucleation of microtubule assembly. However it is not clear why γ tubulin is limited to the centrosome when it could possibly nucleate microtubules in solution. The relationship between the ring complex and nucleation is also debated (Stearns and Winey, 1997).

γ tubulin has also been found in plants, which, unlike animal cells, lack focused centrosomes and nucleate microtubule assembly at a variety of locations. γ-tubulin

has been identified in at least two algae, two ferns, and five flowering plants, including Arabidopsis and maize (reviewed by Joshi, 1996). Plant γ tubulins are highly conserved between species, with more than 90% sequence identity at the amino acid level. The amino acid sequence from *Chlamydomonas* is 73% identical to that in plants, however they are less identical to fungi and animal homologues (60-70%). The plant γ tubulins also appear to be larger : both maize and *Arabidopsis* polypeptides have a predicted molecular mass of 53 kD (animal γ tubulin have a molecular mass of 50 kD). Plant γ tubulin is also much more widely distributed than its animal or fungal counterparts. It is associated with all microtubule arrays and with the nuclear envelope. Its localisation changes with the cell cycle, and it is especially prominent over nuclear caps in prophase, kinetochore fibres in metaphase, polar caps in late anaphase and phragmoplasts in telophase (Liu et al, 1994).

1.2.2.2 Microtubule Elongation

Microtubules grow by the addition of tubulin dimers to their ends. Initially it was not clear whether this occurred stepwise, one dimer after another, along the 'curls' of surface lattice helices, by lengthwise addition to protofilaments, or via protofilaments sheets. Recent studies using electron cryomicroscopy have shown that growing microtubules have long, curved, sheet-like extensions up to several microns in length, whilst in shrinkage, the protofilaments curl into tight rings. This along with negative stain electron microscopy have shown that tubulin dimers are added to the free end of two dimensional sheets that close continuously at the other end to form the cylindrical wall of the microtubule (Chretien et al., 1995). This would also explain the presence

of the B-lattice organisation of a microtubule, with the 'seam'. It is not known whether the seam plays any functional role in the microtubule (reviewed by (Wade and Hyman, 1997)).

Tubulin assembles into microtubules with the hydrolysis of GTP. In the dimer, both α and β tubulin bind to GTP, but with different affinities. GTP is permanently bound to α tubulin in the N (non-exchangeable) site where it appears to have a structural role. It is buried in the intradimer surface in the three dimensional structure (Nogales et. al, 1998). In the β-subunit, the GTP molecule is reversibly bound to the E (exchangeable) site, which is partially exposed in the dimer but would be buried in the microtubule.

It is unclear how GTP hydrolysis on the addition of tubulin dimers affects sheet closure. It is not thought likely that GTP hydrolysis itself is responsible for the closure of the sheets as microtubules can be assembled in the presence of slowly hydrolysable GTP analogues such as guanylyl-(α,β)-methylene-diphosphonate (GMPCPP). Such microtubules are much more stable than standard GDP bound microtubules, indicating that GTP hydrolysis destabilizes microtubules and favours disassembly (Caplow and Shanks, 1996). Recent observations using electron cryomicroscopy and image analysis have revealed subtle differences in tubulin conformations in GDP-bound and GMPCPP-bound microtubules - in the latter the monomer spacings along the protofilaments are about 1.5 angstrom greater. Analysis of severed microtubules show that there are three conformational states for each microtubule end, corresponding to bound GTP, GDP and inorganic phosphate, and

bound GDP (Tran et al., 1997). These studies strongly indicate that the structural changes in the tubulin molecule within the microtubule surface lattice lead to the macroscopic behaviour of microtubules such as dynamic instability, interactions with MAPs and motor proteins and other enzymes.

1.2.3 Microtubule Dynamics

Microtubule assembly is under strict spatial and temporal control in a cell. Tubulin polymerisation studies *in vitro* suggest that the growth or shortening of microtubules is a simple self-assembly mechanism determined by the concentration of unpolymerised tubulin in solution. However, *in vivo*, the number and distribution of microtubules are not a function of available tubulin in the cell, but depend various signals that promote re-organisation of the microtubule cytoskeleton for various cellular purposes. Indeed one of the prominent and inherent features of microtubules is its 'dynamic instability' (Mitchison and Kirchner, 1984). Microtubules interconvert between periods of growth and rapid shrinkage, with abrupt changes between the two. Transitions from growing to shrinking are called catastrophes, and transitions from shrinking to growing are called rescues. In this concept, all microtubule fibres do not behave uniformly, rather growing microtubules co-exist with another undergoing shortening. Mitchison and Kirchner (1984) attribute this property of Dynamic instability of microtubules to its action as GTPase, which is necessary for its assembly. There is a delay in the hydrolysis of GTP following the addition of tubulin subunits, resulting in a cap of GTP-tubulin at the plus end of the microtubule, with the remaining microtubule containing GDP-tubulin. The model rests on the stabilising

effect of the GTP-tubulin cap, so that if the rate of GTP-hydrolysis exceeds that of tubulin addition, the GDP-tubulin core is exposed, leading to depolymerisation of the microtubule (reviewed by Cassimeris, 1993). This dynamic instability exists and has been observed in individual microtubules by dark field microscopy (Horio and Hotani, 1986). Although there is little biochemical evidence for unhydrolysed GTP in the lattice, it has recently been shown that a few GTP-like subunits at the end of the microtubule will stabilise a microtubule against depolymerisation (Drechsel and Kirschner, 1994). Dynamic instability could be explained as a direct consequence of microtubular structural transition due to GTP hydrolysis. Chretian et. al. (1995) have shown that the during growth, the ends of microtubules are curved, closing into tubes further down the lattice, whilst they curl over and 'peel' off during shrinkage. This could be a result of conformational changes in the tubulin dimer due to GTP hydrolysis (Hyman and Karsenti, 1996).

Microtubule dynamics in a cell can be regulated in two ways: by regulating the growth or shrinkage rates themselves, or by regulating the transition rates between growth and shrinkage. Many factors regulate microtubules directly or indirectly to stabilise or destabilise them.

1.2.3.1 Microtubule Stabilising Factors

Microtubule dynamics is influenced by external factors as well as by the tubulin isotype it is composed of. Erythrocyes, for example, are virtually free of MAPs, and tubulins expressed in these cells consist of mainly one isotype. Brain microtubules,

on the other hand, consist of microtubules of heterogenous tubulin isotypes. Comparison of the dynamics of microtubules of the two cell types in the absence of MAPs revealed that the erythrocyte microtubules are less dynamic, with lower critical concentration for elongation , and rate of association and disassociation of tubulin. Catastrophes were rare, rescues frequent, and shrinkage slow. (Frinczek et al., 1993). These experiments showed that different isotypes lead to different microtubule dynamics.

Tubulins differ not only in isotypes, but also can also be modified post-tranlationally in several ways: phosphorylation, acetylation, detyrosination, and glutamylation. These modifications usually lead to stabilisation of microtubules, and are generally found in differentiated cells such as neuronal cells (see (Mandelkow, 1995)). α-tubulin which has lost its last two carboxy residues (including a tyrosine) is found in very stable neuronal microtubules (Paturele-Lafanechere et al., 1994). Polyglutamic chains attached to C-terminal glutamic acid in α- and β-tubulin are also found in stable neuronal microtubules (Audebert et al., 1994). Gurland and Gunderson (1993) found that long-lived, stable microtubules that have lost their C-tyrosine from α-tubulin selectively break down when phosphatases are inhibited by okadaic acid. This suggests a role of phosphorylation in destabilizing microtubules. Structural changes to the polymer resulting from these modifications are suspected of being responsible for their stability.

The most extensively studied external factor responsible for the regulation of Microtubule Dynamics are MAPs. *In vitro* studies of microtubule dynamics in the presence of brain microtubule associated proteins showed that the MAPs, such as tau

and MAP2, lowered catastrophe rate and increased rescue rate. Each of the MAPs were seen to modulate but not abolish the dynamic behaviour of microtubules (Pryer et al., 1992). Umeyama *et. al.* (Umeyama et al., 1993) studied the effect of MAPs on microtubule dynamics *in vivo*. They microinjected biotin-labeled tubulin to MAP expressing fibroblast cells, and measured the incorporation of tubulin, and turnover of labeled microtubule bundles. They found that microtubules in MAP-expressing cells are very stable *in vivo*. MAPs bind to microtubules and act as a 'hinge', preventing microtubules depolymerising by holding the protofilament sheet together (reviewed in (Wade and Hyman, 1997)).

Recently motor proteins have been shown to play a direct role in regulating microtubule dynamics. It has been shown that in the absence of centrosomes, microtubules can still organise themselves into arrays. In mitotic and cytosolic extracts, microtubule stabilising drugs such as taxol can induce formation of microtubule asters in *Xenopus* even in the absence of centrosomes [Verde, 112 #104]. The minus-end directed microtubule motor protein dynein was thought to be essential role in the organisation of these arrays. Nedelec et. al. (Nedelec et al., 1997) showed that these motors, linked artificially into multimeric complexes, can produce astral arrays of microtubules from purified tubulin *in vitro*. Moreover, after nucleation, microtubules are released from the centrosome at a constant rate [Keating, 1997 #107]. The released polymer appears to glide over the nuclear surface. This gliding motion is a combination of microtubule translocation and microtubule treadmilling (Rodinov and Borisy, 1997). The minus ends of these polymers are unstable and subsequently depolymerised.

1.2.3.2 Microtubule Destabilising Factors

The phosphorylation of MAPs by kinases, including MPF and MAP kinases, in the microtubule-binding domains result in their 'detachment' from the microtubules, allowing the polymers to depolymerise (Shiina et al., 1992) In response to external signals, proteins such as katanin, an ATPase, p56, and Elongation factor 1α(EF1α), an essential component of the eucaryotic translation apparatus, severe stable microtubules and disassemble them to tubulin dimers (McNally and Vale, 1993), (Shiina et al., 1994). Belmont and Mitchison (Belmont and Mitchison, 1996) have also identified the heat-stable oncoprotein18 (Op18/Stathmin) which physically interacts with tubulin dimers and increases the catastrophe rate of microtubules.

Microtubule motors play a role in destabilisation as well as stabilisation of microtubules. The deletion of the gene encoding a kinesin-related protein in yeast, Kip2p, results in almost total loss of cytoplasmic microtubules, while another kinesin, Kar3, alters microtubule dynamics *in vitro*. Deletion of the gene for this protein results in a dramatic increase of cytoplasmic microtubules. A frog kinesin, XKCM1, has also been shown to alter microtubule dynamics [reviewed by Joshi, 1998 #86].

1.2.3.3 Microtubule Dynamics in the cell cycle

Microtubules form the spindle array during mitosis. Kirschner and Mitchison (Kirschner and Mitchison, 1986) provided the first comprehensive model for spindle array formation. They proposed that microtubules grow out from the centrosome,

then rapidly shrink back, exploring the surroundings like a radar. However when it comes into contact with a kinetochore from a condensed chromosome, a capture event takes place, and those MTs with kinetochores are stabilised against shrinkage. This gives rise to a spindle array comprising of two centrosomal poles connected to chromosomal kinetochores via the kinetochore microtubules. Microtubules are also connected pole-to-pole, or with the cellular cortex (astral microtubules).

Heald *et. al.* (Heald et al., 1996) incubated non-centrosomal *Xenopus* egg extracts with DNA coated beads to show that DNA, not necessarily the kinetochore, can self-organise the microtubules into bipolar spindles. In this experiment, microtubules first interacted randomly with the DNA coated beads, then were slowly sorted into axial arrays. These arrays were focussed at the ends to give rise to a bipolar spindle around the DNA coated beads. An antibody against a subunit of cytoplasmic dynein blocked the formation of microtubule foci at the ends of the array, but did affect the assembly of MTs into arrays by the coated beads. This model and further experiments by Merdes *et. al.* (Merdes et al., 1996) suggests that microtubules of mixed polarities are arranged into parallel arrays by kinesin with the plus ends oriented towards the chromatin. Minus-end directed motors such as dynein then translocate to the minus ends of the parallel microtubules, therefy fosusing the filaments at their minus ends as the motor interacts with several filaments together. In Kirschner and Mitchison's model, dynamic microtubules nucleated from the centrosome act as searching devices which are captured and stabilised by the kinetochore. The new model suggests that spindle bipolarity in the result of cytoplasmic assymetry due to chromatin, intrinsic microtubule polarity, and the action of polarity-directed microtubule motors.

Microtubule motors thus appear to play a prominent role in almost all aspects of microtubule dynamics.

1.2.4 Microtubule Motor Proteins

Microtubule motor proteins are proteins that bind to microtubules and move along them by converting chemical energy from ATP hydrolysis into kinetic energy. Motors often carry organelles to their target sites in the cell. Motor proteins can usually travel only in one direction, and are therefore classified as plus-end directed or minus-end directed microtubule motor. Two major classes of microtubule motors, involved in organelle transport and cell division, are the kinesin and dynein superfamilies.

The kinesin molecule consists of two 120kD kinesin heavy chains (KHC) and two 64-kD kinesin light chains (KLCs). It has a rod like structure composed of two globular heads 10 nm in diameter, a stalk, and a fan-like end with a total length of 80 nm. The globular heads are composed of KHCs that bind to microtubules and the KLCs constitute the fan ends. a systematic molecular biology search for kinesin superfamily genes coding for proteins containing ATP-binding and microtubule binding consensus sequences led to the discovery of new kinesin superfamily proteins related to organelle transport. Three major types of KIFs are present classified according to the position of the motor domain: the amino terminal type; the middle type; and the carboxy-terminal type.

Cytoplasmic dynein is a member of the dynein superfamily of proteins. It is a large multisubunit complex. It has two heavy chains (530kD), three intermediate chains (74 kD), and four light intermediate chains (55kD). It also contains phosphate binding pockets, called P-loops, in its central region. The central and C-terminal ends of dynein are predicted to form a globular domain which interacts with microtubules and provides the motor, whilst the N-terminal region binds to its cargo. Cytoplasmc dynein also interacts with the large (10 subunit) protein complex dynactin. Subunits of dynaction are thought to link dynein to its cargo. (Reviewed by Hirokawa, 1998).

1.3 Microtubule Functions in the Cell

1.3.1 Cell Shape and Polarity

In many cases, the particular shapes of differentiated cells are regulated by the presence of microtubules. The most well-known example is the case of neorons where both the dendritic processes and the axon are composed of microtubules organised in a polarised manner. Bass and Ahmed (1993) studied the contribution of microtubule transport and assembly for establishing the the axonal microtubule array using the properties of the anti-microtubule drug vinblastine. At nanomolar levels, the drug inhibits microtubule assembly and limits the rate at which the polymer exchanges subunits with the soluble tubulin pool. Therefore any changes in microtubule distribution could not be due to assembly but transport of microtubules. Axons grown in the presence of vinblastine showed the same uniformly plus end distal oriented microtubules as control axons, revealing that the transport of microtubules are

responsible for establishing their polarity orientation. The authors then depolymerised most microtubules in cultured with a more potent drug, allowed a burst of reassembly from the centrosome and added vinblastine to prevent further reassembly. Over time, the microtubules were gradually depleted from the cell centre and accumulated in the periphery and within developing axons, again revealing that microtubules released from the centrosome are actively transported towards the cell periphery and then into the axon.

Yu et al (1996) used biotynalated tubulin to show microtubule assembly and transport for axonal growth. Cultured neurons with short axons were microinjected with biotynalated tubulin, and the axons were subjected to immunoelectron microscopic analysis after being allowed to grow. Analysis showed that the majority of the polymer in the newly grown region of the axon were labelled, but varying amounts of unlabelled polymer were also present, indicating that both microtubule growth and microtubule transfer occur during axonal growth.

A microtubule motor may be responsible for transport of microtubules to the cell periphery and into developing processes. Sharp et al (1997) expressed the mitotic motor protein CHO1/MKLP1 in the insect ovarian Sf9 cells, and these normally rounded cells grew processes. The microtubules within the cells initially accumulated at the periphery of the cell body and then within the processes. The microtubules in the processes had either the nonuniform microtubule polarity pattern of dendrites or the uniformly plus-end distal pattern characteristic of axons. These studies show that motor drive microtubule to the cell epriphery and into developing processes, in a manner that sets up distinct patterns of microtubule-polarity orientation.

1.3.2 Organelle transport

Eucaryotic cells have highly regulated membrane trafficking pathways that function to mediate exchange of protein and lipid between distinct membrane-bound compartments or organelles. Transport intermediates that utilize these pathways must often travel significant intracellular distances to reach specific target organelles. Early electron microscopic studies identified short (25-30 nm) crossbridges between membraneous organelles and microtubules, prompting the idea that these might be motor proteins responsible for organelle transport along microtubules (Hirokawa, 1982). The application of video enhanced microscopy revealed in real time the bidirectional movements of several kinds of membraneous organelles along the axon. It also proved that membraneous organelles move along microtubules (Brady et al., 1982).

In many cell types microtubules are nucleated during interphase from a peri-nuclear microtubule organising centre (MTOC) and radiate out towards the cell periphery to form an extensive network throughout the cytoplasm. Organelles of the central membrane system and their transport intermediates diferentially distribute within this microtubule array, with the endoplasmic reticulum (ER) and early endosomes preferentially distributed towards the plus ends of microtubules in the cell periphery, and the golgi, late endosomes and lysosomal membranes clustered near the minus ends of the microtubules in the vicinity of the nucleus. In the absence of microtubules this spatial arrangement is lost and membrane traffic between organelles and to the

cell surface becomes much less efficient (Cole and Lippincott-Schwartz, 1995). Microtubules and their associated proteins therefore play a fundamental role both in the organisation of organelles and in the efficient transport of protein and lipid between these structures in higher eucaryotes. The focus is on answering the question - how do they do it?

Studies with the drug brefeldin A (BFA) , which reversibly dissociates from membranes a complex of peripheral membrane proteins involved in regulating membrane traffic and induces rapid tubulation of Golgi, endosomal and lysosomal membranes, have revealed that membrane tubules can also serve as transport intermediates in pathways through which organelles communicate. BFA reveals the dynamic morphological characteristics of organelles are coupled to their capacity to move bidirectionally on microtubules. Golgi membranes, normally based at the minus ends of microtubules, extend along the plus ends in the presence of BFA. BFA treatment causes membranes of the trans-golgi network (TGN) first to extend towards the plus ends to fuse with the endosomal system, then to colaps at the micus end near the MTOC. Change in the cytosolic pH also results in redistribution of the late endosomes and lysosomes. Most organelles therefore have the ability to bind to both plus- and minus-end directed motor proteins and shared activator molecules may direct the direction of organelle movement (Cole and Lippincott-Schwartz, 1995).

Kinesin has been shown to interact with ER membranes. Immunofluorescence studies with anti-kinesin antibodies show punctuate staining patterns which are closely associated with ER membranes. Supression of kinesin heavy chain expression in cultures rat hippocampal neurons by antisense oligonucleotides resulted in the

retraction of the ER network from the periphery into the center of the cell, without affecting the distribution pattern of microtubules (Feiguin et al., 1994).

The Golgi complex receives, processes and sorts lipidsand protein arriving from the ER. They utilise microtubules to cluster towards the cell centre. Drugs such as taxol or nocodazole result in redistribution of the golgi to the priphery of the cell - they remain functional but can no longer direct material to specific domains on the plasma membrane. Cytoplasmin dynein has been implicated in the 'capture' and minus end directed movement of exogenously added Golgi membranes to semi-intact Chinese Hamster ovary cells, and may be the motor responsible for the nalogous process of clustering of transport intermediates during normal transport between ER and Golgi. Kinesin also affects golgi transport - supression of kinesin heavy chain expression by anti-sense oligonucleotides was shown to inhibit the extension of TGN-derived tubules in the presence of BFA. Similar results were seen by injecting anti-kinesin antibodies.

1.3.3 Microtubules and Cell Division

Microtubules play a key role in cell division by forming the mitotic spindle which is essential for segregation of chromosomes into the daughter cells. The centrosomes and the spindle pole bodies (SPBs) are the two organelles responsible for nucleating the polymerisation of microtubules from free tubulin subunits and organising them into arrays for specific purposes in interphase, mitosis and meiosis. Both the centrosome and the Spindle Pole body duplicate only once per cell cycle, so there are only one or two of them depending on the stage of the cell cycle. A centriole is a short

cylinder consisting of nin triplet microtubules, and the centrosome can be defined as a pair of centrioles surrounded by pericentriolar material. Substances in the pericentriolar material, rather than in the centrosome itself, appears to be responsible for microtubule nucleation. The SPB is a disc-shaped structure embedded in the nuclear envelope that organises nuclear microtubules from one face and cytoplasmic microtubules from the other. SPBs do not have centrioles, instead it consists of several layers.

As the cells enter M-phase, the interphase microtubules dissolve and a bipolar spindle is assembled. Several microtubule severing factors have been discovered, which may be trigger the depolymerisation of interphase microtubules at the G2/M boundary. P56, extracted from Xenopus, binds to monomeric tubulin as well as tubulin subunits in microtubules, and incubation of p56 with monomeric tubulin inhibits microtubule severing activity. It is also less effective in microtubules atbilised by p220 or MAP2 , and electron microscopic obsevartions suggest that p56 attaches to microtubules and produces a structural change that results in kinks and breaks in the lattice [Shiina, 1992 #72]. A second factor, katanin, was purified from sea urchins (McNally and Vale, 1993). Katanin is a heterodimeric protein composed of 81 kD and 60 kD polypeptide subunits. Katanin reversibly severes and disassembles microtubules in a few minutes, proving that severing does not involve proteolysis or protein denaturisation. Katanin also has microtubule stimulated ATPase activity, and requires ATP to severe microtubules. Neither katanin nor p56 can severe taxol-stabilised microtubules. The third severing factor, also extracted from Xenopus, is p46, which was sunsequently found to be the Xenopus elongation factor, EF-1α. It shows microtubule severing activity in vitro. In addition, microinjection of the recombinant

EF-1α into cultured mammalian fibroblasts causes rapid destruction of cytoplasmic microtubule networks. P48 cannot severe microtubules immobilised on a slide - it possibly requires microtubules to be mobile (Shina et al., 1994).

The cell continues in M-phase with the formation of the spindle. The mechanism of spindle assembly is varied - it differs between meiotic and mitotic systems, between somatic, embryonic and gametic cells. However, all eucaryotic cells have certain essential features - two spindle poles from which dynamic microtubules of uniform polarity emanate, with minus ends at the poles and plus ends at the spindle equator. The chromosomes capture and stabilise microtubule plus ends via their kinetochores and move to the metaphase plate. Chromosomes are then separated as they are pulled towards the poles by the microtubules during anaphase, possibly due to the action of minus-end directed motor proteins.

Bipolar spindles are necessary in cell division, and in somatic cells, centrosomes are necessary for bipolar spindles. Centrosomes nucleate a polarised array of microtubules with the minus ends attached to the γ-tubulin complex. In meiotic grasshopper spermatocytes the spindle slowly dissolve if the centrosomes are removed, and spindles will not form at all if the centrosomes are removed from the cytoplasm prior to the nuclear-envelope breakdown. Centrosomes replicate and separate to form the ends of the bipolar spindle at the beginning of M-phase. If centrosomes do not replicate or separate properly, a monopolar spindle forms. Therefore centrosomes are required both to nucleate a polarised array of microtubules and dictate spindle polarity. Astral microtubules interacting with minus-end directed dynein that are anchored in the cytoplasm may serve to pull the centrosomes apart.

Other centrosomal motor proteins include XKLP2 and the BimC subfamily of kinesin like motor proteins. Recent data also suggest that phosphorylation may be necassary for the regulation of centrosome separation. Mutations that cause the loss of function of the protein kinase aurora in Drosophila prevent centrosome separation. Centrosomes, however, do not appear to be necessary for spindle maintenence during late anaphase.

Microtubules in the spindle are stabilised kinetochores by the 'search and capture' model which applies to most mitotic cells. Echinoderm egg and newt lung egg kinetochores appear to stabilise the spindle; in the absence of chromosomes, centromeres nucleate two asters instead of a bipolar spindle. It therefore appears that kinetochores are necessary for bipolar spindle formation.

The hypothesis that chromosomes themselves are involved in organising microtubules into a spindle was first formed when Karsenti et. Al (1984) showed that phage DNA induces spindle formation when microinjected into meiotic Xenopus eggs. Recent data support this hypothesis - when early prophase chromosomes are exposed to the centrosome by mechanical disruption of the nuclear envelope with a microneedle, a bipolar spindle forms prematurely. Micromanipulation of metaphase chromosomes have shown that microtubule mass increases when a chromosome is present in the spindle (Zhang and Nicklas, 1995).

Conclusively data showing that the chromosomes themselves and not the kinetochores are involved in spindle assembly came with experiemnts where magnetic beads coated with plasmid DNA were shown to induce bipolar spindle assembly in *Xenopus* egg M-

phase extracts. As plasmid DNA does not contain any centromeric sequences, the chromatin that forms from it does not contain kinetochores. Time-lapsed recordings of chromatin induced spindle assembly showed that microtubules first aggregated around the chromatin and then coalesced into bundles. In the final stages of spindle assembly, the distal ends of the microtubule bundles were were pinched together to form spindle poles. This movement was dependant on cytoplasmic dynein. This demonstrated that the microtubule minus ends were found at the poles in these in vitro spindles. This centrosome- and kinetochore-free system is the clearest example that chromatin alone can organise microtubules into a bipolar spindle. A family of chromosomal proteins that may function in spindle assembly is the chromokinesins, which includes *Nod* in *Drosophila*, XKLP1 in *Xenopus*, chromokinesin in chicken and Kid in human. These proteins, apart from organising the microtubules into spindles, are also proposed to be responsible for the polar ejection forces that push chromosomes away from the spindle poles and causer them to congregate at the metaphase plate.

Nonkinetochore spindle microtubules turn over quickly in metaphse compared to interphase microtubules, due both to increased number of catastrophes and increased rate of microtubule growth in metaphase. XKCM1 was the first endogenous regulator of catastrophe to be identified, and is a kinesin-related protein. It is homologous to the human kinetochore protein MCAK. Op18/stathmin is a phosphoprotein that is present at elevated levels in some cancer cells. Immunodepletion of either XKCM1 or Op18/stathmin from Xenopus egg extracts results in aberrant spindle assembly. Spindles in these extracts have centrally localised chromatin from which an array of long microtubules emanates. Analysis of the effect of immunodepletion of these

proteins on individual microtubile dynamics revealed that these proteins increased the number of catastrophes, without affecting other proprties of microtubule dynamics.

M-phase microtubules also exhibit a poleward microtubule flux at late metaphase/anaphase - kinetochore microtubule polymerisation at the plus ends is balanced by constant depolymerisation at the minus ends. When plus-end dynamics at the kinetochor are inhibited, microtubule poleward flux continues. The motor for microtubule poleward flux, is, therefore likely to be found at microtubule minus ends or associated with the spindle matrix.

1.4 Microtubule Associated Proteins

1.4.1 General Introduction

A number of additional proteins have been found to co-purify with tubulin when microtubules are extracted from a variety of tissues. These proteins are known as microtubule associated proteins (MAPs), and they appear to play a crucial role in the regulation of properties and functions of microtubules *in vivo*. Although tubulin has been found to self-assemble into microtubules in the absence of MAPs (Caplow, 1992), MAPs isolated from a variety of sources promote microtubule assembly *in vitro*. Due to an abundance of microtubules within neurons, there has been a wealth of information concerning MAPs derived from neuronal microtubules.

1.4.1.1 Neuronal Microtubule Associated Proteins

All brain MAPs studied so far possess a positively charged domain that binds the negatively charged microtubule surface. Depending on their microtubule interaction motifs, MAPS can be divided onto two categories : Type 1 MAPs, such as MAP1A and MAP1B, containing a multiply repeated KKEX motif, and Type 2 MAPs, such as Tau and MAP2, which contain three or four imperfect amino acid repeats.

MAP1A and MAP1B share partial sequence homology. They are both synthesized as a polyprotein coupled to a light chain (Langkopf et al., 1992). MAP1A however has a novel micotubule binding motif which is unique as it is acidic rather than basic (Cravchik et al., 1994). Another basic protein, LC3, is abundant in neurons and binds to both MAP1A and MAP1B , and this could modulate the interactions of both the MAPs with microtubules (Mann and Hammarback, 1994).

Variations in the microtubule binding structure of the two types of MAPS could allow them to bind either with different affinities or along different sites in the microtubule. *In vitro* studies with MAP1 and MAP2 showed that both bind a common sequence within the variable C-terminal region of different β-tubulin isoforms. Therefore it can be inferred that both types of MAPs bind on the same region of the microtubule surface. However there are functional differences between the MAPs - Type 2 MAPs have been shown to promote microtubule assembly more efficiently than MAP1A or MAP1B (Olmsted, 1986)

1.4.1.2 Non-Neuronal Microtubule Associated Proteins

MAPs have also been identified in non-neuronal cells. MAP4 was the first non-neuronal MAP to be discovered in the rapidly growing HeLa cell line (Bulinski and Borisy, 1979). This is a pure cell line and can be subject to large scale culture, and therefore sufficient tubulin concentrations could be extracted for the identification of a MAP. MAP4 has been shown to be of the Type II category, containing 4 imperfect repeats (and one pseudo-repeat) of 32 amino acids in its C-terminal domain. MAP4 has since been isolated from and sequenced in human, bovine and mouse non-differentiated tissues, and studies of its expression and developmental regulation suggests that it is important in microtubule dependant processes, particularly in the cell cycle (Bulinski, 1994)

MAPs have also been isolated from non-mammalian cells. MAPs of mass similar to MAP4 has been identified from *Drosophila* (Goldstein et. al, 1986), *Xenopus* (Gard and Kirchner, 1987; Faruki and Karsenti, 1994), diatoms (Wordeman and Cande, 1987) and budding yeast (Irminger-finger et. al, 1996). The Drosophila 205kD MAP shares the properties of microtubule assembly, but protein sequence information demonstrates that it is unrelated to MAP4.

In *Xenopus* at least three MAPs have been identified so far, and their role in microtubule dynamics, particularly cell cycle-dependant changes, have been extensively studied. The first MAP to be discovered in this organism was the 215 kD Xenopus-MAP (X-MAP) (Gard and Kirchner, 1987). It was shown to promote elongation of microtubules specifically at the plus end. It is also developmentally

regulated and is phosphorylated during mitosis. The second *Xenopus* MAP to be discovered, of 220 kD, is also phosphorylated during mitosis, its phosphorylation diminishes its ability to bind to taxol-stabilised microtubules or to stabilise microtubule growth from purified centrosomes (Shiina et al., 1992). A third Xenopus 230kD MAP4-like protein has been shown to be a MAP by *in vivo* cellular distribution, and its ability to bind specifically to taxol microtubules. This protein is heat-stable and immunologically related to MAP4. It could also be phosphorylated in mitotic extracts as it shows a shift in gel mobility. The purified 230kD MAP promotes elongation of microtubules by lowering the critical concentration of tubulin necessary for microtubule assembly. It promotes microtubule elongation from both the plus and minus ends of axonemes (Faruki and Karsenti, 1994).

The lowest eucaryote to demonstrate the presence of MAPs is the budding yeast *Saccharomyces cerevisiae*. The gene, termed MHP-1 (MAP-homologous protein 1) was isolated by expression cloning using antibodies specific for the Drosophila 205kD MAP (Irminger-finger et. Al., 1996). MHP-1 codes an essential protein of 1398 amino acids, and its microtuble biding C-terminal domain shares a short sequence of homology with tau. MAP2 and MAP4. It does not, however, share sequence homology with the 205K *Drosophila* MAP. It is therefore possible that regardless of sequence homology, the MAPs may share structural similarity. As with other MAPs, MHP1 is also anomolously retarded on an SDS-PAGE gel. It is highly charged and the putative microtubule-binding domain is followed by an acidic COOH-terminal region. However, the protein contains alternating acidic and basic regions, and its acidity gradually increases from the N-terminal region to the C-trminal region. Deletions of MHP make the cell non-viable, whilst its overexpression results in the

increased formation and stabilisation of cytoplasmic microtubules (Irminger-finger et al., 1996).

1.4.2 Tau

Tau was one of the first MAPs to be identified. It was purified from pig brain, and subsequently found to be a potent promoter of microtubule assembly *in vitro* (Goedert et al., 1994). It is found mainly in axons of neurons in mammalian cells. There are six known tau isoforms, produced from a single gene by alternative splicing. The expression of the tau isoforms are developmentally regulated (Kosik et al., 1989).

As a type II MAP, all tau isoforms contain three or four tandem repeats of 31 or 32 amino acids located at the C-terminal end, each containing the characteristic pro-gly-gly-gly motif . The extra repeat in the isoforms with the four repeats is inserted within the first repeat of the isoforms of three repeats in a way that preserved the periodic pattern(Goedert, 1989). Twelve residues are identical in the four repeats, and a further six residues are identical in three of the four repeats. The N-terminal end of the protein is the projection domain, determining the spacing between adjacent microtubules(Chen et al., 1992). Some of the tau isoforms contain an additional 29 or 58 amino acid insert near the N-terminus (Goedert et al., 1994). There is also a charge separation between the two ends of the protein - while residues 1-125 in the N-terminus are predominantly acidic, the C-terminal residues (126-250) are basic (Goedert et al., 1994).

The only known post-translational modification of tau is phosphorylation (Goedert et al., 1994). This is significant as phosphorylated tau is far less effective than nonphosphorylated tau in promoting microtubule assembly. There are 17 ser-pro and thr-pro sites in tau where it can be phosphorylated, and indeed they have been phosphorylated *in vivo* by several known kinases - it can act like a 'sponge' for kinases (Drewes et al., 1997; Drewes et al., 1992; Goedert et al., 1994; Mandelkow et al., 1995; Mandelkow, 1995; Mandelkow et al., 1992). Hyperphosphorylation of tau is found in neurofibrillary tangles formed in Alzheimer's disease (Kosik, 1994).

Comparison of the pattern of recombinant tau with that of native tau shows that the four major tau isoforms in the adult human brain correspond to isoforms with three or four repeats without N-terminal inserts and to isoforms with three or four repeats containing the first N-terminal insert of 29 amino acids. Isoforms with three or four repeats with the 53 amino acid N-terminal insert are also found but at lower levels. These findings reflect the levels of mRNA transcripts encoding the various tau inserts. Transcripts encoding isoforms with three or four repeats, and those with the first N-terminal insert, are found throughout the adult human brain and their levels do not vary much between diferent regions (Goedert, 1990). Transcripts encoding the isoforms with 58 amino acid insert are found only at low levels. However in foetal brains as well as in immature brains, only transcripts encoding isoforms with three repeats are found. Transcripts of four repeat isoforms or with N-terminal inserts are not detected. The developmental shift of tau bands from a simple foetal pattern to a more complex adult pattern therefore involves the transition from the expression of three repeat isoforms and no inserts to the expression of all six isoforms (Goedert, 1990).

1.4.2.1 Functions of Tau

Tau has several distinct effects on microtubules *in vitro*: It binds to them, promotes their nucleation and elongation, protects against disassembly and induces them to form parallel arrays called bundles (Brandt and Lee, 1993; Brandt and Lee, 1994; Gustke et al., 1994).

1.4.2.2 Distribution

Tau is found mainly in differentiated cells, and is heterogenously distributed both within cells and between different cell populations. Whilst the six tau isoforms are found in the central nervous tissue, Big Tau, characterised mainly by the presence of an additional exon, is found in the peripheral nervous system (Goedert et al., 1992). Different neuronal cell types express different isoforms of tau. Pyramidal cell bodies in all layers of the adult human cerebral cortex encode isoforms with three or four repeats. In the hippocampus, cells express three repeat isoforms. Four repeat isoforms are also found in the pyramidal cells of the subiculum and hippocampus, but not in the granule cells (Goedert et al., 1994).

Within neurons, tau is mainly axonal. Antibodies that recognise all tau isoforms label axons and only a small number of neuronal cell bodies and dendrites in adult brain from a variety of species. Tau is more widely dispersed in immature cells, however - in juvenile cat brain a larger number of cell bodies and dendrites are labelled. A small number of glial cells also show staining using anti-tau antibodies. There is also a

nuclear variant of tau (Bassell et al., 1994). Intracellular sorting may take place at the level of the transcripts, which come in sizes between 2.5 and 8 kB and may contain targetting information. Microtubules may play a role in distributing tau, because mRNA is transported along them (Bassell et al., 1994).

1.4.3 Alzheimers Disease.

Alzheimer's disease is a neurodegenerative disease, which, unlike other such diseases like schizophrenia and Huntingdon's disease, is characterised by two main features in the postmortem brain. One is the senile plaque, mainly consisting of extracellular aggregates in a dense plaque core or as diffuse infiltrate in portions of the neuropil. The second characteristic is the neurofibrillary tangle, found within the neuron in the cerebral cortex and hippocampus and in some subcortical nuclei. (reviewed by (Kosik, 1994)).

The senile plaques consist of the βamyloid peptide, part of the amyloid precursor protein (APP), a large glycoprotein that spans the membrane once. Defective cleaving of a 100-110 Kd fragment of APP which includes the Aβ region by an unknown enzyme called α-secretase leads to the accumulation of the Aβ fragment into aggregates that form the plaques (Esch et al., 1990; Haas et al., 1994).

The fibrous component of the disease, not normally seen in the cytoskeleton, is known as the paired helical filament (PHF). It consists of two subunit strands helically wrapped around each other. Treating the tangles with pronase removes a fuzzy coat to reveal a pronase-resistant core (reviewed by (Goedert et al., 1994)). Biochemical

studies have shown that PHF is composed of abnormally phosphorylated tau (Greenberg and Davies, 1990). The N- and C-terminal regions of tau form the fuzzy coat, while the microtubule-binding repeat region forms the pronase-resistant core. Sequence analysis of the core fragments have revealed that both three-repeat and four-repeat isoforms contribute to the core of PHF, but only three repeats are protected (Jakes et al., 1991). Recombinant tau fragments with three MT-binding repeats can also form filaments like those found in Alzheimer's disease (Crowther et al., 1992).

Tau in PHF is abnormally phosphorylated and has greatly diminished ability to bind to microtubules, although how phosphorylation inhibits binding of tau to microtubules and subsequently promotes its assembly into PHFs is not clear (Morishima-Kawashima et al., 1995). Since the phosphorylation is much greater and many more sites than that of normal tau, it is likely that increased activity of a specific tau kinase rather than the decreased activity of a phosphatase that is responsible for PHF formation. Identification of these kinases and/or phosphatases could provide a clearer understanding of the mechanisms of Alzheimer's disease (reviewed by (Goedert et al., 1994)).

1.4.4 MAP2

MAP2 is another type II neuronal MAP. Like tau, MAP2 is heat stable, and has a homologous repeat domain near the C-terminal end (Matus, 1994). However, unlike tau, MAP2 found in the brain has three repeats, and a four repeat MAP2 is found in glial cells (Doll et al., 1993). The N-terminal domain of MAP2 also has a much larger extension than tau. Another similarity with tau is that MAP2 has several isoforms

produced by the alternative splicing of a single gene (Garner and matus, 1988). There are two high molecular weight forms of MAP2, MAP2a and MAP2b, and a low molecular weight form, MAP2c. The different isoforms are developmentally regulated. MAP2b is expressed constitutively throughout life, MAP2a is expressed only in mature neurons, while MAP2c expression is high during development (Binder et al., 1984; Kalcheva et al., 1998).

In mature neurons, MAP2 has been localised to dendrites, although MAP2c has been localised to axons as well (Matus, 1994) (Okabe and Hirokawa, 1989) (Garner and matus, 1988)]. MAP2 has been shown to bind to microtubules in a positively cooperative manner, leading to clustering of MAP2 on the microtubule surface, a feature that distinguishes MAP2 from tau (Wallis et al., 1993).

MAP2c, the low molecular weight form of MAP2, was initially identified as a 70kD microtubule binding protein cross-reactive with only a limited number of monoclonal anti-MAP2 antibodies. MAP2c is abundant in the immature nervous system and disappears in mature neurons.

MAP2c consists of the extreme N-terminal and C-terminal functional ends of MAP2. In its C-terminal, it contains the 32 amino acid repeats characteristic of Type II MAPs (Garner et al., 1988). It is also heat-stable. In its N-terminal end, it contains the cAMP-dependent protein kinase binding site (Kindler et al., 1991). This is a defining feature of MAP2 as tau and MAP4 do not contain this site. All forms of MAP2 also contain multiple repeats of the motif proline-glutamic acid-serine- threonine (PEST) (Friedrich and Aszodi, 1991). This is a feature of many proteins that are programmed

for proteolytic destruction, and this could be one of the features regulating the developmental and cellular distribution of the protein.

1.4.5 MAP4

MAP4 was the first known non-neuronal MAP. Although originally purified from HeLa cells, it was subsequently found in all cells except adult human brain and mature sperm. Immunoelectron microscopy revealed that MAP4 was present along the length of apparently all cellular microtubules, on all classes of microtubules within the mitotic spindle, and on microtubules formed after mitosis or drug-induced polymerisation (DeBrabander et al., 1981).

The molecular weight of the native MAP4 molecule was calculated as approximately 440 kD. However the molecular mass calculated from it deduced amino acid sequence is approximately 125 kD (Bulinski, 1994). All MAP4 preparations studied to date consist of multiple species of the protein. Structural data suggest that MAP4 is a highly elongated protein with two distinct domains (similar to other TypeII MAPs) - the C-terminal domain that binds microtubules and the N-terminal domain that projects from the microtubule surface. It is heat stable. The N-terminal projection domain possesses a series of 13 amino acid repeats of unknown functional significance. This region is acidic. In contrast, the C-terminal domain has a net basic charge and is highly conserved within species. It contains the repeat sequences present in tau and MAP2. However, there are some differences between the neuronal MAPs and MAP4 within the microtubule-binding domain - it does not share sequence homology in regions flanking the MT-binding repeats (Aiwaza et al., 1991; Chapin

and Bulinski, 1991). The proline rich region of MAP4 is also more extensive. MAP4 is also alternatively spliced to produce four isoforms containing three, four or five imperfect repeats. The isoform expressed in these experiments contained five repeats. The second of these five repeats is markedly different from the other repeats, and has a long spacer sequence (Bulinski, 1994).

In vitro studies have shown that, like tau and MAP2, MAP4 promotes microtubule assembly and stability (Aiwaza et al., 1987). *In vivo* studies using GFP-tagged MAP4 revealed that MAP4 reorganises microtubules into bundles and stabilises microtubules against depolymerisation by the drug nocodazole (Olson et al., 1995). However, studies involving immunodepletion of MAP4 from the cell did not reveal any effect (Wang et al., 1996).

MAP4 is found in dividing cells, and regulates the depolymerisation of interphase microtubules as the cell enters mitosis. It has been revealed that MAP4 is a target of the cdc2 kinase (Ookata et al., 1995; OOkata et al., 1997). MAP4 has been shown to be phosphorylated by the cdc2 kinase it its proline-rich C-terminal region, and phosphorylation of the MAP supressed the ability of MAP4 to stabilise microtubules (Ookata et al., 1995; OOkata et al., 1997). Therefore microtubule dynamics in the cell through the cell cycle appear to be regulated directly by MAP4.

1.5 Microtubules in Yeast

1.5.1 Fission Yeast Cytoskeleton

Fission yeast are ascomycete yeast that belong to the genus *Schizzosaccharomyces,* and share the property of dividing by medial fission. The fission yeast *S. pombe* has been at the forefront of cytoskeleton research due to the relative simplicity of its cytoskeletal organisation, which reflects a lifestyle based almost exclusively on growth and division, and without complications faced by higher eucaryotes such as changes in cell shape and movement.

Microtubules in *S. pombe* are composed of 2 α-tubulin, 1 β-tubulin and 1 γ-tubulin genes (Horio et al., 1991) (Yanagida, 1987). The β-tubulin is 76% homologous to chicken β-tubulin, and the α-tubulin is 76% homologous to porcine brain α-tubulin (Yanagida, 1987). Gene disruption experiments showed that the α1 tubulin as well as the β and γ tubulins is essential for cell survival, but the α2 tubulin is non-essential (Yanagida, 1987). Although sequencing of the fission yeast genome is not complete, data from genetic, western blotting and DNA hybridisation approaches suggest that no more tubulins will be discovered (Hagan, 1998) (Yanagida, 1987).

The two α tubulin genes also differ in their regulation. Transcription of α1 appears to be modulated, whilst that of α2 appears constitutive. The amounts of α1 and α2 polypeptides produced, as estimated by using lacZ fused genes or by gel electrophoresis are similar (Adachi et al., 1986). It is possible that α1mRNA are short-lived, or that α2 mRNA are more stable in transcription.

1.5.2 Regulation and Function

Microtubules in fission yeast play a role in the determination of cell shape, in nuclear and organelle positioning, and in mitosis and cell division (reviewed by (Hagan, 1998). Microtubules in interphase fission yeast cells extend between the ends of the cell. Between four to eight tubulin staining elements can be seen by indirect immunofluorescence, and each of these elements possibly contain two to three microtubules (Hagan and Hyams, 1988). Treatment of fission yeast cells with microtubule depolymerising agents resulted in the disruption of the rod-like shape of the cell into branches or bends (Umeneso et al., 1983). Tubulin mutants, such as *nda2* and *nda3*, showed a similar phenotype(Toda et al., 1983). However it was not clear whether microtubules played a diect role in these changes, or a secondary role due to excessive mitotic delay resulting from these treatments. Morphogenetic mutants, such as *tea1, tea2, ban3.2, ban4.1* and *mal3*, which showed no appreciable delay in mitosis but showed abnormalities in micrrotubule arrangements in the cell provided direct evidence for the role of microtubules in cell morphology (Mata and Nurse, 1997), (Verde et al., 1995). *Tea* mutants are bent or T-shaped, and a basket of short microtubules surrounds the nucleus. *Ban* mutants are bent, and the interphase microtubules form a thick bundle on one side of the cell.

Microtubules are also responsible for the positioning of several organelles, such as the nucleus, golgi apparatus, and the mitochondria in fission yeast. Yaffe et. al. (1996) revealed that the *ban 5.4* mutant had asymmetrically distributed mitochondria. Genetic analysis revealed that ban 5.4 is an allele of *atb2*, which codes for α2 tubulin.

Cold sensitive nda3 (β-tubuling coding) mutants also showed an asymmetric distribution of mitochondria after incubation at lower temperatures. These experiments provided genetic evidence for the role of microtubules in mitochondrial movement (Yaffe et al., 1996). Ayscough *et. al* (1993) revealed that disruption of microtubules in fission yeast by thiabendazole (TBZ) resulted in the disassociation of Golgi stacks (Ayscough et al., 1993). Microtubules also appears to position the interphase nucleus to the centre of the cell (Hagan and Yanagida, 1997).

1.5.3 Microtubules in Mitosis

The dynamic properties of microtubules are essential for the eucaryotic cell to undergo the various stages of the cell division cycle. The fission yeast is a good system to study the changes in microtubules as they show distinct rearrangements at defined points in the cell cycle.

Most of the S. pombe cell cycle is occupied by interphase, when the cell extends in size from 7μm to 14 μm. At this stage, three to eight microtubules extend across the length of the cell from the two tips (Hagan and Hyams, 1988). (Pichova et al., 1995) have also reported the presence of a network of cytoplasmic microtubules beneath the plasma membrane. These are helically arranged and similar to plant cell types where randomly and helically distributed cortical MTs form a peripheral network and are known to control the pattern of cell wall deposition and cell elongation via transmembrane wall synthetases. The possible roles of cytoplasmic microtubules have

been discussed earlier. Cell elongation ceases and the cytoplasmic microtubules disappear at the G2/M boundary (Mitchinson and Nurse, 1985).

The transition in fission yeast from interphase to mitosis is rapid, and denoted by the appearance of two anti-tubulin staining dots on the edge of the nucleus, the spindle pole bodies (SPBs), with the concomitant disappearance of the cytoplasmic interphase microtubules (Hagan and Hyams, 1988). At the beginning of mitosis the entire nucleus fluoresces with high anti-tubulin antibodies, indicating the import of tubulin into the nucleus. A short bar extends between the two SPBs which then forms the prophase spindle. As the spindle elongates, the chromosomes migrate to the centre of the cell to form the metaphase plate (Ding et al., 1997). There are two sets of microtubules in the intra-mitotic spindle - one extends between the two SPBs, interdigitating with one another to form a region of overlap; the other extends from the SPBs to anchor to the kinetochores of the chromosomes. Possibly due to the contribution of kinetochores to the signal, metaphase spindles appear thicker at the ends than in the middle when viewed by immunofluorescence microscopy (Hagan, 1998).

As the chromosomes segregate in anaphase A, the kinetochore microtubules shorten and decrease in number (Ding et al., 1993) and the spindle continues to elongate (anaphase B). Elongation of isolated spindles from *nuc2-* cells of *S. pombe* after addition of ATP and tubulin suggests that a mechanochemical system at the zone of microtubule interdigitation co-operates with tubulin polymerisation at the post-distal microtubule ends to drive spindle elongation. Kinesin-like proteins may drive such interactions. Rather unusually, in the fission yeast anaphase B is initiated slightly

before anaphase A. When the nuclei have been pushed towards the cell ends in late anaphase, the spindle breaks down and microtubules appear in the middle of the cell in a pattern called the post-anaphase array (PAA) (Hagan and Hyams, 1988). Initially it was thought that these microtubules came from two discrete microtubule organising centres (MTOCs) - supporting this was data from Horio et. al (1991) which showed by electron microscopy that several individual microtubules extended from an amorphous mass in late mitosis. However Pichova et al (1995) showed by novel immunofluorescence microscopy that the microtubules of the PAA extend as a ring in the cell equator. The ring appears after actin has appeared in the same region (Marks et al., 1986), and suggests co-operation of the microtubules and F-actin in marking the location of the division plane.

At the start of anaphase, astral microtubules also become associated tangentially with the outer cytoplasmic face of the SPBs and persist till the end of anaphase B (Hagan and Hyams, 1996). They are not dependent on the initiation of anaphase, however, as they are also present in mutants that cannot undergo the metaphase/anaphase transition (Hagan and Hyams, 1996).

1.5.4 Microtubules in Budding Yeast

The budding yeast *S. cerevisiae* contains two α-tubulin genes, *TUB1* and *TUB3* (Schatz et al., 1986), and a single β-tubulin gene, *TUB2* (Neff et al., 1983). The two budding yeast α-tubulins are 72-74% homologous to porcine α-tubulin (Yanagida, 1987). Biochemical characterisation of purified budding yeast tubulin has revealed

that both the growing and noncatastrophic shortening rates of yeast tubulin were much smaller than those of brain microtubules. Yeast microtubules were also rarely rescued from catastrophic shortening and usually depolymerised completely, usually back to the axonemal seed (Davis et al., 1993).

There are few microtubules in the unbudded or interphase state of the budding yeast, as seen by EM and immunofluorescence studies, and thier distal ends are often close to the edge of the cell (Kilmartin and Adams, 1984). The budding yeast microtubule organising center, which is the spindle pole body, is embedded in the nuclear envelope and nucleates microtubules from both the cytoplasmic and nuclear faces (Byers and Goetsch, 1975). The initiation of DNA synthesis in budding yeast coincides with bud emergence and is followed soon after by the formation of a mitotic spindle (Pringle and Hartwell, 1981). Studies of budding yeast microtubules using GFP-tubulin have revealed that *S. cerevisiae* interphase microtubules are more dynamic than mitotic microtubules, possibly because the cytoplasmic microtubules must locate the bud site so that the nucleus and subsequently the spindle can be orientated (Carminati and Stearns, 1997).

The mitotic spindle apparatus occurs through a series of steps in the budding yeast cell cycle, as revealed by EM and immunofluorescence studies (Pringle and Hartwell, 1981). The SPBs duplicate at approximately the G1/S transition. The nucleus then migrates to the mother-bud junction, and the SPBs separate from one another to form a spindle. One SPB remains proximal to the neck, while the other traverses the nuclear envelope. (Vallen et al., 1995). Pole-to-pole microtubules originate at one pole and terminate very close to the other (Page and Snyder, 1993). The number of

discontinuous microtubules within the spindle approximates the number of chromosomes within the cell, suggesting that each *S. cerevisiae* chromosome is connected to the SPB by a single microtubule (Page and Snyder, 1993). The spindle initially elongates slowly, then at a rapid rate. Rapid oscillations of the elongating spindle suggest that when one pole is moving towards the neck, the other pole is moving distally, separating into mother and bud, until the spindle reaches its maximum length (Yeh et al., 1995). These oscillations are absent from dynein mutants, suggesting an important role for dynein in spindle movement (Yeh et al., 1995). Cytoplasmic microtubules also grow out of either pole body and interacts with the cortical ends of both mother and bud. The sweeping and shrinking behaviours of cytoplasmic microtubules at the cortex are fequent in budded cells and associated with the movement of the spindle to the site of microtubule attachment. This suggests that cytoplasmic microtubules play a rolein in proper orientation of the spindle during mitosis (Carminati and Stearns, 1997; Yeh et al., 1995).

Microtubule dynamics in budding yeast has been shown to be regulated by microtubule motors. In the absence of dynein, rates of polymerisation and depolymerisation were significantly slower, and catastrophe frequencies were reduced by half (Carminati and Stearns, 1997; Yeh et al., 1995). The kinesin-related protein Kar3p caused destabilisation of the minus ends of microtubules (Endow et al., 1994) and limited the number and length of cytoplasmic microtubules (Saunders et al., 1997). Other non-motor proteins have been reported to co-localise to tubulin and regulate microtubule function Bik1 p is reported to be required for microtubule formation and stabilisation and for pindle pole body fusion during conjugation(Berlin et al., 1990). recently an essential *S.cerevisiae* gene, *MHP1*, was revealed to code for

cytoplasmic microtubules play a rolein in proper orientation of the spindle during mitosis (Carminati and Stearns, 1997; Yeh et al., 1995).

Microtubule dynamics in budding yeast has been shown to be regulated by microtubule motors. In the absence of dynein, rates of polymerisation and depolymerisation were significantly slower, and catastrophe frequencies were reduced by half (Carminati and Stearns, 1997; Yeh et al., 1995). The kinesin-related protein Kar3p caused destabilisation of the minus ends of microtubules (Endow et al., 1994) and limited the number and length of cytoplasmic microtubules (Saunders et al., 1997). Other non-motor proteins have been reported to co-localise to tubulin and regulate microtubule function Bik1 p is reported to be required for microtubule formation and stabilisation and for pindle pole body fusion during conjugation(Berlin et al., 1990). recently an essential *S.cerevisiae* gene, *MHP1*, was revealed to code for a microtubule associate protein which is immunologically similar to the mammalian MAP4, and essential for the formation and/or stabilisation of budding yeast microtubules (Irminger-finger et al., 1996).

2. METHODS AND MATERIALS

2.1 Yeast Strains

The strains of Schizosaccharomyces pombe used are listed in table 2.1 below.

Strain	Source Reference
972h⁻	A gift from Paul Nurse
leu1.32h⁻	A gift from P. Nurse
nda2-KM52h⁻	(Toda et al., 1983)
nda2-KM52h⁺	(Toda et al., 1983)
nda3-KM311h⁺	(Toda et al., 1983)
nda3-KM311h⁻	(Toda et al., 1983)
SP1002 *(h⁺leu1ura4ade6-M210kin1::ura4⁻)*	(Levin and Bishop, 1990)

Table 2.1 . *Schizosaccharomyces pombe* strains used in this work.

2.2 Plasmids

2.2.1 Plasmids used in subcloning are listed below

Plasmid	Source Reference

pBR322	(Bolivar et al., 1977)
pBluescript	Stratagene
pGEM 5X	Promega
pUC19	(Yannisch-Perron et al., 1985)
pREP1	(Maundrell, 1993)

Table 2.2. A list of all the plasmids used for cloning in this work, with references for their sources of origin (restriction MAP of pREP1 is shown in the figures 2.1)

2.3 Escherichia coli strains used

The strains of E. coli used were

JA226 (*recBC, leuB6, trpE5, HsdR*$^-$, *Hsd M*$^+$, *lacY*, E600)

DH5α (*supE44-,lacU169,φ80lacZΔM15, hsdR17, recA1, endA1, gyrΔ96, thi-relA1*)

BL21-DE3 (*hsdS,gal,λcIt$_s$ 857ind1 sam7ninSlacUV5T7gene1*)

Figure 2.1 Restriction MAP of pREP1 (Maundrell, 1993)

2.4 MATERIALS

2.4.1 Chemicals

All chemicals were purchased from Sigma or BDH unless otherwise stated. Media reagents were supplied by Difco.

2.4.2 Media

The *E. coli* strain JA226 was maintained on Luria-Bertani (LB) medium (10 g/l bactotryptone, 10 g/l NaCl and 5 g/l yeast extract). Transformants were selected and maintained on LB with 100 μg/ml ampicillin.

Yeast cells were maintained on yeast extract (YE) (5 g/l yeast extract and 30 g/l glucose) or Edinburgh minimal medium with phthalate (EMMp) (20 g/l glucose, 5 g/l NH_4Cl, 2.2 g/l Na_2HPO_4 and 3 g/l phthalic acid) supplemented with 10,000X minerals stock, 1000X vitamins stock (Alfa *et al.*, 1993) and 75 μg/ml adenine, leucine or uracil as required. Solid media was made with the addition of 20 g/l agar. Repression of transcription from the *nmt1* promoter (Maundrell, 1990; Maundrell, 1993) was achieved by the addition of 4 μg/ml thiamine.

2.4.3 Plasmids

The plasmid listed in table 2.2 were used for subcloning the MAPs into one of the pREP series of vectors . For expression in yeast, the vectors pREP1vectors carrying the inducible *nmt1* promoter were used (Basi *et al.*, 1992; Maundrell, 1993).

2.4.4 PCR Primers

Oligonucleotides (Table 2.3) were synthesised by PE-Applied Biosystems UK

nmt1	5' atg tgc agc gaa act aaa acc 3'
nmt2	5' ata tgc ttg aat ggg gct tcc 3'

Table 2.3 Oligonucleotides

2.5 PREPARATION AND MANIPULATION OF PLASMID DNA

2.5.1 Extraction of Plasmid from Bacteria

A single colony of transformed E. coli was inoculated into 10 mls of LB + ampicillin (100 μg/ml), and incubated overnight at 37^0C, 225rpm. 1-3 mls of the overnight culture was pelleted. The pellet was resuspended in P1, the Cell Resuspension Solution (50 mM glucose, 25 mM Tris-Cl, 10 mM EDTA, pH 8.0). The cells were lysed using the P2, Cell Lysis Solution (0.2N NaOH, 1% SDS), and the proteins precipitated by adding P3, the Neutralising Solution (1M Potassium Acetate, 3% acetic acid). This results in a floculant precipitate which is pelleted in a microfuge by centrifuging for 10 mins, 4^0C.

2.5.2 Phenol:Chloroform Extraction of DNA

Contaminating proteins were removed from solutions of DNA by extraction with an equal volume of phenol:chloroform (1:1) followed by phase separation at 13,000 rpm for 10 mins. Tris (pH 8.0) equilibrated phenol was purchased from Fisons.

2.5.3 Precipitation of DNA

DNA was precipitated from aqueous solution by the addition of 0.1 volume of 3 M sodium acetate pH 5.2 and 2 volumes of ice cold 100% ethanol, mixed and incubated at -20°C for 10 mins. Precipitated DNA was pelleted by centrifugation at 13,000 rpm for 10 mins, washed in 70% ethanol, air dried and dissolved in TE (10 mM Tris-HCl, pH 8.0, 1 mM EDTA) or sterile water.

2.5.4 Determination of Nucleic Acid Concentration

The concentration of nucleic acids in an aqueous solution was determined by spectrophotometry at 260 nm. An absorbance of 1.0 cm^{-1} was taken to be equivalent to 50 μg/ml DNA. The concentration of very small amounts of DNA was estimated by spotting 0.5 μl of the DNA solution onto a 1% (w/v) agarose plate containing 0.5 μg/ml ethidium bromide, and comparing the intensity of the fluorescence with that of known standards on a UV light box. The standards used were prepared from HindIII/EcoRI digested λ DNA.

2.5.5 Restriction Analysis

Restriction enzymes and the corresponding reaction buffers from New England Biolabs, and Gibco BRL were used in cloning and restriction analysis. All reactions were carried

out in the supplied buffers following manufacturers recommendations. To avoid the possibility of 'star activity' the glycerol concentration was adjusted such that it was never more than 8% (v/v) of the total reaction volume.

2.5.6 Agarose Gel Electrophoresis

DNA was size-fractionated through SeaKem GTG agarose (Flowgen Ltd) using a horizontal submerged minigel apparatus (Pharmacia). Gels were made with 0.7 - 2.0% (w/v) agarose in 1X TBE buffer (9 mM Tris-borate, 0.1 mM EDTA) containing 10 ng/ml ethidium bromide added. DNA was mixed with 1/2 vol FOG loading buffer (15% (w/v) Ficoll 0.25% (w/v) Orange G) prior to loading. The gel was submerged in 1X TBE and electrophoresed at 8 Volts/cm. Lambda DNA (Boehringer Mannheim) cut with HindIII/HindIII.EcoRI or a 123 base pair ladder (Sigma), was used as DNA standard size markers . DNA was visualised by illumination with medium wave (302 nm) ultraviolet light.

2.5.7 Blunt-ending DNA Fragments

Blunting the termini of DNA fragments by filling-in the recessed termini was performed using 5 units of Klenow enzyme (MBI Fermentas) 1X Klenow buffer (50 mM Tris-HCl, pH 8.0, 5 mM $MgCl_2$, 1 mM DTT) and 100 μM dNTPs in a final volume of 40 μl and incubating at room temperature for 15-20 mins

2.5.8 Dephosphorylation of Plasmid DNA

Following restriction digestion, vector DNA was routinely dephosphorylated using 2 units (per mg plasmid) of calf intestinal alkaline phosphatase (CIAP) (MBI Fermentas) (Sambrook *et al.*, 1989) added directly to the restriction digest. The DNA was incubated at 37°C for 30 mins and then electrophoresed through an agarose gel for purification.

2.5.9 Recovery of DNA Fragments from Agarose Gels

The required fragment was excised from the gel using a clean razor blade with minimum exposure to UV light. DNA was extracted from the agarose using the Geneclean Kit (Bio 101, Anachem.) following the recommended procedure.

2.5.10 Ligations

Ligations of vector and insert were performed using T4 ligase (MBI Fermentas) for both cohesive-end and blunt-end DNA. 10 ml reactions containing 5 units T4 ligase (10 u for blunt ends), 1X ligase buffer (40 mM Tris-HCl, 10 mM $MgCl_2$, 10 mM DTT, 0.5 mM ATP) and a vector to insert ratio of 1 to 5 were incubated at 16°C overnight.

2.5.11 Cloning in *E.coli*

2.5.11.1 Preparation of Competent Bacteria

Competent bacterial cells were prepared using the calcium chloride method (Sambrook *et al* 1989), and frozen at -70°C as 200 ml aliquots containing 30% (v/v) glycerol. For greater transformation efficiency a modified Hanahans Protocol was used. 20 ml SOB media (20 g/l tryptone, 5 g/l yeast extract, 0.5 g/l NaCl, 2.5 mM KCl and 10 mM $MgCl_2$)

was inoculated with a single colony from a freshly plated culture and incubated at 37°C for about 4 hrs until a density of A_{650}=4.5 was obtained. The bacteria were then chilled on ice for 15 mins before centrifugation at 3,500 rpm at 4°C for 10 mins. The pellet was washed once in ice cold TFB (10 mM MES pH 6.2, 100 mM KCl, 45 mM $MnCl_2$, 10 mM $CaCl_2$, 3 mM hexamine cobalt chloride) and centrifuged again at 3,500 rpm, 4°C. The pellet from this second spin was resuspend in 1.6 mls cold TFB supplemented with 50 ml of DTT (2.25 M Dithiothreitol in 40 mM potassium acetate, pH 6.0) and incubated on ice for 5 mins. 50 ml DMSO (Sigma) were added and the cells were mixed gently and left on ice for a further 10 mins. Finally, a second aliquot of 50 ml DTT was added, the cells were mixed gently and incubated for at least 5 mins on ice. At this point the cells were transformed directly or frozen in glycerol as with the calcium chloride method.

2.5.11.2 Transformation of Competent Bacteria

5 ml of ligation reaction were added to 200 ml of competent bacteria in a 6 ml Falcon tube (Becton Dickinson, 2063) and left on ice for 30 mins. The cells were heat shocked at 42°C for 90 secs and put on ice for 2 mins before recovery in 800 µl SOC (SOB with 20 mM Glucose) (prewarmed to room temperature) at 37°C for 1 hour. Transformants were selected on LB plates containing 100 µg/ml ampicillin overnight at 37°C. Control transformations were included in each experiment. These included a ligation reaction of vector alone to determine the background of vector religation; a transformation with 10 µl water (ie. "no DNA"control), and a transformation with 5 ng undigested pBluescript as a standard of the efficiency of the transformation in a particular experiment.

2.5.11.3 Amplification and Recovery of Plasmid DNA

Plasmid DNA was amplified by inoculating a single colony of *E.coli* containing the required plasmid into LB-broth with ampicillin and growing at 37°C with shaking at 250 rpm. To analyse ligation reaction products 2 ml cultures were grown for 4-5 hrs or overnight, cells were harvested from 1.5 ml of this culture and the pellet resuspended in 150 µl solution I (50 mM Tris/HCl, 10 mM EDTA, pH 8.0). The cells were lysed by the addition of an equal volume of solution II (200 mM NaOH, 1% SDS), and mixed by gentle inversion and kept at room temperature for 4-5 mins. This solution was neutralised by the addition of solution III (2.55 M KAc, pH 4.8) mixed immediately by gentle inversion. An equal volume of phenol-chloroform was added directly to this viscous solution, mixed well and microfuged 1300 rpm for 10 mins. The precipitate of SDS, proteins and genomic DNA collects at the aqueous interface. The extracted plasmid DNA was recovered from the aqueous phase by ethanol precipitation at -20°C and dissolved in water with 50 µg/ml RNase A.

Plasmid DNA to be sequenced was prepared using a Qiagen mini-prep kit. This system follows a similar protocol to that above but the plasmid DNA is purified from the cell lysate using an anion-exchange resin resulting in a purer DNA sample that yields higher quality sequence data. For large scale preparations of plasmid DNA 100-400 ml cultures were grown overnight and the plasmid extracted using the Qiagen Midi or Maxi-Prep Kit (Qiagen Ltd.).

2.5.12 Preparation of Yeast Genomic DNA

The required yeast strain was inoculated into 30 ml of the appropriate medium and grown overnight at 25°C, 30°C or 36°C (as specified), with shaking at 160 rpm, until saturation. Cells were harvested by centrifugation at 2,500 rpm for 5 mins, and protoplasted by resuspension in 1.5 ml of solution SP1 (1.2 M D-sorbitol, 50 mM sodium citrate, 50 mM sodium phosphate, 40 mM EDTA) containing 3 mg of Zymolyase, and incubation at 37°C for approximately 20 mins with occasional shaking. To stop the digestion the cells were centrifuged and carefully resuspended in 500 µl 5X TE, then lysed by the addition of 50 µl of 10% SDS, and incubation at 65°C for 20 mins. 200 µl of 5M potassium acetate was added and the solution was incubated on ice for 30 mins. The solution was then microfuged at 13,000 rpm for 5 mins at room temperature, and the supernatant collected and extracted with 400 µl of phenol:chloroform. Following ethanol precipitation the DNA was resuspended in 300 µl TE overnight. Contaminating RNA was removed by incubation at 37°C for 1 hour with 50 ng RNase A. The DNA was precipitated with 500 µl isopropanol, and resuspended in 100 µl TE. The concentration and quality of the DNA was estimated by running 5 µl on a 0.7% agarose gel.

2.5.13 Polymerase Chain Reaction

Polymerase chain reactions (PCRs) were performed on 2-10 ng of template DNA in 50 µl volumes in the presence of 10 pmoles of each primer, 400 µM each deoxyribonucleic acid (Pharmacia), 2 mM $MgSO_4$, vent buffer (10 mM KCl, 10 mM, $(NH_4)_2SO_4$, 20 mM Tris-HCl (pH 8.8), 2 mM $MgSO_4$, 0.1% Triton X-100) and 1 unit of vent polymerase (New England Biolabs Ltd.). The reaction was denatured at 95°C for 2 mins prior to the addition of the polymerase and start of the cycles. In general reaction conditions used a

denaturation stage of 95°C for 30 secs; an annealing temperature 5-10 degrees below the estimated melting temperature (T_m) of the primers (where T_m =4(G+C) + 2(A+T)) (Suggs *et al*, 1981) for 30 secs, and an extension stage at 72°C for 30-60 secs for 30 cycles, followed by a final extension at 72°C for 10 mins.

2.6 PREPARATION AND ANALYSIS OF PROTEINS

2.6.1 Extraction of Protein from *S. pombe*

Proteins were extracted from fission yeast using a method modified from Booher *et al* (1989). 50 ml yeast cultures were grown to a cell density of 1 x 10^7 at 29°C. The cells were harvested by centrifugation at 2,500 rpm at 4°C for 3 mins and the pellet washed once in 10 ml PBS (Phosphate Buffered Saline; 137 mM NaCl, 3 mM KCl, 8 mM Na_2HPO_4, 1 mM KH_2PO_4, pH 7.4), then once in 1 ml of PBS before resuspending in 250 µl freshly prepared extraction buffer (25 mM Tris, 80 mM ß-glycerophoshate, 15 mM *p*-nitrophenylphosphate, 20 mM EGTA, 15 mM $MgCl_2$, 1 mM DTT, 0.1 mM NaF, 0.1% Nonidet P-40, 1 mM PMSF (phenylmethylsulphonyl fluoride) and 10 µg/ml each of leupeptin, aprotinin, and pepstatin). To break open the cells an equal volume of ice cold 500 µm acid washed glass beads (Sigma) were added to the cell pellet. This mixture was then vortexed vigorously for 30 secs at 30 second intervals on ice for 6 mins. The resulting slurry was centrifuged at 13,000 rpm at 4°C, for 2 mins, and the supernatant collected. Protein concentration determined using the Bradford protein assay (Biorad).

2.6.2 Sodium Dodecyl Sulphate-Polyacrylamide Gel Electrophoresis (SDS-PAGE)

Discontinuous SDS-PAGE was performed using resolving gels of 7% acrylamide overlaid with a 5% stacking gel. A 30% (w/v) acrylamide stock was used (Acrylamide : Bisacrylamide, 37.5 : 1). The resolving gel contained 400 mM Tris-HCl, pH 8.8 and 0.1% SDS (v/v), which was mixed prior to the addition of 0.1% (v/v) N,N,N',N'-tetramethylethylenediamine (TEMED, Sigma) and 0.05% (w/v) ammonium persulphate for polymerization. The stacking gel was prepared in the same way and contained 100 mM Tris-HCl, pH 6.8, 0.1% SDS, 0.2% TEMED and 0.4% ammonium persulphate. Protein samples were prepared in 1X sample loading buffer (50 mM Tris-HCl, 100 mM DTT, 2% SDS, 0.1% bromophenol blue, 10% Glycerol, pH) and boiled for 5 mins. Electrophoresis was performed using the Mighty Small electrophoresis system (Hoeffer) with protein electrophoresis buffer (25 mM Tris-HCl, 200 mM glycine, 0.1% SDS). Gels were run at 25-50 volts. High molecular weight markers (Sigma 6H) were used as standards.

2.6.3 Analysis of Proteins by Coomassie Staining

Following electrophoresis, proteins on a SDS-PAGE gels were fixed and the protein visualised by emersion in 0.25% (w/v Coomassie Brilliant Blue R250 (Sigma), 50% (v/v) methanol, 10% (v/v) acetic acid at room temperature with gentle agitation overnight. The stain was then removed and the gel destained with successive washes in destain (35% (v/v) methanol, 12% (v/v) acetic acid) until the background was clear.

2.6.4 Analysis of Proteins by Immunoblotting.

Following SDS-PAGE, proteins were transferred to immobilon-P (Millipore) membrane, which was permeablised by treatment with methanol prior to use. Transfer was for 16 hrs at 10 volts when using the BIORAD wet electroblotting system, or for 1 hour at 25 mA when using a Millipore Semi-dry system. Transfer buffer was the same for both systems (12.5 Tris, 96 mM glycine and 0.01% (w/v) SDS, pH). Methanol was omitted from the transfer buffer to aid the transfer of large proteins. Following transfer the membrane was incubated for 1 hour in PBS containing 2% (w/v) dry milk powder, washed 10 mins with PBST (PBS with 0.2% (v/v) Tween 20) and incubated overnight at 4°C with the primary antibody (see Table 2.4 for the details of the antibodies used), diluted in PBST containing 2% (w/v) dry milk powder and 0.01% (w/v) sodium azide. The filter was then washed 3 times for 10 mins in PBST before incubating for 1.5 hrs at 4%C with the appropriate secondary antibody (Table 2.3), diluted 1:100 in PBST/2% (w/v) dry milk powder (Marvel). Finally, the blots were washed 2 times for 15 mins in PBST before detection with ECL chemiluminescent reagents (Amersham).

Table 2.4 Antibodies used for Immunoblotting

Antibody	**Type**	**Origin**	**Dilution**	**Source**
TP70	polyclonal	anti-rabbit	1/10000	J-M. Gallo
α-MAP2	polyclonal	anti-rabbit	1/20	A. Matus
MPM1	polyclonal	anti-rabbit	1/1000	J.C. Bulinski
Goat α-rabbit IgG	horseradish peroxidase conjugated		1/100	Sigma

Rabbit α-	horseradish	1/100	Sigma
mouse IgG	peroxidase		
	conjugated		

2.7 YEAST CELL BIOLOGY

2.7.1 General

2.7.1.1 Re-Isolation of Yeast Strains

Yeast strains were stored on glycerol at -70°C and were re-isolated by patching a small amount of the frozen glycerol stock onto a YE plate and incubating at 25°C for 3-4 days. The yeast were then streaked to single colonies on a YE plate and incubated for a further 2 days before replica plating onto YE with 20 μg/ml phloxin B (Magdala red) at 25°C to test ploidy; YE with phloxin at 36°C to test for a *cdc* phenotype and onto MM without the appropriate supplement to determine auxotrophy where applicable. Single colonies with the correct phenotype were maintained on solid media for use in this study.

2.7.1.2 Mating Type Testing

The mating type of strains isolated in this study were determined by mating with test strains of known phenotype as described in Alfa *et al.* (1993).

2.7.2 Yeast Transformation

2.7.2.1 The Alkaline Cation Method

The lithium acetate protocol was used for all routine transformations. The method described in Alfa *et al* (1993) was followed with the only exception being the use of YE or MM media rather than MB.

2.7.2.2 Electroporation

100 ml cultures were grown in minimal medium (diploids were grown in YE) to a density of A_{595}=0.5. Cells were harvested and washed 3 times in 10 ml of ice cold 1.2 M sorbitol. Finally, the cells were resuspended in 1.2 M sorbitol to give a final cell density of 10^9 cells/ml. Keeping the cells on ice, 0.5 μg of DNA was mixed with 100 μl of cells and dispensed into a prechilled 0.2 cm BIORAD gene pulsar cuvette. An electric pulse was applied to the cells at a setting of 1.6 kV, 25 μF and 200 ohms. 800 μl of 1.2 M sorbitol was added and 100-200 μl aliquots of this cell suspension were plated onto selective minimal medium. Plates were incubated at 25°C or 29°C for 6-7 days.

2.7.3 Yeast Classical Genetics

2.7.3.1 Tetrad Analysis

Tetrads were dissected from a 2 day old mating mix or from isolated diploid strains sporulated on minimal medium (MM or ME). YE medium with adenine (YEA) plates were carefully prepared ensuring a flat even surface. Using a sterile tooth pick a colony of sporulating diploids was streaked thinly, in a straight line down the left hand side of the

plate. A micromanipulator (Singer Instruments) was used to dissect 10-20 asci from vegetative cells, and position them 6 mm apart in a line perpendicular to the initial streak. The plate was then incubated at 19°C, 25°C or 30°C for 5-24 hours to allow the asci walls to break down and the spores to be released. The spores from each ascus were dissected 6 mm apart in a straight line and the plate was incubated at 25°C for 3-4 days. Spores from each tetrad were scored for viability and auxotrophy.

2.7.3.2 Random Spore Analysis

A sterile tooth pick was used to transfer a scraping of cells from the centre of a three day old mating mix into 1 ml of sterile water containing 0.5% (v/v) glusulase (Sigma). The cells were vortexed and incubated at 37°C over night to digest the walls of the vegetative cells and the asci. The spores were washed twice in sterile water and the spore concentration was estimated using a haemocytometer. 200 spores were plated onto YEA and the required selective media.

2.7.4 **Overexpression of** *MAPs*

Inserts containing a MAP was subcloned into the pREP1 vector (Maundrell, 1993) creating plasmid pRep1-MAP (Table 2.5 shows the multiple cloning sites of the pREP/pRIP series of vectors). pRep41-MAP was transformed into a *leu 1.32*$^{-}$ strain or the strains listed in table 2.1 by the lithium acetate procedure and transformants were selected on media containing 4 μM thiamine.

MAPs were overexpressed when the transformed strains were grown for more than 12 hours in medium without thiamine. A pre-culture of transformed cells were set up in

minimal medium containing thiamine and supplements overnight at 29^0C. Cells were washed three times in minimal medium without thiamine, and then suspended in medium with or without thiamine at a concentration of 1 X 10^5 cells/ml and grown at 36^0C, 29^0C and 20^0C. Cells were counted at intervals using a haemocytometer to measure cell growth in the presence or absence of MAPs.

Removal of thiamine from the medium turns on the nmt promoter of pREP1 (detailed in chapter 3). The 12-hour lag in the promoter being turned on is due to the presence of intracellular thiamine (Maundrell, 1990).

Table 2.5 Characteristics of the pREP and pRIP expression vectors(Maundrell, 1993)

Vector	**MCS**	**Marker**
pREP1/pRIP1	Nde1/ Sal1/BamH1/Sma1	LEU2
pREP2/pRIP2	Nde1/ Sal1/BamH1/Sma1	ura4+
pREP3/pRIP3	Bal1/Sal1/BamH1/Sma1	LEU2
pREP4/pRIP4	Bal1/Sal1/BamH1/Sma1	ura4+

2.8 CYTOLOGY

2.8.1 Staining of Nuclei with 4', 6-diamino-2-phenylindole (DAPI)

A 1 ml sample of a cell culture was washed twice in PEM (100 mM PIPES, pH 6.9, 1 mM EGTA, 1 mM $MgSO_4$), and then the pellet was resuspended in a further 50-100 μl of

PEM. 5 µl of this cell suspension was spread onto a microscope slide and dried for 30 secs on a hot block. A 2.5 µl drop of mounting medium (50% (v/v) glycerol, 1 ng/µl DAPI, 1 µg/µl *p*-phenylenediamine (antifade) was placed on to the cells. A coverslip was applied with slight pressure and sealed with nail varnish.

2.8.2 Localisation of Microtubules (Methanol Fixation Method) and MAPs

Microtubules were localised using the Methanol fixation Method. Cells in early log phase (approx 2 X 10^6 cells/ml) were rapidly filtered through a chilled 2.5 cm Millipore membrane disc using a Buchner flask fitted with a Whatman filter apparatus. Cells from the filter paper were carefully washed and suspended in methanol previously chilled to -20^{0}C. Cells were further left for exactly 8 mins in methanol at -20^{0}C, then washed three times with 10 mls PEM. The cell walls were then digested by resuspending the cells in PEMS containing 1mg/ml Lysing enzyme (sigma) and 0.3 mg/ml zymolase 20T, at a concentration of 5 X 10^7- 1 X 10^8 cells/ml, and incubating at 37^{0}C till 10% of the cells have lost their walls (within 5-15 mins). After washing immediately with PEMS to remove the enzymes, the cells were incubated for 30 mins PEMBAL. The samples were then aliquoted into Eppendorf tubes, centrifuged (3000 rpm, 3 mins), and the pellet resuspended in 50-100µl of the appropriate concentration of primary antibody (table 2.6). The samples were incubated overnight at room temperature. The following day, the samples were washed three times in PEMBAL, and incubated 8 hours in the dark in a rotary invertor with 50 µl 1in 50 dilution of rhodamine or fluorescein conjugated secondary antibody. The secondary antibody was then washed off with PEMBAL, and the cells

resuspended to a concentration of approx. 3 X 10^7cells/ml in PEMBAL. 50 µl of cells were applied to round 13mm poly-lysine coated cover slips and dried using a hairdryer. Each coverslip was inverted into 2 µl of mounting medium (10 µl of DAPI/antifade and 90 µl elvanol or 50% glycerol), and sealed using nailpolish. The cells were viewed under a fluorescence microscope.

Table 2.5 Antibodies used in Immunofluorescence

Antibody	**Type**	**Origin**	**Dilution**	**Source**
TP70	polyclonal	anti-rabbit	1/100	J-M. Gallo
α-MAP2	polyclonal	anti-rabbit	1/5	A. Matus
MPM1	polyclonal	anti-rabbit	1/100	J.C. Bulinski
Goat α-rabbit IgG	rhodamine conjugated		1/50	Sigma
Rabbit α-mouse IgG	rhodamine conjugated		1/50	Sigma

2.8.3 Localisation of Mitochondria

Cells in medium with and without thiamine were grown for approx. 24 hours, till they expressed the particular phenotype. The cells were then resuspended to a concentration of 2 X 10^6 cells/ml, in medium containing 500 nM mitotracker (Molecular Probes), the mitochondria-selective dye. The cells were further incubated with shaking for 30 minutes under growth conditions, then mounted on a coverslip and observed under a fluorescence microscope rhodamine filter.

2.8.4 Localisation of vacuoles

The vacuole staining dye, FM4-64 (Molecular Probes), was kept at a stock concentration of 80 μM in DMSO.

Cells were grown to exponential phase in medium with or without thiamine, then resuspended in medium containing 16 nM FM4-64, at a concentration of 1 X 10^6 cells/ml. Cells were incubated for 15-30 mis at optimum growth conditions, then washed three times in YES and observed under a fluorescence microscope (rhodamine channel).

2.8.5 Microscopy and Photography

Cells were viewed with a Zeiss photomicroscope II fitted with epifluorescence optics using a planachromat 63X 1.25 NA objective. DAPI and Calcofluor staining was viewed using the 48 77 02 filter set, and the rhodamine staining using the 48 77 12 filter set. Images were either photographed using Kodak T-MAX 400 ASA film developed according to the manufacturers instructions, and printed onto Rapitone P1-4 paper (Agfa), or transferred directly into an Improvision file using OpenLab computer software. The captured images were then printed using a Fotofun printer.

3. Cloning and expression of Tau, MAP2c and MAP4 in *Schizosaccharomyces pombe*

3.1 Introduction

3.1.1 Microtubules in *S. pombe*

The fission yeast *S. pombe* is an ascomyte that divides by binary fission. It is 3-4μm in diameter and 7-15 μm in length. It undergoes a typical eucaryotic cell cycle, and the length of the cell provides a convenient indicator of the cycle point.

Fission yeast microtubules are polymers of α- and β- tubulin (Yanagida, 1987). γ-tubulin, arranged in a ring as part of the microtubule organising centre, acts as a nucleating template for their polymerisation (Horio, 1994). There are two α-tubulin genes in fission yeast (*nda2* + and *atb1*+) (Adachi et al., 1986), a single β-tubulin gene (*nda3*+) (Hiraoka et al., 1984) and one gene encoding γ-tubulin gene (*gtb1*+/*tug1*+) (Horio et al., 1991).

Microtubules in *S. pombe* were first observed by electron microscopy by McCully and Robinow (1971). Hagan and Hyams (Hagan and Hyams, 1988) provided the first comprehensive data on the arrangement of microtubules through the fission yeast cell cycle using immunofluorescence microscopy.

As in other eucaryotes, cytoplasmic microtubules in fission yeast arise from MTOCs and extend between the ends of the cell at interphase. As the cell enters mitosis, the interphase microtubules depolymerise, and an intranuclear spindle is formed from the two spindle pole bodies (see chapter 1 for details). Following mitosis, cytoplasmic microtubules are re-instated from a pair of γ-tubulin containing MTOCs at the cell equator (Hagan and Hyams, 1988) (Horio et al., 1991). Although biochemically, the microtubules in fission yeast are similar to higher eucaryotes they are easier to study in *S. pombe* because (a) cells contain fewer microtubules whose organisation has been determined in great detail (Ding et al., 1993) and (b) there are conditional mutants of fission yeast that affect microtubule arrangement. Conditional mutants provide a way to directly compare the effect of the functional and mutant protein, without the danger of artifacts due to unknown secondary targets as is sometimes the case with drugs and other biochemical studies. Therefore *S. pombe* conditional mutants can be used as a valuable tool to study eucaryotic microtubule function.

3.1.1.1 Conditional microtubule mutants in S. pombe

Mutants of both the α-1 and β-tubulin gene, named *nda2*-KM52 and *nda3*-KM311 respectively, in *S. pombe* are lethal in the cold (20^0C), showing that both these genes are essential. Both show similar phenotypes which indicate some of the functions the microtubules perform in the cell. Some of these phenotypes include:

- nuclear division arrest at pro-metaphase, indicating that microtubules are essential for spindle formation, which in turn is essential for chromosome separation.

- nuclear displacement, which indicates that the location of the nucleus within the cell may be microtubule-dependant (Hagan and Yanagida, 1997)
- condensed chromosomes
- branching of cells, indicating that cell morphology and microtubule organisation have a close relationship
- failure to execute cytokinesis, which is evidence for the existence of a cytokinesis checkpoint that monitors spindle integrity (Fankhauser et al., 1993)

The α-2 tubulin mutant, *atb-2*, also show some of the above characteristics, notably the formation of branched cells. However deletion of this gene is not lethal, thereby indicating α-2 tubulin is not essential (Adachi et al., 1986). Morphogenetic mutants which have defective microtubule organisation also reveal more about the how and why microtubules influence cell shape. Some such mutants are *tea1* and *tea2* (Mata and Nurse, 1997), which result in T-shaped cells; *ban 3.2* (Verde et al., 1995) which is bent , and *mal3* (Beinhauer et al., 1997).

Microtubule mutants have also been isolated according to their resistance or sensitivity to tubulin inhibitors. *Ben* mutants, which which were identified as resistant to the benzimidazole compounds thiabendazole (TBZ) and benomyl, were mapped to the β-tubulin locus (Roy and Fantes, 1983). Other mutants mapped to this locus were supersensitive to TBZ or a combination of TBZ and cold. Mutants located to the *nda2* locus did not show any greater resistance or supersensitivity compared to the wild type strains. Another mutants, *ben4*, is resistant to benomyl but not TBZ, and is cold sensitive. *Ben4.C10* may provide clues to the interaction of the actin and microtubule

cytoskeletons as it is both resistant to benomyl and sensitive to actin gene dosage (Fantes, 1989).

3.1.2 *pombe* as a model organism for the study of heterologous gene expression

Fission yeast has many characteristics that make it an excellent model for the expression of eucaryotic genes. Although it is a relatively simple eucaryote, it shares many cellular properties with larger more complex organisms (Zhao and Lieberman, 1995). It has a short doubling time and can be easily manipulated in the laboratory (Moreno et al., 1991) (Alfa et al., 1993)

At the gene level, mammalian introns can be spliced in fission yeast (Kaufer et al., 1985) and endogenous introns can also be spliced when a component of the yeast spliceosome, U2 snRNa, is replaced by the human equivalent (Shuster and Guthrie, 1990). In addition, mammalian promoter and poly(A) signals are functional in *S. pombe* although not in *S. cerevisiae* (Russell, 1989). The conservation of gene activity between *S. pombe* and mammals was clearly demonstrated by the functional complementation of the fission yeast *cdc2.33* mutant by the human homologue (Lee, 1987). *S. pombe* can therefore provide a novel host system to investigate the structure, function and expression of eucaryotic genes, especially those of mammalian origin (Lee, 1987).

The differences between fission yeast and higher eucaryotes is often advantageous in making it the preferred organism for studying higher eucaryotic gene functions, as there will be no endogenous effect. Broker et. al (Broker et al., 1987) expressed active human antithrombin III in *S. pombe,* whilst Tournier et. al. (Tournier et al., 1996) expressed the human cyclin-dependant kinase inhibitor $p21^{cip1}$ in fission yeast in order to investigate its role in the cell cycle checkpoint pathway. Recently, mammalin proapoptotic genes of the Bcl-2 family, BAK and BAX, were expressed in *S. pombe* to further examine their function as regulators of apoptosis (Fraser and James, 1998). This chapter describes the expression of mammalian MAPs *S. pombe* in order to determine their role as unique probes of microtubule function in yeast.

3.1.3 Fission Yeast Vectors

3.1.3.1 General Features

The common features of *S. pombe* vectors are an autonomous replicating sequence (*ars*), a yeast selectable genetic marker, and unique restriction sites for cloning. Most are also shuttle vectors and contain a bacterial origin of replication (*ori*) and selectable marker such as an antibiotic resistance gene.

In *S. pombe*, autonomous replication sequences are defined as sequences which promote high-frequency transformation and yield mitotically unstable transformants containing unrearranged plasmid. The most commonly used *ars* in fission yeast is

derived from a 2μm circular plasmid of *S. cerevisiae*. However, these plasmids have a low copy number, and transmission through mitosis and meiosis is poor. Transmission frequency of *ars* and its *S. pombe* homologue, ars1, through mitosis and meiosis can be greatly improved by a *S. pombe* EcoR1 fragment called *stb*. Although it is not an *ars*, it increases copy number to about 100/cell and stabilises the plasmid by some unknown function (Russell, 1989). Transformation efficiency can also be increased by co-transforming an *ars* and *non-ars* plasmid together, resulting in co-polymerisation of the two plasmids. Lee and Nurse (1987) exploited this strategy in cloning a complementing human homologue of *cdc2+* by the co-transformation of a $cdc2^{ts}$ strain with a human cDNA library made in a non-*ars* plasmid together with an *ars* plasmid (Lee, 1987).

Selectable genetic markers are required in vectors so that cells having the DNA vectors could survive compared to cells without vectors for the particular genetic strain. This ensures that the selected cells/colonies have the required vector DNA. The most widely used selectable marker systems involve genes that complement *S. pombe* mutations which prevent growth in medium lacking leucine, *leu1.32,* due to lack of 3-isopropylmalate dehydrogenase, or uracil, *ura4-294, ura4-D6, ura4-D18 etc,* due to a mutant orotidine-5'-phosphate decarboxylase (Zhao and Lieberman, 1995). The *leu1-* mutants can be complemented by both fission yeast *leu1* and *S. cerevisiae* LEU2 genes, and *S. pombe ura4* and *S. cerevisiae* URA3 can similarly complement ura4 deficient strains. However LEU2 and URA3 are inefficiently expressed in fission yeast, and require multiple plasmid copies to compensate. (Russell, 1989)

3.1.3.2 Expression Vectors in S. pombe

The original general-purpose fission yeast cloning vectors such as pDB248X and YEp13 , LEU2.2μm/pBR322 containing vectors, had the disadvantage of being poorly transmitted through mitosis and meiosis, and were therefore often lost after a few generations. pFL20 contains *stb* and *ars* as well, and is mitotically more stable, and has high copy number. It is therefore useful for expression of foreign genes, and active human antithrombin III was expressed in pFL20 (Russell, 1989).

Most fission yeast vectors incorporate specific promoters to regulate cDNA expression. The *S. pombe adh* (alcohol dehydrogenase) gene promoter has been widely used, as the *adh* gene is highly expressed in *S. pombe*., and is constitutive in glucose- and glycerol/ethanol containing medium. The plasmids pEVP11 and pART1 contain the *adh* promoter. pSM1 encodes the simian virus 40 (SV40) early promoter. It is weaker than the adh promoter and is therefore useful when overexpression of a gene would be toxic to the cell.

The most common promoters for fission yeast expression vectors are *adh+* (constitutive high expression); *fbp+* (carbon source responsive); a tetraccycline-repressible system based on the CaMV promoter; and the *nmt+* (no message in thiamine) promoter, which is the most frequently used (Forsburg, 1993).

3.1.4 Some commonly used vectors are (Forsburg, 1993)

Vector	Promoter	Activity

pART1-lacZ	adh	constitutive,
pSM-lacZ	SV40 promoter	constitutive
pSLF101-lacZ	CamV promoter, Tet operator	
REP3X-lacZ	nmt1+ promoter	full strength
REP41X-lacZ	nmt+ promoter	weaker
REP81X-lacz	nmt+ promoter	weakest

3.1.5 The pREP/pRIP series of Vectors

The pREP is an extrachromosomally replicating plasmid and pRIP is an integrative expression plasmid containing the promoter and polyadenylation signal of the nmt+ gene of *S. pombe*. The difference between pREP and pRIP is that pREP contains the S. pombe *ars1* gene (origin of replication), and is therefore maintained extrachromosomally in high copy number. Each series of these vectors either contain the *S. Cerevisaie* LEU+ gene or the *S. pombe ura4+* gene as the selectable marker, combined with one of two alternative multiple cloning sites (Table 3.2) (Maundrell, 1993).

The *nmt1+* gene, on whose promoter these plasmids are based, is involved in thiamine biosynthesis. Therefore the *nmt1+* promoter is regulated by the levels of available thiamine. In minimal medium in the absence of any exogenous thiamine, the intracellular thiamine concentration is approximately 10pmol/10^7 cells,and the promoter is totally derepressed. When thiamine is added to the medium, this is

actively taken up by the cells and as the intracellular thiamine concentration rises rapidly, *nmt1*+ transcription being concurrently repressed. In three hours, *nmt1*+ mRNA is undetectable. If the cells are then washed and allowed to grow in thiamine-free medium, the internal thiamine concentration gets reduced by dilution as the cell mass doubles, and when the concentration falls to 50pmol/10^7 cells, *nmt1*+ mRNA transcription is re-installed. (Maundrell, 1993).

Highly expressed fission yeast promoters contain the TATA sequence, as in other metazoans, and the transcription start site (tsp), normally occurs in a tightly defined region 25-30 bp downstream. The *nmt1*+ promoter contains the sequence 5'-ATATATAAAlocated 25 bp upstream from the tsp. Basi et al (1993) made stepwise deletions in the TATA box and quantified the effects of the mutations by assaying the expression of the chloramphenicol acetyl-transferase (CAT)-encoding gene (cat) cloned downstream. The progressive truncation of the TATA box resulted in a concomitant decrease in promoter strength both in terms of CAT mRNA and CAT activity loss in the cell extracts. Both the levels of promoter induction, as well as residual expression levels in the presence of thiamine were decreased . However the tsp was unaffected. These mutations were used to construct weaker pREP vectors, the pREP41 and the pREP81(weakest) series. (Basi et al., 1993). (Maundrell, 1990).

3.2 Methods

3.2.1 Cloning of tau, MAP2c and MAP4 into pREP1

The longest human tau, with four repeats and an N-terminal 56 amino-acid insert, htau40, in the vector pRK172 (from M. Goedert), was initially subcloned into puc19 vector as an Nde1/EcoR1 fragment. Tau was then subcloned into pREP1 as an Nde1/BamH1 insert.

The rat three-repeat MAP2c (from A. Matus)was cloned into pREP1 by creating an Asc1 restriction site before the 'start' site of the MAP2c sequence, and before the Nde1 site in pREP1, using linkers. MAP2c was then subcloned directly into pREP1 as an Asc1/blunt ended fragment.

Human MAP4 in pGEM, the five-repeat isoform of MAP4 (from J.C. Bulinski), was initially subcloned into pBluescript as an spe1/Cla1 fragment. It was then subcloned onto pREP 1 as an Sal1/blunt fragment.

3.2.2 Expression of Tau, MAP2c and MAP4 in *S. pombe*

pREP1-tau, pREP1-MAP2c and pREP1-MAP4 were transformed into *S. pombe* *leu-1.32h-* strain using the lithium acetate method (described in chapter 2). The cells were harvested to detect the presence of the MAPs, by centrifugation. The cells were then broken in the presence of equal amounts of cold 500μm glass beads and an equal volume of lysis buffer (as described in chapter 2), in the rpesence of the following

protein inhibitors: 0.1mM phenylmethylsulfonyl fluoride, 20μg/ml leupeptin, 20μg/ml aprotinin, 20μg/ml pepstatin.

Expression of MAPs in *S. pombe* was determined by western blotting. The anti-tau antibody TP70 (a kind gift from J.M. Gallo) was used at a concentration of 1/10000 dilution to determine the expression of tau; the anti-MAP2 antibody (a kind gift from A. Matus) was used at a concentration of 1/20 to determine the expression of MAP2c; the anti-MAP4 antibody MHP1 (a kind gift from J. Bulinski), was used at a concentration of 1/1000 dilution to determine the presence of MAP4.

3.2.3 Growth of *S. pombe* expressing Tau, MAP2c and MAP4 in the presence of thiabendazole (TBZ)

Cells containing pREP1-tau, pREP1-MAP2c and pREP1-MAP4 were streaked on to minimal medium with and without thiamine and containing the microtubule destabilising agent thiabendazole at concentrations of 0, 5, 10, 20 and 40 μg/ml. The cells were then grown at 36^0C, 29^0C and 20^0C.

3.3 Results

3.3.1 Tau, MAP2c and MAP4 inhibited the growth of *S. pombe* in varying degrees

As an initial indicator of the effects of the expression of the heterologous MAPs on the microtubule cytoskeleton in fission yeast, the growth of cells transformed with the three plasmids was determined in the presence and absence of thiamine at 20, 29 and 36^0C.

Tau appeared to inhibit fission yeast growth at all three temperatures (fig 3.1). At all three temperatures, there was an initial lag period when the cells grew slowly both in the presence and absence of thiamine. This lag phase lasted for 20 hours at 36^0C and 29^0C (Fig. 3.1 a and b), and lasted up to 30 hours at 20^0C (fig. 3.1 c). The cells then entered log phase. The doubling time in log phase in the absence of thiamine increased by 77% at 36^0C, 60% at 29^0C, and 125% at 20^0C, compared to that in the presence of thiamine. At 36^0C, the cells reached stationary phase at approximately 30 hours. Cells expressing tau reached stationary phase at 2.2×10^7 cells/ml, compared to cells not expressing any MAP, which continued to grow to 3.5×10^7 cells/ml (Fig. 3.1 i). At 29^0C, between 21 and 30 hours, tau expressing cells grew at a slower rate than the controls, but after 30 hours, the rate of growth of both control and tau expressing cells were almost equal, judging from the slope of the graph (Fig. 3.1ii). At 20^0C, cells in the presence and absence of thiamine grew at almost identical rates upto 44 hours, then cells expressing tau grew much more slowly (Fig. 3.1iii) compared to the control.

MAP2c-pREP1 cells grew slower than tau-pREP1 cells even in the presence of thiamine. However, MAP2c also appeared to inhibit growth in the absence of thiamine (fig. 3.2.i,ii and iii). As with tau, there was an initial lag phase before the cells entered log phase. In cells carrying the MAP2c plasmid, doubling times

increased by 180% at 36^0C, 75% at 29^0C and 128% at 20^0C in the absence of thiamine in the log phase.

MAP4 also showed the growth inhibition trend seen in the other two MAPs, but less pronounced (fig. 3.3 i,ii and iii). As with tau, there was a lag phase of 20 hours at 36 and 29^0c and 30 hours at 20^0C, before the cells entered log phase. Doubling times at log phase increased by 12.5%, 83% and 33% at 36, 29 and 20^0C respectively in the absence of thiamine, compared to cells in the presence of thiamine under the same conditions. At 36^0C, the cells expressing MAP4 showed a slower in growth rate compared to the control cells. The growth rate then increased, but continued to be lower than the control, as judged by the slopes of the line graph (Fig. 3.3 i). At 29^0C, differences in growth rate between cells in the presence and absence of thiamine could be seen after 20 hours (Fig. 3.3 ii). However, the growth rates for both continued to be much slower than tau or MAP2c till 28 hours. After 30 hours, the slope became much steeper for both the control and MAP4 expressing cells, but the MAP4 expressing cells had a slightly smaller slope compared to the control. At 20^0C, cells overexpressing MAP4 began to show a slowdown in growth compared to the control (Fig. 3.3 iii). This difference increased as the control cells continued to show a faster growth rate, and this rate took a sharp incline at 72 hours. In contrast, the growth rate of MAP4-expressing cells continued to show a slow increase, thereby resulting in a progressively greater difference in growth rates between cells in the presence and absence of thiamine with increased time.

Figure 3.1 Tau inhibits fission yeast growth at three temperatures, 36^0C, 29^0C and 20^0C. Human htau40 was expressed in fission yeast under the control of the thiamine repressible promoter *nmt1*.

(i). Growth in the presence (open square) and absence (closed diamond) of thiamine at 36^0C.

(ii). Growth in the presence (open square) and absence (closed diamond) of thiamine at 29^0C

(iii). Growth in the presence (open square) and absence (closed diamond) of thiamine at 20^0C

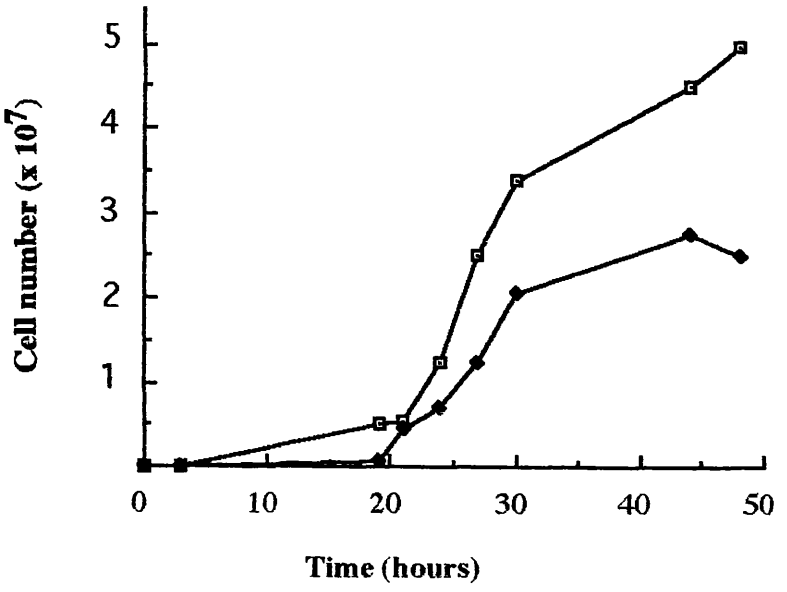
Cell number (x 10^7)
5
4
3
2
1
0
10
20
30
40
50
Time (hours)

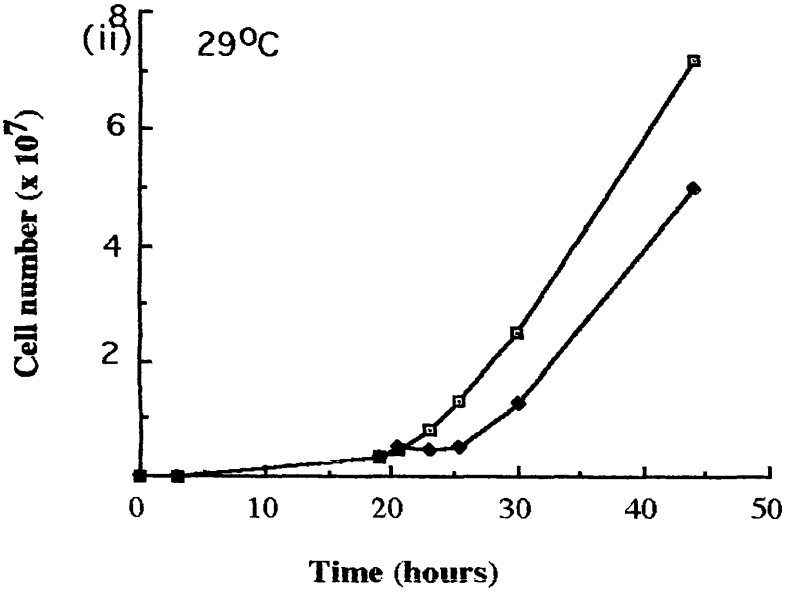
(ii)
29°C
Cell number (x 10^7)
8
6
4
2
0
10
20
30
40
50
Time (hours)

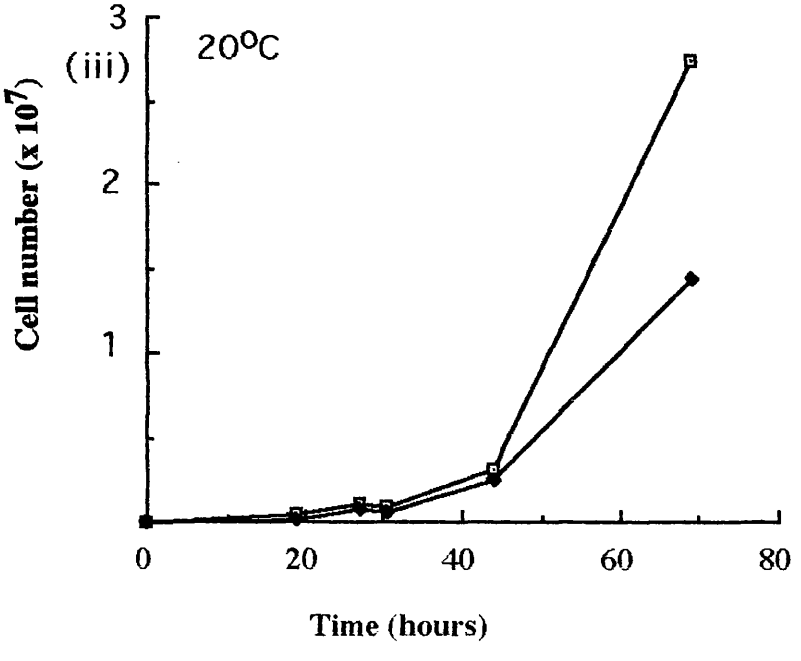
(iii)
20°C
Cell number (x 10^7)
3
2
1
0
20
40
60
80
Time (hours)

Figure 3.2 Rat MAP2c, expressed under the control of the thiamine repreessible nmt1 promoter, inhibits fission yeast growth at three temperatures, 36^0C, 29^0C and 20^0C.

(i). Growth in the presence (+T) and absence (-T) of thiamine at 36^0C.

(ii). Growth in the presence (+T) and absence (-T) of thiamine at 29^0C

(iii). Growth in the presence (+T) and absence (-T) of thiamine at 20^0C

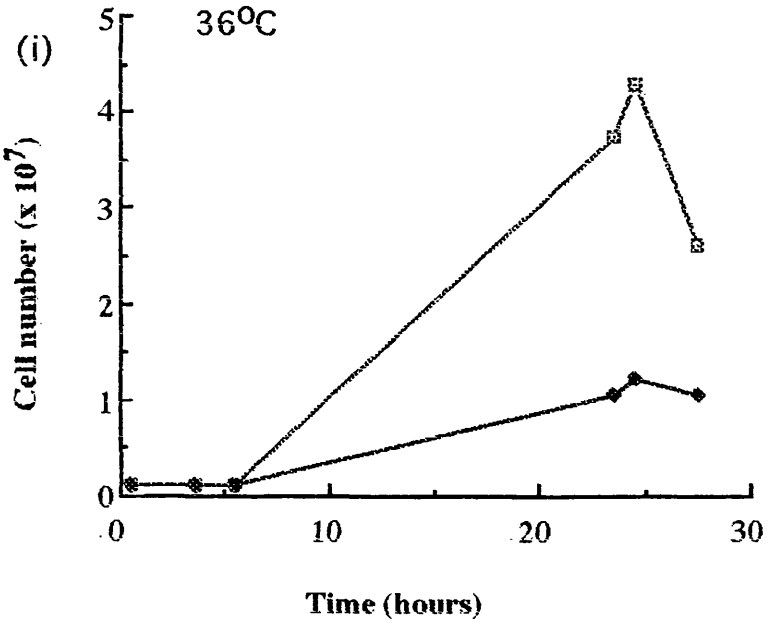
(i)
36°C
Cell number (x 10^7)
0
1
2
3
4
5
0
10
20
30
Time (hours)

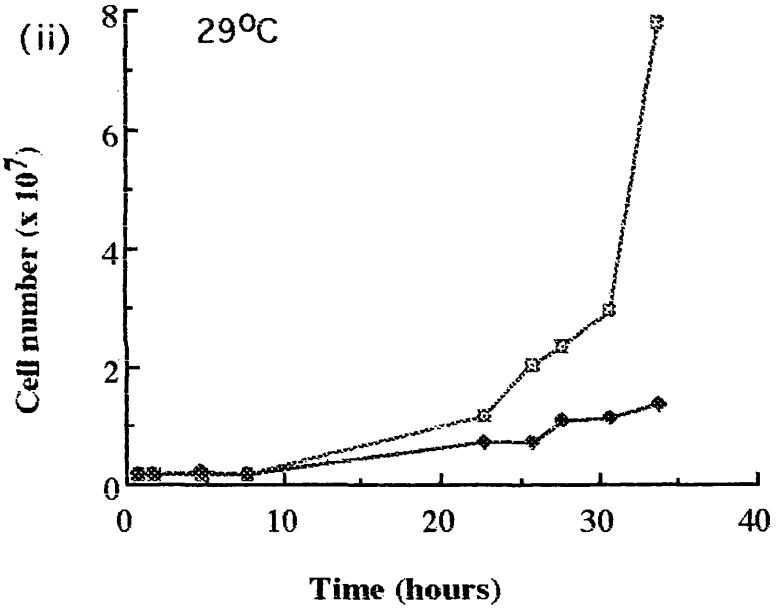
(ii)
29°C
Cell number (x 10^7)
0
2
4
6
8
0
10
20
30
40
Time (hours)

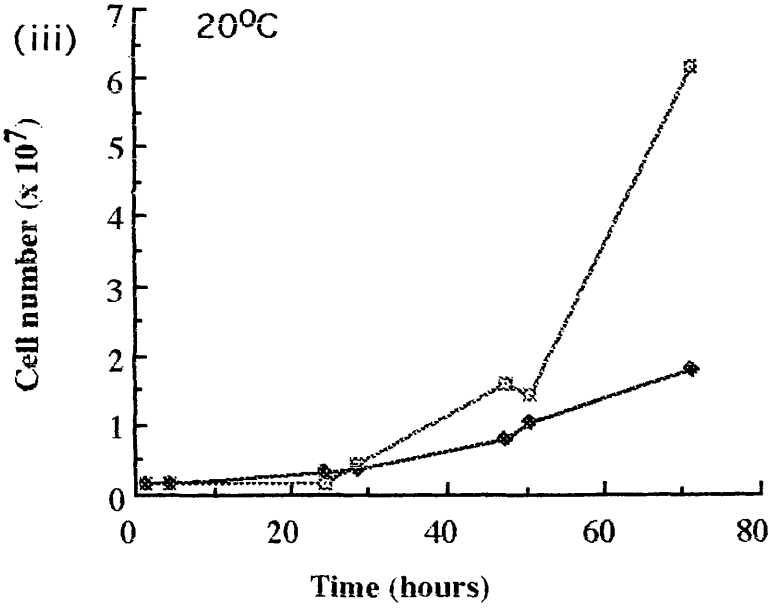
(iii)
20°C
Cell number (x 10^7)
0
1
2
3
4
5
6
7
0
20
40
60
80
Time (hours)

Figure 3.3. Human MAP4, expressed under the control of the thiamine repressible nmt1 promoter, inhibits fission yeast growth at three temperatures, 36^0C, 29^0C and 20^0C.

(i). Growth in the presence (open square) and absence (closed diamond) of thiamine at 36^0C.

(ii). Growth in the presence (open square) and absence (closed diamond) of thiamine at 29^0C

(iii). Growth in the presence (open square) and absence (closed diamond) of thiamine at 20^0C

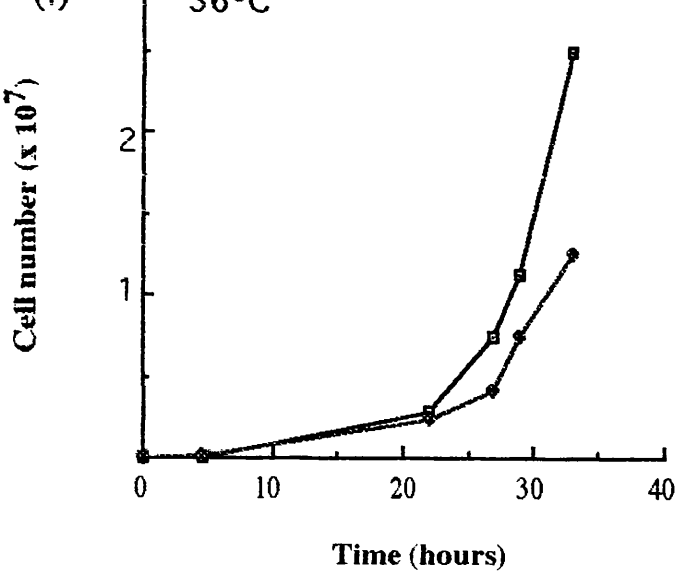
Cell number (x 10^7)
2
1
0
10
20
30
40
Time (hours)

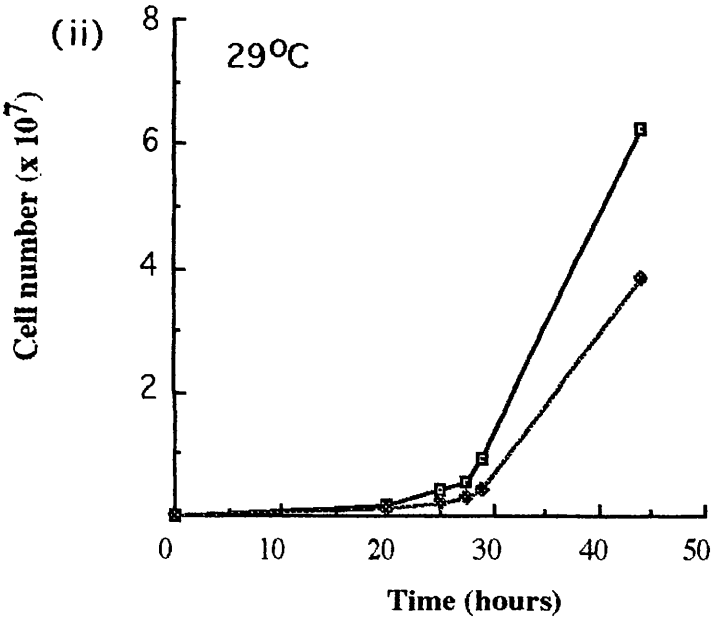
(ii)
29°C
Cell number (x 10^7)
8
6
4
2
0
10
20
30
40
50
Time (hours)

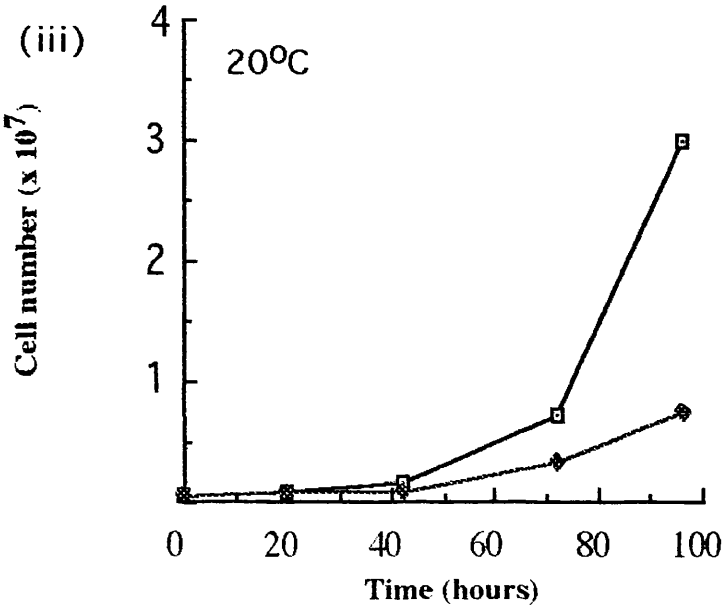
(iii)
20°C
Cell number (x 10^7)
4
3
2
1
0
20
40
60
80
100
Time (hours)

3.3.2 The expression of tau, MAP2c and MAP4 is confirmed by western blotting

To confirm that the inhibition of growth was due to the expression of MAPs, protein extracts were prepared from cells grown in the presence and absence of thiamine for approximately 36 hours, and immuno-blotted using anti-tau, anti-MAP2c and anti-MAP4 antibodies.

Blotting with anti-tau TP70 antibody revealed no expression of tau in the presence of thiamine (+T) and the expression of a 64kD protein corresponding to the molecular weight of tau in the absence of thiamine (-T) (figure 3.4 a).

Figure 3.4 b shows a western blot of a protein extract from cells expressing MAP2c with an anti-MAP2c antibody. No protein expression was detected in the presence of thiamine. In the absence of thiamine, a band at 70 kD, the molecular weight of MAP2c was detected after 36 hours. However the blot also revealed numerous lower molecular weight bands, suggesting the protein has been partially proteolysed. This was repeated a number of times, and the proteolysed bands were seen on every occassion despite the inclusion of protease inhibitors in the extraction solutions.

Figure 3.4c shows a western blot stained with the anti-MAP4 antibody, MHP1. The blot shows no protein expression in the presence of thiamine, but the appearance, in the absence of thiamine, of a band at 125kD, which is the actual molecular weight of

Figure 3.4 Western Blotting confirms that the MAPS tau, MAP2c and MAP4 have been expressed in the absence but not in the presence of thiaminein fission yeast

A. Western blotting using the polyclonal anti-tau antibody TP70 reveals a 64kD band in the absence of thiamine.

B. Western Blotting using anti-MAP2c polyclonal antiserum reveals a band at 70kD, corresponding to the molecular weight of MAP2c on an SDFS-page gel, as well many smaller bands which suggest partial proteolysis of the protein.

C. Western Blotting using the polyclonal anti-MAP4 antibody MHP-1 reveals a 125kD band, corresponding to the actual moecular weight of MAP4, in the absence of thiamine.

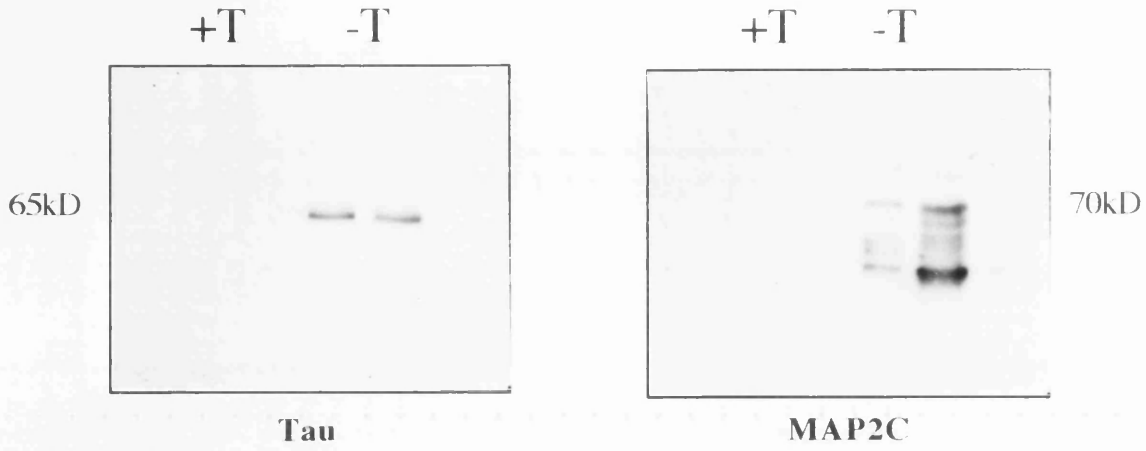
+T
-T
65kD
+T
-T
70kD
Tau
MAP2C

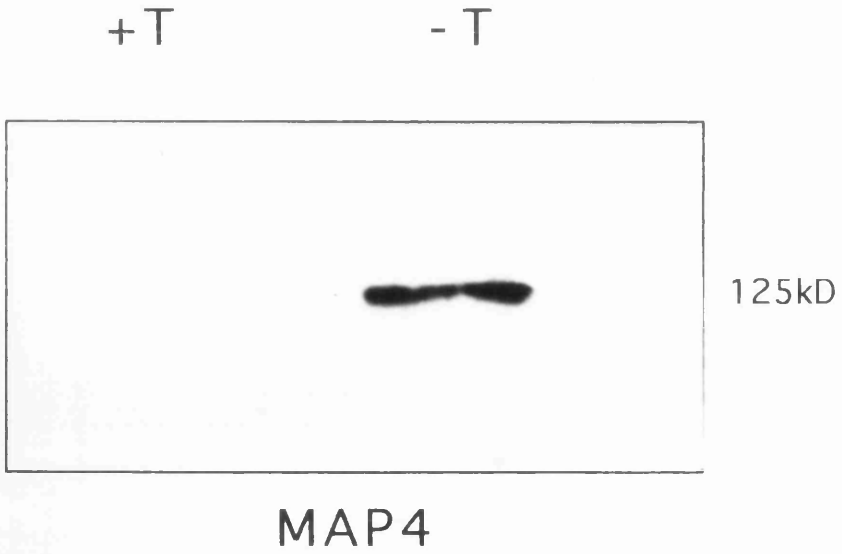
+T
- T
125kD
MAP4

MAP4 from its amino acid sequence, but not the expected value from gel electrophoresis (Bulinski, 1994)

3.3.3 Tau, MAP2c and MAP4 have different morphological effects on *S. pombe*

Growing cells expressing pREP plasmids containing a MAP insert in the absence of thiamine showed not only an inhibition of growth, but also morphological changes compared to cells grown in the presence of thiamine or cells containing pREP1 only (without any MAP cDNA insert). Cells expressing each MAP showed distinct morphologies (Fig. 3.5)

In the absence of any MAP expression, wild type cells, containing only the empty pREP vector, appeared as cylindrical cells 6-14μm long (Fig. 3.5a)

The majority of cells expressing tau looked normal. After 28-30 hours in the absence of thiamine, 1-2% of cells showed branching (as seen in fig. 3.5 b) , another 1% was 2-3 times longer than average, usually with multiple septa (seen in fig. 3.5 b).

Cells expressing MAP2c for 28-30 hours generally appeared longer than controls (Fig. 3.5c), and more than 25% of cells had a 'bulbous' shape either at the end or in the centre of the cell. Like tau, 1-2% of cells also exhibited the branching or 'T-phenotype' (not shown).

Figure 3.5 Overexpression of tau, MAP2c and MAP4 in *S. pombe* results in different morphologies in the yeast.

A. Fission yeast cells in the absence of MAPs, containing pREP only, grown in the absence of thiamine for 30 hours.

B. Fission yeast cells containing pREP1-tau, grown in the absence of thiamine for 30 hours. Cells are either similar to the controls, or long with multiple septa, or branched.

C. Fission yeast cells containing pREP1-MAP2c, grown in the absence of thiamine for 30 hours. Cells are long, bent, and some have a 'bulbous' end.

D. Fission yeast cells containing the plasmid pREP1-MAP4, grown in the absence of thiamine.

Bar 10 μm

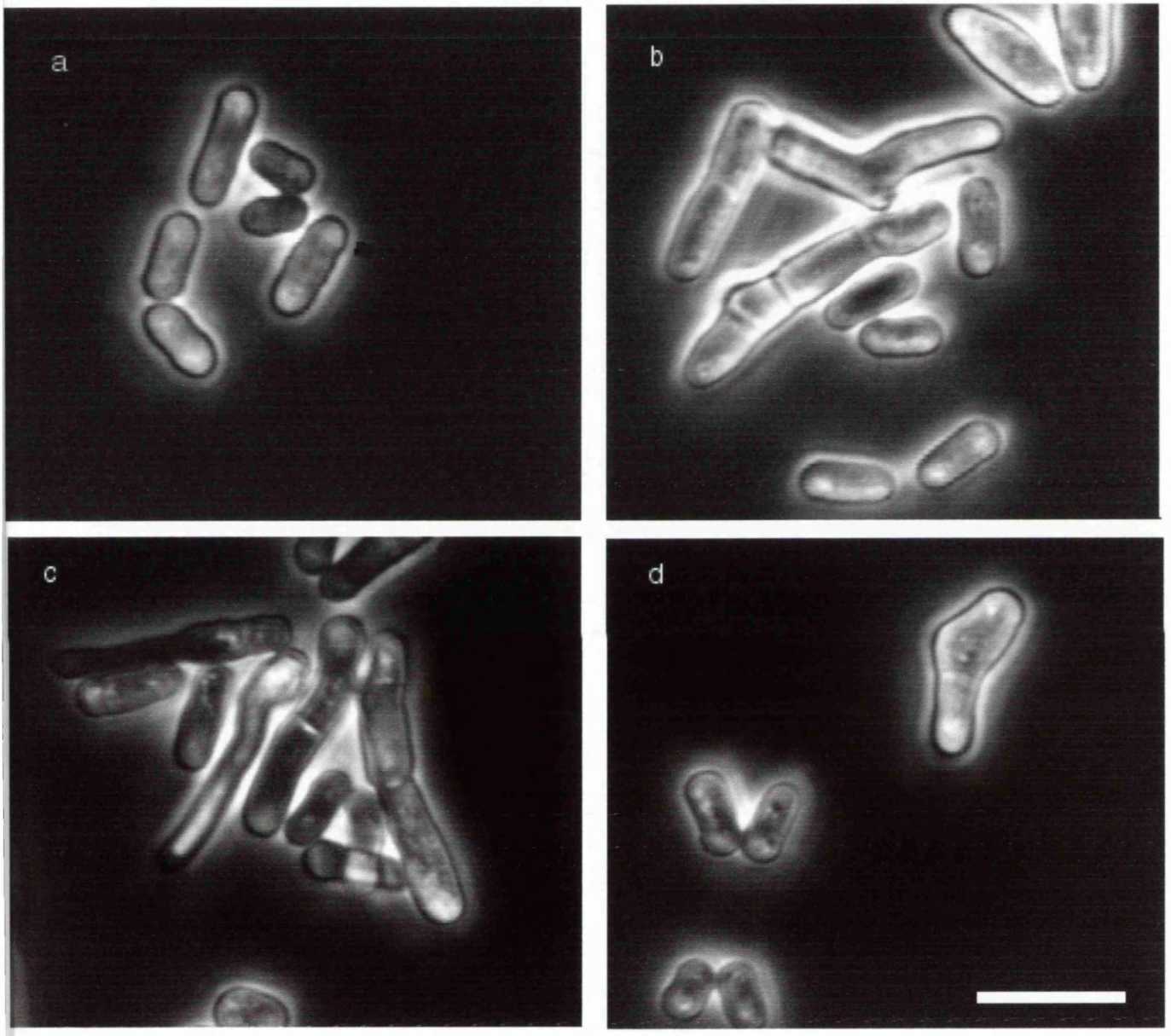
a
b
c
d

MAP4 expressing cells did not appear to increase in length. However more than 30% of cells appeared bent after 28-30 hours in the absence of thiamine (Fig. 3.5 d). Up to 5% of these cells also appeared hammer-shaped (not shown).

3.3.4 Tau, MAP2c and MAP4 show variations in cell length in *S. pombe*

As seen in Fig. 3.5, some cells expressing MAPs appeared longer. Cell length was therefore measured, of 30 or more of each category of cells expressing tau, MAP2c and MAP4 for 30 hours (at late log phase), to determine whether there was variation in distribution of cell length due to the effects of the different MAPs. It appeared that the expression of tau and MAP2c did indeed result in a significant number of cells growing longer (Fig. 3.6). Control cells containing only the pREP vector did not exceed 16m in length, and 96% of the cells were 6-15μm in length. Similar results were obtained from the lengths of cells expressing MAP4, with 95% of cells ranging from 4-15μm, and 5% of cells in the range of 15-25μm. The cell lengths of cells expressing tau showed a wider distribution. While the majority of tau expressing cells (81%) were of the 'normal' range of 6-15μm, 8% were 15-25μm long, and 11% were even longer, in the range of 25-35μm. No wild type cells of this length were detected. It is MAP2c, however, that appears to have the most potent effect on cell length. Only 56% of cells are of the normal 6-15μm size range, but the large minority, 44% were longer. 5% of MAP2c expressing cells were as long as 35-45μm (3-4 times longer than the average wild type cell), longer than cells in any of the other categories. 34 % of MAP2c expressing cells were 15-25μm long, compared to only 4-5% for control and MAP4

3.6 Overexpression of tau, MAP2c and MAP4 result in variation in cell length in *S. pombe*. Fission yeast cells not expressing any MAP (control), expressing tau, MAP2c and MAP4, were grown in the absence of thiamine for 30 hours. The length of cells were then measured for at least 40 cells expressing each MAP. As cell length varied over a wide range, the number of cells within a range were expressed as a percentage of total number of cells measured. The length of MAP4 expressing cells showed variations similar to the control, and none were longer than 16μM. Both tau and MAP2c showed longer cells upto 35μM long. Only MAP2c showed cells as long as 40μM.

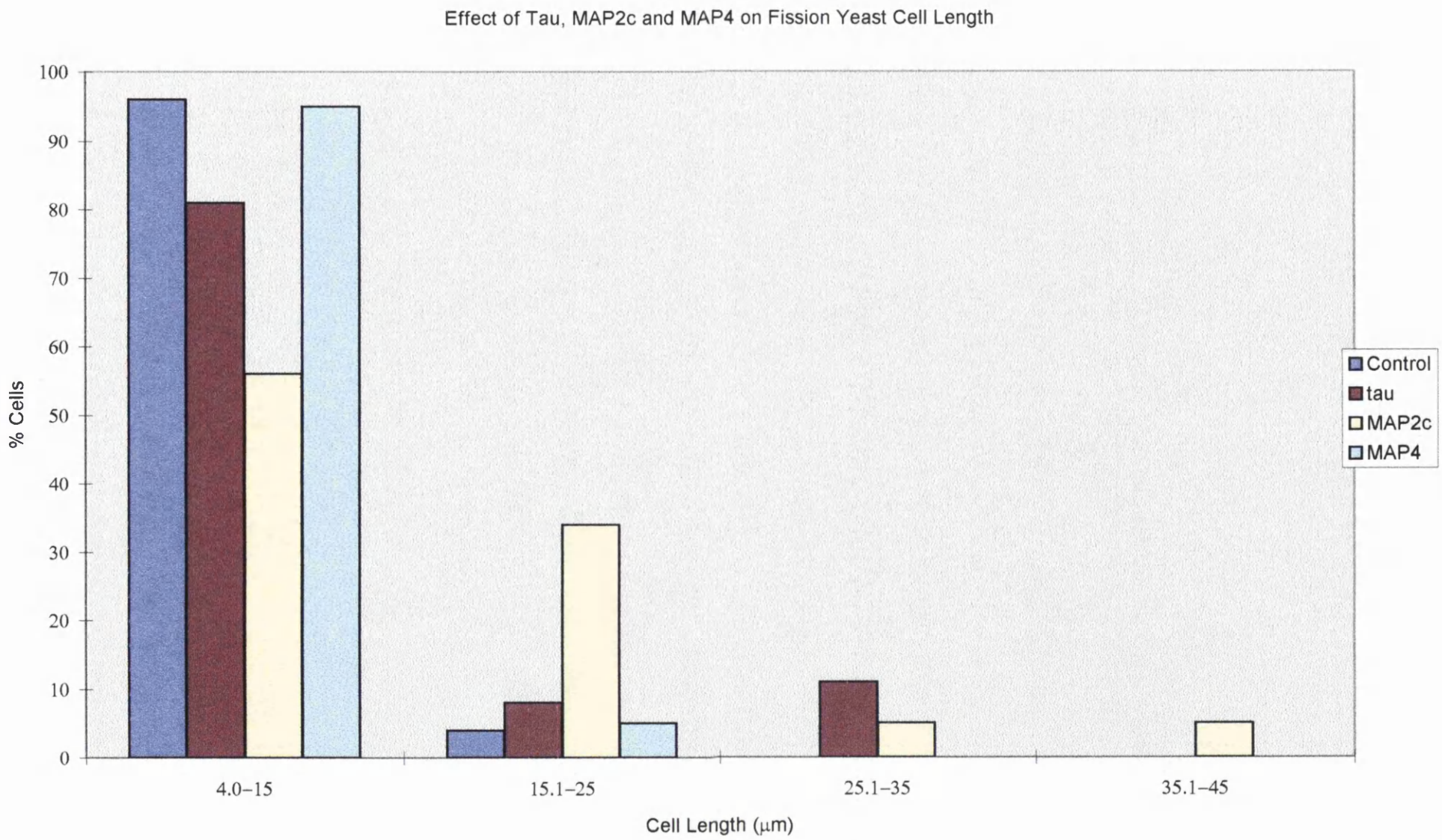
Effect of Tau, MAP2c and MAP4 on Fission Yeast Cell Length
100
90
80
70
60
50
40
30
20
10
0
% Cells
4.0–15
15.1–25
25.1–35
35.1–45
Cell Length (μm)
Control
tau
MAP2c
MAP4

expressing cells, and 8% of tau expressing cells. Another 5% of cells expressing MAP2c were 25-35μm long, while 11% of cells expressing tau were in this size range.

3.3.5 MAP2c but not tau slows entry into mitosis for G2-arrested cells

Cell length in fission yeast is usually an indicator of its phase in the cell cycle. Since a significant number of cells expressing tau and MAP2c showed a significant increase in length compared to the controls, these two MAPs could affect the entry of fission yeast cells into mitosis. We therefore investigated whether the MAPs tau and MAP2c interfere with the progression of cells in G2 phase. Temperature-sensitive *cdc25.11* cells expressing tau or MAP2c or containing only the pREP1 plasmid, were grown in medium without thiamine to express MAP for 24 hours, then blocked at G2 by shifting to the restrictive temperature (36^0C). On shifting the cells back to permissive temperature (25^0C), MAP2c cells showed peak septation 40 min later than the control, while tau cells showed peak septation 40 minutes earlier compared to the control (fig. 3.3.5). These results indicate that tau and MAP2c may affect the cell cycle in different ways.

3.3.6 Tau, MAP2c and MAP4 does not rescue the cold sensitivity of *nda2* and *nda3*

As MAPs are generally believed to stabilise microtubules, the MAPS tau, MAP2c and MAP4 were expressed in the fission yeast tubulin cold-sensitive mutants *nda2* and *nda3* at the restricitve temperature, 20^0C, to determine whether the MAPs would have

Figure 3.7 MAP2c but not tau slow down the exit of cdc25 cells from G2. *cdc25.211* cells containing pREP1 alone, pREP1-tau and pREP1-MAP2c were grown at 25 ^{0}C for 24 hours in the absence of thiamine. The cells were then shifted to 36^{0}C for 4 hours to block the cells at G2. After blocking, the cells were shifted again to 25^{0}C and the number of septa being formed were counted every 20 minutes to measure exit from G2 phase. Tau reached peak septation 40 minutes before the control, while MAP2c reached peak septation 40 minutes after the control cells.

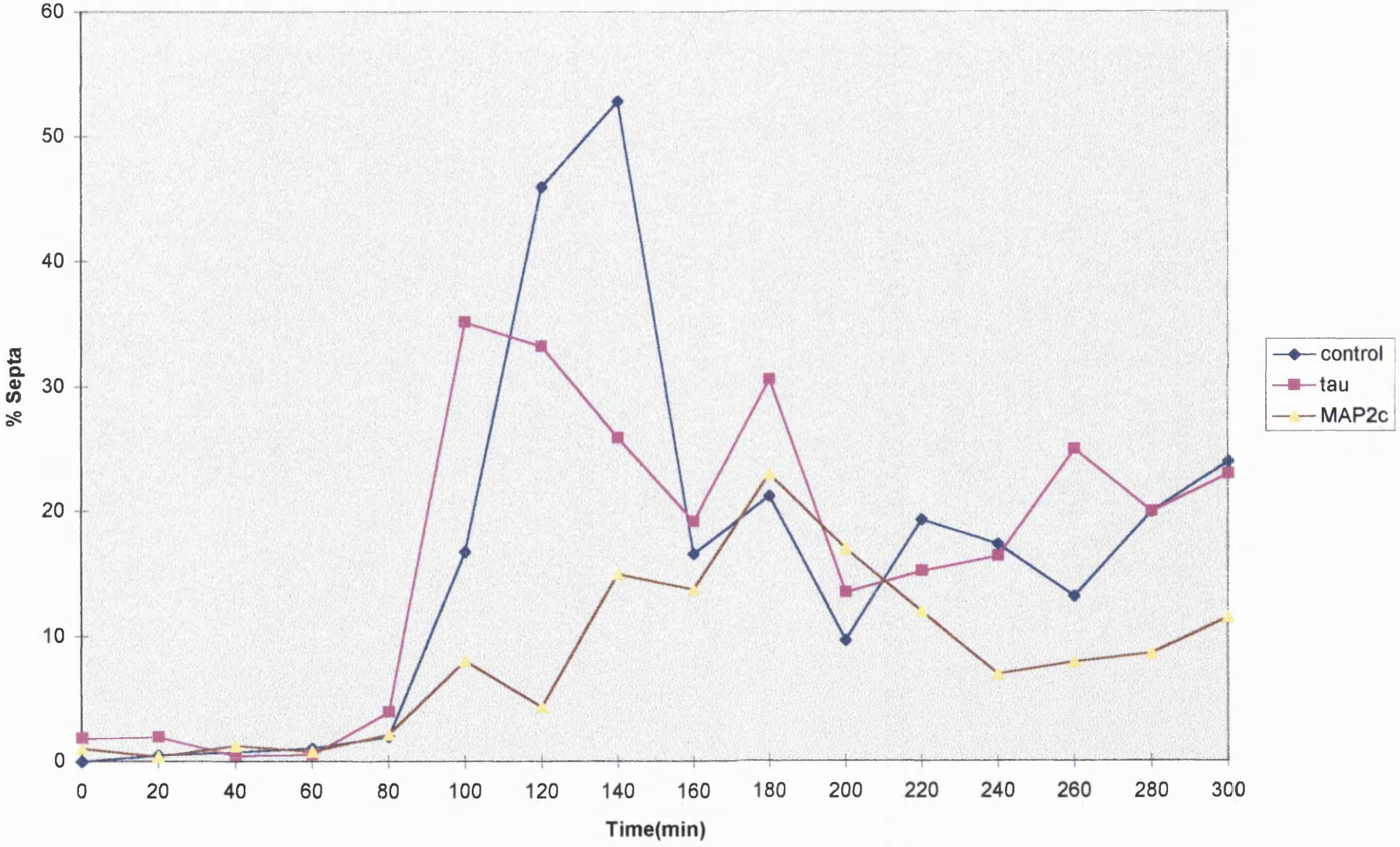
60
50
40
30
20
10
0
% Septa
0
20
40
60
80
100
120
140
160
180
200
220
240
260
280
300
Time(min)
control
tau
MAP2c

any effect on the cold-sensitivity of these mutants. None of the MAPs showed any effect on the cold sensitivity of the *nda* mutants (not shown)

.

3.3.7 Tau and MAP2c rescue the thiabendazole sensitivity of fission yeast at 20^0C.

Cells expressing tau, MAP2c and MAP4 were grown in the presence of different concentrations of thiabendazole (TBZ) to determine whether they prevented the drug's microtubule depolymerising effect. Figure 3.7 shows the effect of MAPs on the TBZ sensitivity of *S. pombe* at 36^0C, 29^0C and 20^0C. Figure 3.7.a shows the the growth of *S. pombe* at 36^0C, in the presence of, from left to right, 0, 5, 10, 20 and 40 μg ml^{-1} TBZ. +T indicates the preence of thiamine (and therefore MAPs are not being expressed), -T indicates the absence of thiamine, and therefore the expression of MAPs. Cells grew at all concentrations of TBZ except at 40 μg ml^{-1} TBZ, irrespective of the expression of MAPs.

Figure 3.7 b shows the growth of *S. pombe* at 29^0C, in the presence of TBZ at concentrations as described above. Once again the cells grew at all concentrations of TBZ except at 40 μg ml^{-1} TBZ, irrespective of the expression of MAPs.

Figure 3.7c shows the growth of S. pombe in the presence of TBZ concentrations described above, at 20^0C. In the presence of thiamine, cells grew at 5 and 10 μg ml^{-1} TBZ, but were sensitive to 20 μg ml^{-1} TBZ. Expression of tau or MAP2c overcomes this sensitivity, but not MAP4 (not shown). All cells were sensitive to 40μg ml^{-1} TBZ.

3.8 Tau and MAP2c rescue the sensitivity of fission yeast to the combined effects of cold and thiabendazole. Cells were grown in minimal medium containing, from left to right, thiabendazole (TBZ) concentrations of 0, 5, 10, 20 and 40 μg/ml. The top row shows cells grown in the presence of thiamine (control), and the bottom row shows cells grown in the absence of thiamine. In each plate, the left half expressed tau and the right half expressed MAP2c. At 36^0C (a) and 29^0C (b), cells were resistant to TBZ concentrations as high as 20μg/ml, but sensitive to 40μg/ml TBZ, and the expression of tau or MAP2c did not reveal any change. At 20^0C, control (+ thiamine) cells were sensitive to 20μg/ml TBZ, and both tau and MAP2c appeared to rescue this sensitivity.

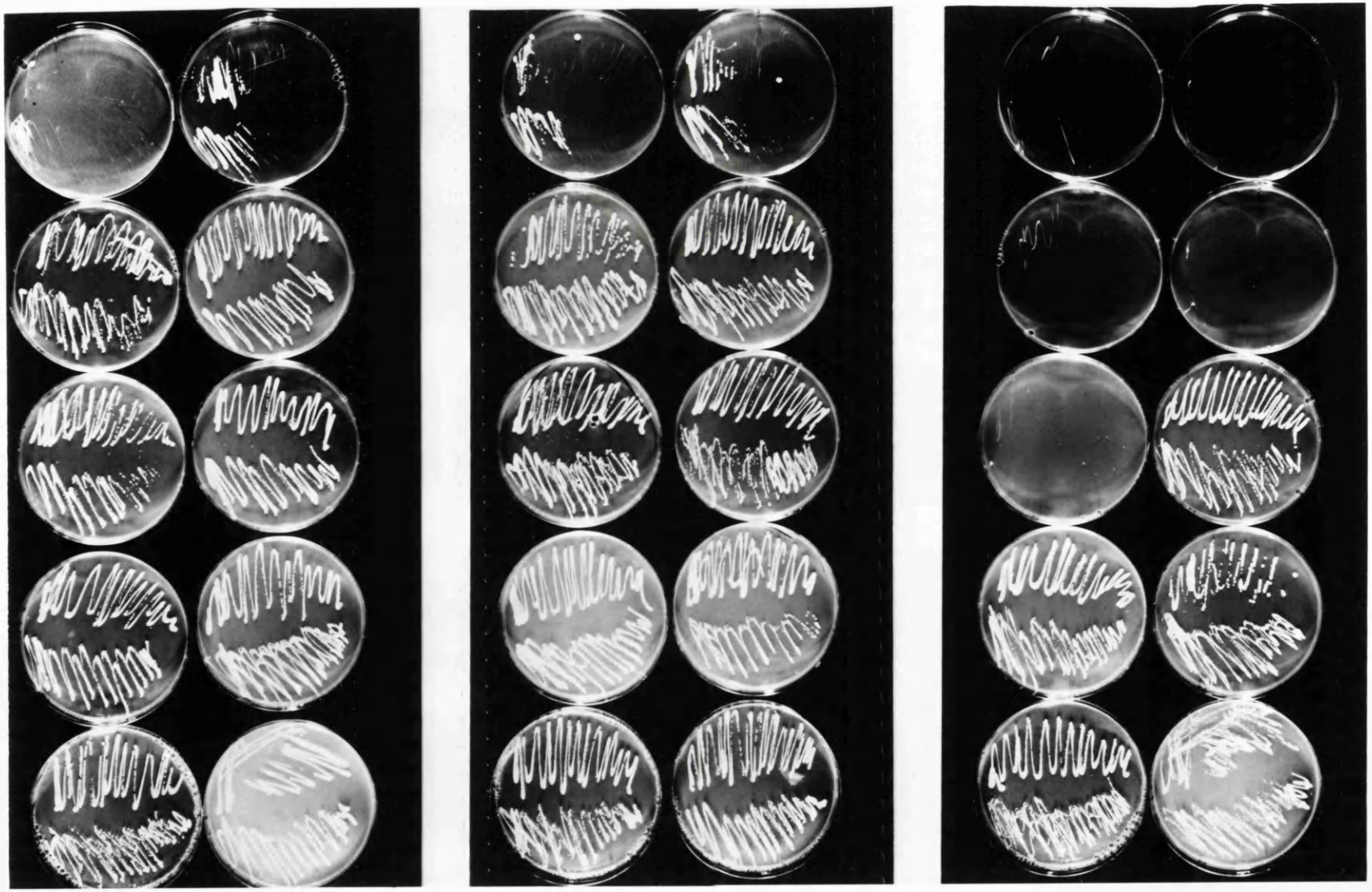

3.4 Discussion

This chapter describes the first experiments designed to explore the effect of the ectopic expression of the well-characterised mammalin MAPs, tau, MAP2c and MAP4 in a genetically tractable lower eucaryote. All three MAPS i.e. tau, MAP2c and MAP4 have previously been studied in different cell systems with low endogenous activity in order to better understand their functions *in vivo* (Sadot et al., 1995) (Baas et al., 1991; Barlow et al., 1994; Chen et al., 1992; Chen et al., 1992; Hirokawa et al., 1996). Tau has been studied extensively in neuronal cell lines such as PC12 (Hanemaaijer and Ginzburg, 1991), non-neuronal cell lines such as Chinese Hamster Ovary (CHO) cells (Preuss et al., 1997; Preuss et al., 1995), and insect cell lines such as Sf9 (Chen et al., 1992) (Baas et al., 1991). MAP2c has also been studied in Sf9 cells (Chen et al., 1992) (Leclerc et al., 1996), while MAP4 has been compared to tau in CHO cells (Barlow et al., 1994) (Olson et al., 1995). All MAPs appear to stabilise microtubules in all of these systems. Both tau and MAP2c are reported to form microtubule bundles in Sf9 cells. However expression of tau results in one long process with the microtubules arranged in an axon-like manner, while MAP2c results in several short neurite-like processes, indicating differing functional roles for the two MAPs In non-neuronal cells such as CHO cells, both the neuronal MAPs have been reported to form circular bundling of microtubules. MAP4, unlike tau, did not cause microtubule bundling in the CHO cells as reported by Barlow *et. al.*(1994). However, Olson et. al. (1995) have reported that MAP4 stabilses microtubules as measured by resistance to nocodazole depolymerisation in both CHO cells and BHK cells.

The present studies have shown that all the three MAPs, tau, MAP2c and MAP4 have an inhibitory effect on the growth of fission yeast. Given the high degree of amino acid sequence homology between the tubulin genes of yeast and mammals (Yanagida, 1987) it might be expected that MAPs would bind to microtubules and stabilise them. If as a result it takes longer for the cytoplasmic microtubules to depolymerise, entry into M- phase could be delayed, resulting in slower growth. A dynamic, tighly regulated spindle is required for cell division, and MAPs may also affect slow down cell division by interfering with spindle dynamics.

For each of the MAPs, the change in doubling time was temperature-specific. All three MAPs show greatest inhibitory effects of growth at 20^0C. Microtubules tend to depolymerise in the cold, although this property is not fully understood (Watson et al., 1990). MAPs may stabilise these microtubules but slow down their dynamics, resulting in their greater doubling times. MAP2c induced the greatest increase in doubling time at 20^0C compared to the other temperatures. This could be due the the way in which MAP2c interacts with the microtubules in the cold. MAP4 showed little difference in doubling times with change in temperature. MAP4 may have less of a stabilising role as it is generally found in non-differentiated cells with dynamic microtubules which are regulated for cell division. In mammalian cells, MAP4 interacts with cyclin B to target $p34^{cdc2}$ kinase which regulates M-phase microtubule dynamics (Ookata et al., 1995). As the $p34^{cdc2}$ kinase is conserved in fission yeast (Lee, 1987), MAP4 may have a similar effect, possibly replacing an endogenous fission yeast MAP activity, and therefore not affect cell growth greatly. Tau could act

in a manner similar to MAP2c, as they are both neuronal MAPS. However, it could have a lesser effect due to a possible lower binding or stability. Tau confers drug stability, but not cold stability to microtubules in insect ovarian Sf9 cells (Baas et al., 1994). Therefore it may not have a stabilising role in the cold in fission yeast either.

The differences in the rate of growth in the presence of the different MAPS could be due to the differences in their ability to stabilise microtubules. MAPs are thought to stabilise microtubules by binding to the microtubules by their C-terminal domain. According to the 'jaws' model of MAP-microtubule interaction (Mandelkow, 1995; Preuss et al., 1997), the C-terminal domain can be divided into two parts, the catalytic domain, consisting of the 18-amino acid imperfect repeats, and the targetting domain, consisting of the sequences flanking the repeats on both sides. This model postulates that the targetting domain is responsible for targetting the MAPs to the microtubules, and causing tight but unproductive binding, so that there is no increase in microtubule stability or nucleation. The repeats then act catalytically to promote microtubule stability and nucleation, which can lead to bundling. In addition, MAPs could also act as physical spacers beteween microtubules, explaining why the long arms of MAP4 or MAP2 lead to wider spacing between microtubules (Chen et al., 1992). In the present studies, tau has four repeats, MAP2c has three repeats anf MAP4 has five repeats. As the repeats are essential in the 'jaws' model for microtubule stabilising functions of the MAPs, the number of repeats rather than the differences between the MAPs could also be a reason for the observed differences in the rate of growth. This can be further clarified by expressing three-repeat tau in *S. pombe* and comparing its overexpression to that of three-repeat MAP2c and four-repeat tau. Binding of MAPs to microtubules

is regulated by phosphorylation (Mandelkow, 1995). There are several target sites for proline-directed kinases such as MAPK and GSK3 in the flanking regions constituting the targetting domain, while other kinases, such as MARK, target sites in the repeat regions. MARK has been reported to be potent in detaching MAPs from microtubules by phosphorylating the KXGS motifs in the repeats (Drewes et al., 1997). The *S. pombe* kin1 protein shows more than 50% homology to the MARKs (Levin and Bishop, 1990), and could phosphorylate the heterologous MAPs expressed in fission yeast (see chapter 4). Variations in the possible nature and degree of phosphorylation of the two MAPs could also account for their differences in inhibiting the rate of growth of *S. pombe.* The tubulin sequence of *S. pombe* could also result in differences in binding of the two MAPs. MAP2 has been reported to bind to two different subdomains of the C-terminus of β-tubulin from bovine brain, one with a sequence that is constant among isoforms, and another which exhibits variations between isoforms(Cross et al., 1991). The constant C-terminal sequence of the β-tubulin showed differential interaction of MAP2 and tau (Cross et al., 1991), indicating that binding to microtubules is specific for MAPs even though the microtubule binding repeats are similar in all MAPs.

MAP2c appears to be the most potent inhibitor of *S. pombe* growth. Proteolysis of this protein could remove some key regions which could either (a) make it bind to the microtubules more tightly due to removal of certain amino acids in the C-terminal region (b) it could lack the regions containing key amino acids that require to be phosphorylated in order to 'inactivate' the protein and allow microtubule

depolymerisation or (c) it could have smaller 'arms'possibly leading to closer spacing between microtubules which could affect microtubule dynamics and stability.

Western Blotting shows that all three MAPs were expressed. However, it is not clear what state the proteins exist in in fission yeast. Tau shows an intact band at 65kD, which is similar to bands from proteins expressed in brain, and recombinant tau expressed in *E. coli* (Goedert, 1989) (Goedert, 1990). The anti-tau antibody used, TP70, is a polyclonal antibody and recognises both phosphorylated and non-phosphorylated forms of tau. Although only one intact band is seen, and not several bands as would be expected if differential phosphorylation of tau occurred, the structure of tau has been shown to contain so many target motifs for so many kinases, including the cdc2 kinase (Goedert et al., 1994; Mandelkow, 1995), that it is unlikely that tau would not be phosphorylated at all in *S. pombe*. Western blotting with specific antibodies that detect phosphorylated tau would confirm whether or not tau is phosphorylated in *S. pombe*.

MAP2c appears to be partially proteolysed, and this may affect the way it interacts with microtubules in *S. pombe*. The primary structure of MAP2, including MAP2c, shows multiple repeats of the motif proline-glutamic acid- serine-threonine (PEST) (Matus, 1994). This motif is generally present in proteins destined for eventual proteolytic destruction, and could regulate the function and subcellular distribution of MAP2 and MAP2c in neuronal cells. The recognition of these PEST sequences in *S. pombe* could explain why MAP2c appears partially proteolysed.

MAP4 shows a band corresponding to its size according to its amino acid sequence. However, all MAPs generally show a 'drag' for unknown reasons so that its apparent molecular weight is higher than its molecular weight according to its amino acid sequence. It is possible thats a part of the MAP4 sequence was reaaranged or eliminated from the plasmid in *E. coli*, as it is a large insert in a large plasmid, and this was not obvious due to the location of the restriction sites of the enzymes used.

Both tau and MAP2c are neuronal MAPs, whilst MAP4 is a non-neuronal MAP. Neurons have processes such as axons and dendrites, which retain their shape due to 'stiff microtubules'. The stiffness of the microtubules is attributed to MAPS such as tau and MAP2, which provide added stability to the fibres running down the processes [reviewed by Matus, 1994 #34]. In non-neuronal mammalian cells, expression of high levels of tau and MAP2 alters the microtubule arrangement of the cells such that they become independent of the organising centres and are found free in the cytoplasm with a tendency to form bundles. Expression of both tau and MAP2 in insect Sf9 cells have been reported to result in induction of processes with axon-like microtubule organisation (Baas et al., 1991) (Chen et al., 1992). Tau and MAP2c could have a similar stabilising effect on *S. pombe* microtubules. It has been suggested that the *S. pombe* interphase microtubules run along the long axis of the cell beacuse this could be the most energetically favourable mode of microtubular growth (Mata and Nurse, 1997). The resulting decrease in microtubule dynamics due to the MAPs could result in long fibres and send signals to the cell to extend in a manner similar to the development of neuronal processes. Although the extension is usually in the two longitudinal tips, the increased stability conferred on the microtubules by the presence

of the MAPs could lead the microtubules to grow in other directions resulting in 'processes' being formed in the 'sides' of the cell and leading to branched or 'T-shaped' cell morphology.

The cell length of fission yeast is also an indicator of its phase in the cell cycle. The MAPs tau and MAP2c, and particularly MAP2c, may prevent microtubule depolymerisation, and therefore delay the onset of M-phase, resulting in continuation of cell growth. Block-release experiments with *cdc25.211* cells expressing tau and MAP2c show that indeed MAP2c, which cause a minority of wild type cells to grow to 2.5 times its normal length, does slow the exit from G2. Therefore it interferes with the onset of M-phase in some way. However, tau appears to hasten the exit from G2 to M-phase compared to the control. It is possible that tau but not MAP2c is a substrate of cdc2 kinase, and its phosphorylation by the kinase decreases its microtubule stabilising ability. Tau expressed in Chinese Hamster Ovary (CHO) cells have been shown to be completely phosphorylated at the onset of M-phase, and detached from microtubules (Preuss et al., 1995). Tau may behave similarly in the fission yeast. Many tau expressing long cells (such as one seen in Fig. 3.5 b) are multiseptate, suggesting that tau does not interfere with the entry into mitosis, but has an effect on cytokinesis. It has been reported that in PC12 cells, tau interacts with the neural plasma membrane through its amino-terminal projection domain (Brandt, 1995). The role of tau may be more complex than merely stabilising microtubules, and its interaction with the plasma membrane suggests that tau may also interact with the proteins of the septa and perhaps this slows or prevent cytokinesis in certain cases. Thurston *et. al* (1991) have also reported the localisation of tau to the nucleolus of

cells, suggesting a role for tau in ribosomal biogenesis or protein synthesis. Tau could therefore influence the regulation of the cell cycle.

Nda2 is a mutant fission yeast α1-tubulin gene, and *nda3* is a mutant fission yeast β-tubulin gene, which make the strains cold -sensitive. None of the MAPs had any detectable effect on the cold-sensitivity of these mutants. MAPs may not be able to bind to the microtubules at all, as they may have a conformation that does not expose the regions that bind to MAPs. MAPs appear to bind to microtubules through the C-terminal domain of β-tubulin (Cross et al., 1991; Cross et al., 1994). Therefore it is very plausible that some mutation in β-tubulin will affect the ability of MAPs to bind and/or stabilise microtubules. Although MAPs may not bind directly to the α-tubulin, a mutation in α-tubulin could affect the structure of thew tubulin dimer and therefore have repurcussions for interactions with MAPs. Alternatively the MAPs may merely bind to the short microtubule polymers but not be able to use their N-terminal arms to stabilise the polymers.

Thiabendazole depolymerises microtubules in fission yeast, and its effect increases in the cold (Sawin and Nurse, 1998) (Toda et al., 1983) (Umeneso et al., 1983). The exact manner in which thiabendazole acts to depolymerise microtubules is not clear. Fission yeast mutants supersensitive to TBZ map to both the *nda2* and *nda3* regions, coding for α-1 and β tubulin, while the TBZ-resistant mutant, *ben1*, maps to the *nda3* region coding for β-tubulin (Umeneso et al., 1983). Therefore both α- and β-tubulin appears to interact directly or indirectly with the drug to modulate microtubular organisation in the cell. However in the nematode *Haemonchus contortus*, a

photoactive analogue of benzimidazole, with similar biological activity as other benzimidazoles, labeled the N-terminal 63-103 amino acids of β-tubulin-1 (Nare et al., 1996). Tau and MAP2c could prevent the depolymerisation of microtubules due to TBZ by binding to microtubules and physically 'blocking' the drug so that it cannot reach the polymer. However MAP4 should also act in a similar fashion. Instead, it has no effect on TBZ sensitivity of microtubules. It is possible that (a) MAP4 binding to the microtubules is temperature sensitive, and it binds more weakly to microtubules. MAP4 has an extra repeat in the C-terminal region which is different from the other repeats. This repeat could affect the way MAP4 binds to microtubules.(B) as MAP4 is a much bigger protein than tau and MAP2c with much longer 'arms' it could be far less effective in stabilising the MT polymer. MAP4 is also reported to exist as a tetramer (Bulinski, 1993), and this may affect the way it stabilises microtubules in *S. pombe.*

In conclusion, MAPs inhibit the growth of *S pombe* possibly due to their stabilising effect on *S. pombe* microtubules. However the three MAPs, tau, MAP2c and MAP4 possibly act in dufferent ways, and therefore have different effects on the rate of growth and TBZ sensitivity of the fission yeast cells.

4. Effect of the Microtubule associated Proteins tau, MAP2c and MAP4 on fission yeast Microtubules

4.1 Introduction

Microtubules play various vital roles in the cell. Regulating microtubule dynamics for their adaptation to their various roles is the function of the Microtubule Associated Proteins (MAPs). An indication of the crucial role of MAPs is seen in the fact that MAPs have been found in dividing and differentiated cells in organisms from yeast to mammals. MAPs may vary in their amino acid sequence, but they have in common the following features: heat stability, various phosphorylation sites, and most importantly, the ability to bind to and stabilise microtubules via their C-terminal, basic region. A major MAP identified in *Drosophila*, the 205K MAP, was found to be colocalised with the mitotic spindle and cytoplasmic microtubules in immunofluorescence staining of cultures cells (Goldstein et al., 1986). Although it does not have sequence similarity with mammalin MAPs, it is immunologically related to Hela cell MAP4 and as is similar in structural organisation to MAP2. The 205K MAP also has several isoforms, and several potential kinase target sequences, as in tau and MAP2 (discussed later in this section), which raises the possibility of it being regulated by phosphorylation (Irminger-Finger et al., 1990). Microtubule dynamics have been extensively studied in *Xenopus* egg extracts, and several MAPs have been identified. The 215 kD *Xenopus* MAP (X-MAP) promoted elongation of microtubules specifically at the plus ends. Morover X-MAP is developmentally regulated and phosphorylated during mitosis (Gard and Kirchner, 1987). Another 220kD *Xenopus* MAP has also been identified, which is phosphorylated during

mitosis (Shiina et al., 1992). A third, 230K *Xenopus* MAP, purified by temperature-dependant cycles of assembly and disassembly of microtubules, is immunologically related to the Hela MAP4, heat-stable and phosphorylated like mammalian MAPs, and promotes microtubule elongation from axonemes (Faruki and Karsenti, 1994). The budding yeast MAP, MHP1 (MAP Homologous protein 1) is also immunologically related to the *Drosophila* 205K MAP and MAP4. Its C-terminal amino acid sequences are homologous to the microtubule binding domain of MAP2, MAP4 and tau. Immunofluorescence studies and biochemical analyses reveal that it binds to microtubules and mitotic spindles, and is essential for the stabilisation of microtubules (Irminger-finger et al., 1996). The MAPs identified in the nematode, *C. elegans*, have even greater similarity to the known mammalian MAPs. The known *C. elegans* MAP, PTL-1 (Protein with Tau-Like Repeats -1), has two isoforms with four or five tandem repeats that are 50% identical to tau, MAP2 and MAP4 repeats. Both isoforms bind to microtubules and promote microtubule assembly. They also induce the formation of microtubule bundles when expressed in COS cells (Goedert et al., 1996).

In mammals, the heat stable family of MAPs are identified by imperfect repeats of an 18-residue amino acid motif (as discussed in the Introduction). The three most commonly studied MAPs of this type are tau, MAP2 and MAP4. All of them have similar repeats in their C-terminal region, through which they bind to and stabilise microtubules, but unique N-terminal domains. All of them have isoforms some of which are developmentally regulated. However, their presence in mammalian cells vary according to cell type as well as subcellular location : MAP4 is found mainly in non-differentiated cells; tau is found mainly in the axons of neurons and in differentiated cells; MAP2 is found mainly in the dendrites of neurons. The N-

terminal differences, as well as the differences in location, of the different MAPs suggest different functions specific to each MAP in spite of their similarities.

4.1.1 Tau

Tau was one of the first microtubule associated proteins to be identified. It has also generated the great interest due to its role in Alzheimer's disease, where it is found in a hyperphosphorylated state as part of the paired helical filaments (PHFs). Tau in all mammals consists of several isoforms produced by the alternative mRNA splicing of a single gene (Neve et al., 1986). It is found mainly in the axons of neuronal cells (Binder et al., 1985), although it has also been reported in other differentiated cells such as erythrocytes (Sanchez and Cohen, 1994).

Tau from human brain has six known isoforms (Goedert, 1990). They range from 352 to 441 amino acids in length (Goedert, 1989). All tau sequences contain three or four imperfect repeats of an 18 amino acid motif located in the C-terminal half, each containing a characteristic pro-gly-gly-gly motif. The extra repeat in the isoforms with four repeats is inserted in the first repeat in a way that preserves the periodic pattern (Butner and Kirchner, 1991). The N-terminal projection domain appears to determine the spacing between adjacent microtubules (Chen et al., 1992). Some tau isoforms contain an additional 29 or 58 amino acid insert in the N-terminus. These sequences contain a high frequency of prolines and charged amino acids (Goedert, 1989). Three-repeat tau can therefore have no N-terminal insert, or a 29 amino-acid insert, or a 58 amino acid insert. Similarly, four-repeat tau can have no N-terminal

insert, or a 29 amino acid insert, or a 58 amino-acid insert. These combinations result in the six tau isoforms. The adult human brain contains three or four repeat tau without N-terminal inserts or with the first N-terminal insert of 29 amino acids. Isoforms with three and four repeats with the 58-amino acid N-terminal insert are also found at much lower levels. However, foetal and immature brains do not contain any isoforms with four repeats or with N-terminal inserts. Therefore it appears that as the brain develops, tau expression changes from the simpler three-repeat forms with no amino terminal insert to all six isoforms. (Goedert, 1990). The number of repeats also affect its ability to promote microtubule assembly. Rates of assembly were 2.5 - 3.0 times faster in the presence of isoforms containing four repeats when compared with three-repeat isoforms, but the amino terminal inserts did not make any significant difference to assembly rates(Goedert, 1990).

In the rat, another isoform of tau, called big tau, of molecular weight 110kD, has been identified in rat ganglia . Big tau contains sequences identical to the longest of the small tau isoforms, but with an additional 254 amino acid insert in the amino terminal half(Goedert et al., 1992). Big tau is produced from an 8kB mRNA generated by the alternative splicing of the same gene that encodes small tau (Goedert et al., 1992). This may be a tau protein produced specifically in the peripheral nervous system, as RNA blots show that in the peripheral ganglia from adult rats only the 8kB mRNA band corresponding to big tau is found, whereas in ganglia from newborn rats both 6- and 8- kB tau mRNA bands are found. In tissues from the central nervous system only the 6-kB mRNA band was detected (Goedert et al., 1992).

Tau has been shown to bind to microtubules *in vitro* and to stabilise them by promoting their nucleation and elongation, and protecting against disassembly (Brandt and Lee, 1993) (Brandt and Lee, 1994) (Gustke et al., 1994). Tau appears to bind to microtubules with the help of the repeats in the C-terminal domain (Lee, 1989) (Butner and Kirchner, 1991). However both *in vitro* and *in vivo* studies showed that these repeat motifs bound very weakly to microtubules, in contrast to the strong binding of the full length protein (Goode and Feinstein, 1994) (Lee and Rook, 1992). The 'jaws' model has been proposed to explain the tau-microtubule interaction, based on microtubule binding experiments of domains with regions deleted or interchanged. This model suggests that the regions flanking the repeat motif are the 'targetting' domains which position the MAP on the microtubule and cause tight binding. However this binding is unproductive, and the repeat motif is required to promote microtubule assembly or nucleation, although the repeats by themselves do not bind strongly (Goode and Feinstein, 1994). Therefore the MAP functions by a combination of the targetting and catalytic activity. This model has been confirmed *in vivo* by observation of the interaction of different domains of tau with microtubules in transfected CHO cells using immunofluorescence microscopy (Preuss et al., 1997).

Expression of tau in cultured neuronal cell lines and insect cell lines have helped further elucidate the function of tau. Tau is generally located in the axons of neurons. When insect Sf9 ovarian cells are induced to express high levels of tau, they develop processes that are similar to axons in neuronal cells, and contain dense arrays of microtubules (Kosik and McConlogue, 1994). As in axons, the microtubules in these processes are orientated with their plus ends distal to the cell body. There are also bundles of microtubules in Sf9 cell bodies following tau expression (Baas et al.,

1991). Tau appears to play a key role in the stabilisation and elongation of neurite outgrowths when cultured PC12 cells are treated with nerve growth factor (Hanemaaijer and Ginzburg, 1991) (Sadot et al., 1995). Suppression of tau expression using antisense nucleotides inhibit neuronal development (Caceres and Kosik, 1990), suggesting tau plays an important role in neurite polarity. Brandt *et. al* (1995) (Brandt, 1995), have shown that tau can interact with the neural plasma membrane through its N-terminal domain, and this could constitute an important step in neuritic development.

Interaction of tau with microtubules is inhibited by phosphorylation, and this could be one way of regulating microtubule dynamics (Mandelkow, 1995; Preuss et al., 1995; Trinczek et al., 1995). Tau is a phosphoprotein with at least 17 identified phosphorylation sites (Illenberger et al., 1998). *In vitro* studies have shown that several protein kinases act on tau, such as MAP kinase (Drewes et al., 1992), GSK-3 (Mandelkow et al., 1992), cdc2 kinase, or cdk5 (Mandelkow, 1995). A novel MAP-microtubule affinity regulating kinase is p110MARK, which phosphorylates tau KIGs or KCGS motifs in regions flanking the repeat domain. Phosphorylation of Ser262 of tau, which lies within the flanking motif, dramatically reduces microtubule binding (Drewes et al., 1997). *In vivo* phosphorylation studies of tau expressed in CHO and the human neuroblastoma cell line LAN show that there is an endogenous level of tau phosphorylation (Illenberger et al., 1998) (Preuss et al., 1995). Most sites of phosphorylation are in SP or TP motifs, activated by proline-directed kinases, except serine 214 and 262 (Illenberger et al., 1998) (Preuss et al., 1995). Phosphorylation was seen to increase seven-fold in mitosis, when cdc2 kinases are also upregulated, and studies of mitotically arrested cells show that Ser214 is a prominent

phosphorylation site in metaphase, but not in interphase. *In vitro* studies have shown that proline-directed kinases only moderately affect tau-microtubule interactions. However, phosphorylation of Ser214 strongly decreases tau-microtubule interaction *in vitro*, suppresses microtubule assembly, and may therefore be a key factor in the detachment of tau from microtubles in mitosis(Illenberger et al., 1998). This could then lead to rearrangement of microtubules and higher dynamics as seen in mitotic cells (Illenberger et al., 1998). Ser214 is phosphorylated *in vitro* by PKA, and to a lesser extent by PKC (Brandt et al., 1994). Ser 262, on the other hand, is only weakly phosphorylated at interphase and metaphase, but could be briefly phosphorylated at prophase. However it is not known whether MARK, which phosphorylates Ser262, is cell cycle regulated(Illenberger et al., 1998). Another factor is the down regulation of phosphatases such as calcineurin and PP-2a, both of which are capable of removing all phosphates from pre-phosphorylated tau (Mandelkow, 1995). As Ser214 is a prominent site in PHF tau and is part of the epitope for the antibody AT100, the only specific antibody for Alzheimer's tau, it is possible that mitotic mechanisms might lead to Alzheimer's disease.

4.1.2 MAP2

MAP2 is the other major non-motor neuronal MAP. MAP2 has many similarities with tau and is heat stable. MAP2 is a long fibrous molecule that has three or four imperfect repeats containing the pro-gly-gly-gly motif in its C-terminal domain, through which it binds to microtubules, and an N-terminal projection domain (Vallee, 1980). It appears to stabilise and cross-link neuronal microtubules (Matus, 1994).

MAP2 is also found to be phosphorylated on several sites, and can be purified with a cyclic-AMP-dependant protein kinase bound to its projection domain (Vallee et al., 1981).

MAP2 has several isoforms produced by the alternative splicing of a single gene that consists of 20 exons(Garner and Matus, 1988) (Kalcheva et al., 1995). MAP2 has two high molecular weight forms, MAP2a and MAP2b, of 280 and 270 kD respectively in human brains, and a low molecular weight form, MAP2c, of 68kD (Garner et al., 1988). The primary sequence of MAP2c in rat consists of two continuous stretches of amino acids from the extreme ends of MAP2b joined together with 1372 amino acids from the centre of MAP2b, with most of the MAP2b projection domain missing (Papandrikopoulou et al., 1989). MAP2a is similar to MAP2b, with an alternative transcription of at least one extra exon (Kalcheva et al., 1995). Neuronal MAP2 generally has three repeats of the 18 amino acid motif in its C-terminal domain. However, a 4-repeat isoform of MAP2c has been reported in glial cells (Doll et al., 1993)

In mature neurons most MAP2 is associated specifically with the dendrites, although MAP2c is found in axons as well as cell bodies (Garner and Matus, 1988; Okabe and Hirokawa, 1989). The different MAP2 isoforms are also developmentally regulated. MAP2b is constitutively expressed throughout life, MAP2c is expressed at high levels only during development, and MAP2a is found only in the mature neurons of the adult brain (Binder et al., 1984) (Kalcheva et al., 1998). In the rat appearance of MAP2a takes place concommitantly with the disappearance of MAP2c(Kalcheva et al., 1998). This implies different functional roles for each of the three isoforms.

As with tau, MAP2 has been expressed in neuronal and non-neuronal cell lines in an attempt to elucidate its cellular function. As MAP2 localisation may have direct effects on both function and on neuronal morphogenesis, several studies looked at the mechamism of MAP2 distribution. In situ hybridisation has indicated that tau and MAP2 mRNAs extend into the axon and dendrite respectively, while MAP2c mRNA is confined to the cell body (Garner et al., 1988) (Litman et al., 1993). Therefore subcellular localisation of the MAPs could be due to subcellular localisation of the mRNA.

Biotinylated MAP2 was used to study the turnover of MAP2 in axons and dendrites. When injected into cultured spinal cord neurons, MAP2 was initially seen both in the dendrites and axons. However, while dendritic MAP2 stabilised, axonal MAP2 turned over quickly and disappeared (Okabe and Hirokawa, 1989). The primary amino acid sequence of MAP2, including MAP2c, contains multiple repeats of the motif proline-glutamic acid- serine - threonine (PEST), which is contained in proteins marked for proteolytic destruction (Matus, 1994). This mechanism could be activated for axonal destruction of MAP2, but the mechanism is as yet poorly understood.

Transfection of MAP cDNAs into cultured spinal cord neurons revealed that both tau and MAP2c were transported into the axon, but MAP2 was not. Therefore a specific signal suppressing MAP2 transport into the axon may exist (Hirokawa et al., 1996)

As with other MAPs, MAP2 has been shown to stabilise and bundle microtubules *in vitro* (Gamblin et al., 1996) and *in vivo* (Matus, 1994). Expression of segments of

MAP2 and MAP2c into non-neuronal cells such as HeLa cells show that MAP2 causes bundles, and that this does not require the N-terminal domain (Ferralli et al., 1994). As with tau, the C-terminal repeats themselves were insufficient to promote microtubule binding, but required the flanking sequences, particularly in its amino-terminal side, where it is proline-rich. Stepwise increases in length of the flanking sequences led to increased microtubule binding. The strength of binding appeared to correlate directly to bundling and stiffness of microtubules (Ferralli et al., 1994).

The N-terminal projection domain, however, could regulate the spacing between microtubules. Expression of MAP2b and MAP2c in insect Sf9 ovarian cells induced these cells to grow long processes. Electron microscopy revealed that microtubules were more than 50 nm apart in cells expressing MAP2b, but less than 20 nm apart in cells expressing MAP2c (Chen et al., 1992).

MAP2 also appears to impart stiffness to microtubules when expressed in non-neuronal cells. When epithelial cell line PLC cells transfected with MAP2 were treated with cytochalasin B to depolymerise the actin cytoskeleton, the cells grew stiff processes containing MAP2-decorated microtubules (Edson et al., 1993). Experiments with synthetic peptides have shown that MAP2 binds to the microtubule walls using the 18 amino acid motif, while short stretches of 13 -14 amino acids that connect them act as linkers, so that the motifs can bind to neighbouring tubulin dimers and pull the filaments together, reducing their ability to move (Matus, 1994).

The role of MAP2 in neuronal morphogenesis has been shown using antisense oligonucleotides against MAP2 mRNA. In cultures cerebellar neurons, as well as in

the p19 cell line which differentiates into neuroblastoma cells when treated with retinoic acid, antisense oliginucleotides prevented the formation of processes (Dinsmore and Solomon, 1991) (Caceres et al., 1992). Anti-MAP2 oligonucleotides also prevented cell differentiation but cell division continued in spite of the presence of neural differentiation markers (Caceres et al., 1992).

4.1.3 MAP2c

MAP2c, the low molecular weight isoform of MAP2, is abundant in immature neuronal cells where, unlike high molecular weight (HMW) MAP2, it localises to both axons and dendrites. MAP2c appears to bind to dendritic neurons more firmly than to microtubules in axons (Hirokawa et al., 1996).

The microtubule binding domain of MAP2c is identical to that of MAP2b, and as with MAP2b, MAP2c has been shown to bind and stabilise microtubules (Ferralli et al., 1994). Expression of MAP2c in fibroblasts results in bundling of the interphase microtubule network. As with MAP2b, the repeat region plus the proline-rich region were essential for microtubule bundling. However the presence of the amino terminal projection domain confirmed a higher efficiency of microtubule bundling (Umeyama et al., 1993), and therefore this domain may play more than a passive role in microtubule bundling. Introduction of biotinylated-tubulin into the MAP-transfected cells showed that tubulin was incorporated at the distal end of the microtubules. Tubulin turnover was highly suprssed in the presence of MAP2c. Microtubule organisation in fibroblasts in the presence of MAP2c was similar to that in nerve cells,

indicating that MAP2c could play a crucial role in the differentiation of immature nerve cells. (Umeyama et al., 1993). *In vitro* experiments with recombinant MAP2c supported the *in vivo* observations. MAP2c dramatically stabilised microtubules by reducing both the frequency of catastrophes as well the mean length of shortening events, even at very low MAP2c:tubulin ratios. However, MAP2c did not appear saturated even at very high ratios, indicating that MAP2c must not only bind to tubulin molecules of the microtubule lattice, but also with each other, once the first layer is bound to the microtubule surface (Gamblin et al., 1996).

Evidence for the role of MAP2c in neuronal morphogenesis comes from several sources. Suppression of MAP2c with anti-sense oligonucleotides in cultures neurons resulted in a failure of the lamella to form neurites (Caceres et al., 1992). Minor processes were formed when MAP2c was expressed in Sf9 cells (Leclerc et al., 1996). In this role, MAP2c may interact not only with microtubules but also with microfilaments. Cunningham *et. al.* (1997) microinjected tau, mature MAP2 and MAP2c into the human melanoma cell, M2, which lacks the actin binding protein-280 (ABP-280) and forms membrane blebs. Tau and MAP2 rescued the blebbing phenotype. However, MAP2c not only rescued the blebbing, but caused the formation of two distinct structures, an actin-rich lamellae and microtubule-bearing processes (Cunningham et al., 1997). This suggests a distinct role for MAP2c in re-organising the cellular cytoskeleton.

4.1.4 MAP4

Both tau and MAP2 are neuronal MAPs. MAP4 is the most widely studied non-neuronal vertebrate MAP that bears similarity to the neuronal MAPs. It is a heat stable protein with an acidic N-terminal projection domain and a microtubule-binding C-terminal domain. It is a fibrous protein that consists of two 220kD dimers. MAP4 is ubiquitously distributed and has been detected by both indirect immunofluorescence and western blotting in all tissues except mature sperm (Bulinski, 1994). As with tau and MAP2, MAP4 has four isoforms produced by the alternative splicing of a single gene (Chapin et al., 1995; West et al., 1991).

The most common MAP4 isoform, isoform IV, has five imperfect repeats in its C-terminal domain. Four of the five imperfect repeats and the intervening spacer sequences show sequence similarities with the repeat sequences of tau and MAP2. The second repeat, however, is different, with a long spacer sequence and sequence which diverges from the other repeat consensus sequences. However as repeat 2 has an overall positive charge, 10 homologous amino acid residues, and is situated between repeats 1 and 3, it is assumed to be a functional microtubule binding entity. The other isoforms do not have this repeat, and resemble tau and MAP2 more closely in these sequences (Aiwaza et al., 1991; Chapin and Bulinski, 1991; West et al., 1991).

Although MAP4 is similar to the neuronal MAPs in terms of the repeat sequences, C-terminal microtubule binding domain and charge distribution in the molecule, there are also many differences. MAP4 does not share the sequence homology of the regions flanking the repeat domains found in neuronal MAPs. All three MAPs possess a proline-rich basic region just N-terminal to the repeat region. However, this

region is more extended in MAP4, and in contrast to neuronal MAPs, can also bind to microtubules in the absence of the repeat region. This proline rich region in MAP4 also contains consensus sites for phosphorylation by many kinases, which could regulate the binding of MAP4 to microtubules (Bulinski, 1994; West et al., 1991).

Studies have demonstrated that, as with tau and MAP2, MAP4 promotes microtubule assembly and stabilises microtubules *in vitro* (Aiwaza et al., 1987). However, tau and MAP2 are found in differentiated cells which require stable microtubules for their functions. MAP4, on the other hand, is found in dividing cells with dynamic microtubules that periodically reorganise themselves through the cell cycle. Several studies have been done to understand the role of MAP4, as a microtubule-stabilising protein, in the regulation of microtubule dynamics in non-differentiated cells. These have resulted in contradictory reports of MAP4 function. Barlow *et. al* (1994) overexpressed MAP4 in Chinese Hamster Ovary cells and reported no change in microtubule stability of level of polymer (Barlow et al., 1994). In contrast, Olson *et. al* (1995) (Olson et al., 1995) transfected several cells lines such as BHK and CHO with GFP-tagged MAP4 chimeras and studied their function in real time in living cells. They reported that MAP4 reorganises microtubules into bundles and stabilises these arrays against depolymerisation with nocodazole. The basic C-terminal domain alone had the same effect. The projection domain showed no microtubule localisation, but did modulate the association of various binding subdomains with microtubules. Microinjection of intact MAP4 and its C-terminal fragment to PtK cells also promoted microtubule assembly and stabilisation of microtubules, with MAP4 binding to the microtubules *in vivo* (Yoshida et al., 1996). Yet anotherb study of MAP4 overexpression in Ltk- cells found that MAP4 stabilises microtubules as

assayed by resistance to nocodazole, but the entire microtubule binding domain alone was not as efficient in stabilising microtubules as the full-length MAP4. MAP4 overexpression in these cells also appeared to slow down cell growth (Nguyen et al., 1997). On taking the opposite approach and depleting MAP4 from human fibroblasts by seqeustering MAP4 into a MAP4-Antibody complex, Wang *et. al.* (1996) failed to detect any change in microtubule dynamics, post-translational modification or microtubule-dependant organelle transport (Wang et al., 1996). This could indicate that MAP4 function in the cell is compensated by other unknown MAPs.

If MAP4 stabilises microtubules *in vivo* as shown by the studies above, what is its role as the cell enters mitosis and the interphase microtubules depolymerise? The MAP4 sequence has shown consesnsus sequences for protein kinases in its proline rich region. At the onset of mitosis in starfish oocytes, levels of the p34cdc2 kinase activity increases, and the $p34^{cdc2}$/cyclinB complex associates with microtubules in the mitotic spindle and the premeiotic aster (Ookata et al., 1993). This association appeared to take place due to an interaction between cyclin B and MAP4 (Ookata et al., 1995). The cdc2 kinase did appear to target and phosphorylate MAP4 at its proline rich region. This suppressed the ability of MAP4 to stabilise microtubules, although phosphorylation did not prevent MAP4 binding to microtubules. That the phosphorylation of MAP4 at mitosis was specifically by the cdc2 kinase was confirmed by Ookata et. al (1997) using a specific inhibitor of cdc2 kinase, butyrolactone I. Further, the sites of phosphorylation were identified as Ser696 and Ser787, both of which lie within the SPXK consensus sequence for the cdc2 kinase, and are in the proline-rich region of MAP4 (OOkata et al., 1997). Therefore

microtubules dynamics appears to be regulated by the cdc2 kinase at mitosis directly through MAP4.

4.1.5 MAPs in Fission Yeast

Tubulin sequences in fission yeast are homologous to mammalian tubulin sequences by more than 60% (Yanagida, 1987). However only one protein, mal3, has been known to bind to microtubules in *S. pombe*, but its role in the regulation of microtubule dynamics is unknown (Beinhauer et al., 1997). Regions in β-tubulin in chicken that have been shown to interact with MAP2 have sequences very similar in fission yeast, so it is possible that mammalian MAPs could bind to fission yeast microtubules. Therefore in this chapter we study the effect of the MAPs tau, MAP2c and MAP4 on the fission yeast microtubule cytoskeleton by indirect immunofluorescence microscopy in an effort to elucidate the similarities and differences in their function.

4.2 Methods

Cells containing pREP-tau, pREP-MAP2c and pREP-MAP4 were grown in the presence and absence of thiamine for 30 hours. They were then fixed in methanol, and stained with the anti-tubulin antibody TAT-1, and TP70, α-MAP2c antibody and LHB-1 for cells expressing tau, MAP2c and MAP4 respectively. Cells were then mounted with DAP1 in glycerol and observed by fluorescence microscopy.

4.3 Results

4.3.1 Effect of tau on wild type microtubules

In the previous chapter, it was seen that the overexpression of the MAPs tau, MAP2c and MAP4 had distinct effects on fission yeast morphology, growth rate and sensitivity to the microtubule depolymerising drug thiabendazole. As MAPs generally bind to and regulate microtubules, in this chapter we have attempted to study, using indirect immunofluorescence microscopy, how each of these heterologous MAPs affected microtubule organisation in fission yeast.

Indirect immunofluorescence microscopy of control wild type fission yeast cells confirmed the presence of three or four microtubules traversing the length of the interphase cell from pole to pole (Fig. 4.1 a, b). (Hagan, 1998; Hagan and Hyams, 1988). Ectopic expression of tau in the fission yeast did not produce a very strong phenotype (see also the previous chapter). In those cells that did show a phenotype, tau appeared to cause the groups of microtubules to form a single bundle aligned along

Figure 4.1 Immunofluorescence micrographs of microtubules (a and b) and DAPI stained nucleusin wild type fission yeast cells containing the pREP1 plasmid alone. Several microtubules traverse the length of the cell. Bar 10 μm

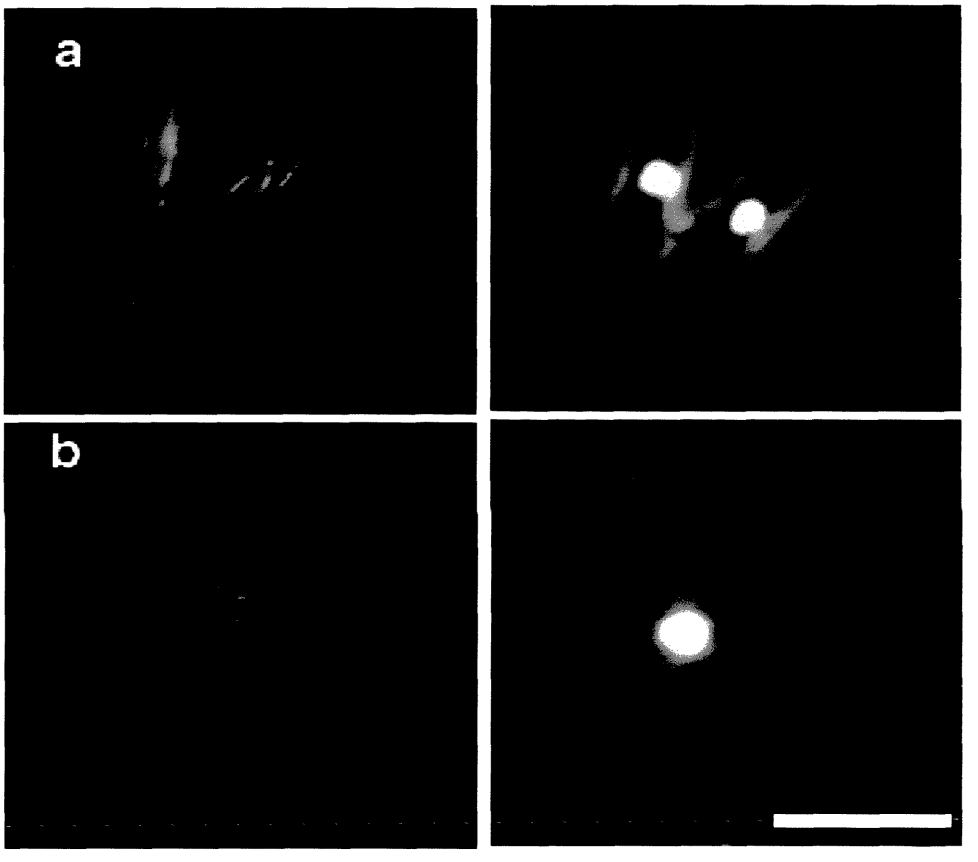
a
b

one edge of the cell. This resulted in a slight curvature of cells(Fig.4.2 a). Most strikingly, tau expressing cells revealed the presence of a stable tubulin staining ring at the cell centre. This structure is of interest as it was not detected in the original description of microtubules in fission yeast (Hagan and Hyams, 1988) and was not detected in control cells. Thus tau appears to stabilise a structure that appears only transiently in the normal cell cycle. Sometimes, microtubule bundles emerged from this region. Some cells appeared elongated following tau expression and lacked interphase microtubules (Fig. 4.2c). This suggests that either the microtubules were depolymerised in these cells, or that tau arrests cell cycle progression at entry to mitosis, the point in the cell cycle where interphase microtubules depolymerise (Fig. 4.2d). Staining of cells overexpressing tau with the anti-tau antibody TP70 revealed that tau appeared to bind to microtubules, and also confirmed that the levels of tau varied considerably in different cells (Fig. 4.3).

4.3.2 Effect of MAP2c on wild type fission yeast microtubules

Cells overexpressing MAP2c, however, showed a stronger phenotype, but distinct from that seen with tau (Fig. 4.4, 4.5). Phenotypes of MAP2c-expressing cells, as revealed by immunofluorescence microscopy, ranged from bent to T-shaped and branched, and contained short microtubules around the nucleus(Fig. 4.4 a, b, c,d). Consistent with this was the appearance of a the high level of background staining of unpolymerised tubulin. As with tau, a number of MAP2c expressing cells were arrested in late anaphase and contained a tubulin staining ring in the cell centre (Fig. 4.4 d). Immunofluorescence staining of these cells with anti-MAP2c antibody confirmed a great variation in the levels of MAP2c expression amongst different cells (Fig. 4.5). Interestingly, strong expression of MAP2c did not always show a strong

Figure 4.2 Immunofluorescence pictures of microtubules and DAPI stained nucleus in wild type cells expressing tau. Microtubules appear bundles and displaced towards the edge of the cell (a), resulting in slight curvature. In late mitosis, a tubulin staining ring appears at the cell centre (b) and microtubules emanating from this ring appear bundled towards the periphery of the cell. Although phenotypically most cells appear similar to the control cells , some appear elongated (c), with depolymerised microtubules. The presence of cells with normal phenotype and microtubule distribution could be a result of low levels of tau expression in the cell. Bar 10 μm

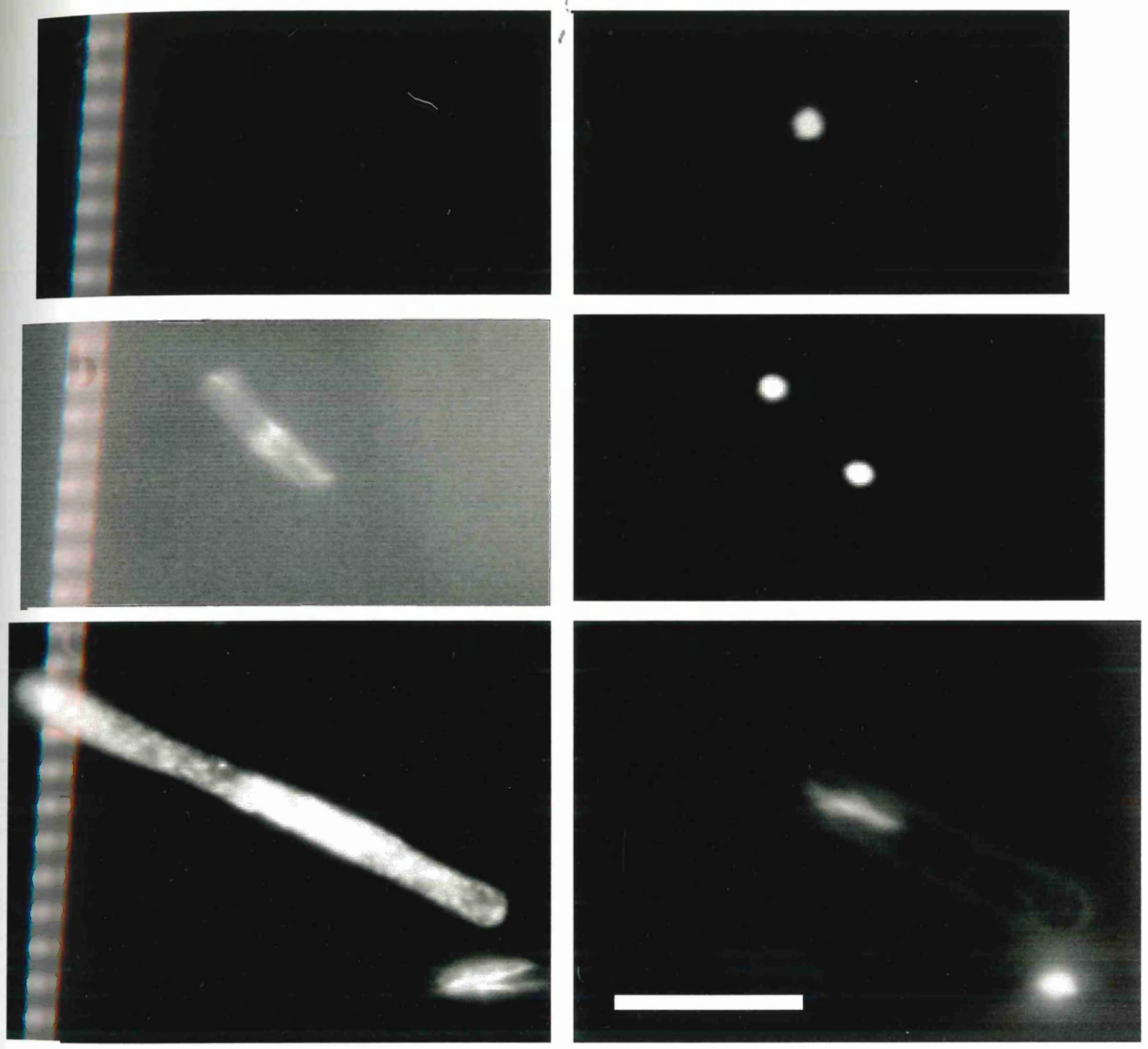

Figure 4.3 Anti-tau staining immunofluorecence picture of wild type cells expressing tau. Tau appears to be localised along the periphery of the cell similar to bundled microtubules, suggesting that tau binds to microtubules. Bar 10μm

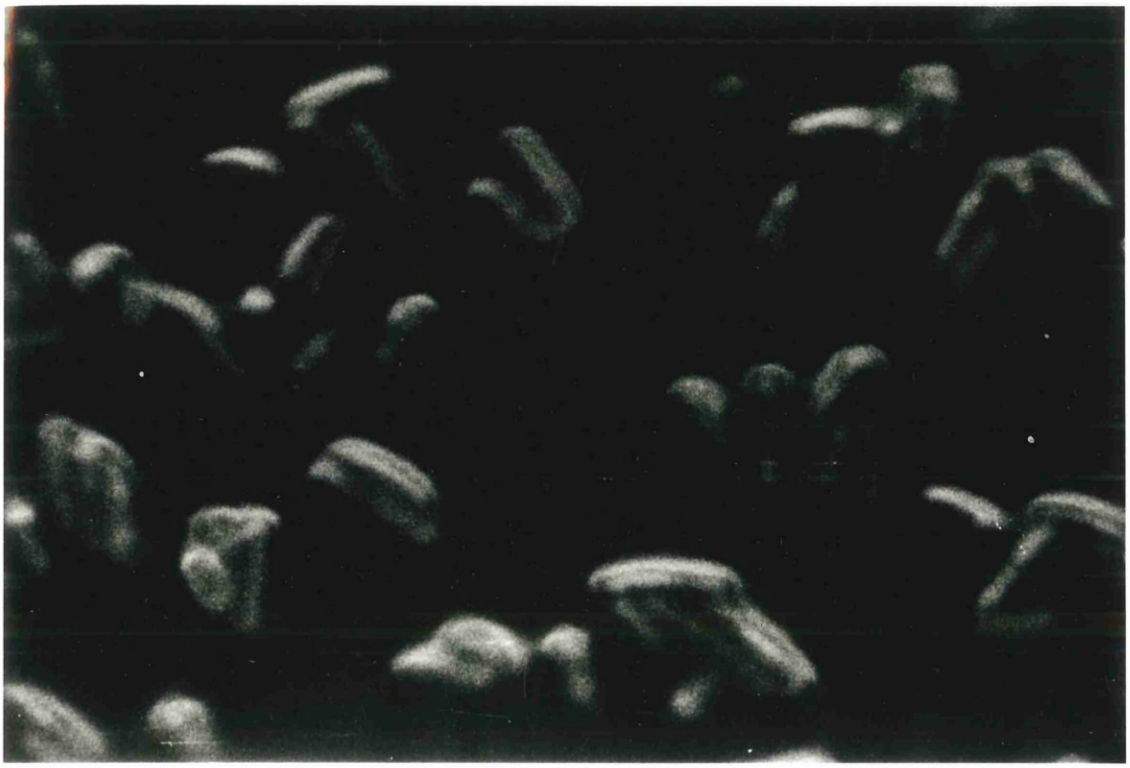

Figure 4.4 Microtubules and DAPI staining mucleus in wild type cells expressing MAP2c. Cells can be slightly bent (a), curved with one end slightly swollen (c), branched (b) or T-shaped (d). In all cases microtubules are short and surround the nucleus. A late mitotic tubulin ring can be seen at the cell equator in dividing cells (d), and microtubules emerge from that region. Bar 10μm

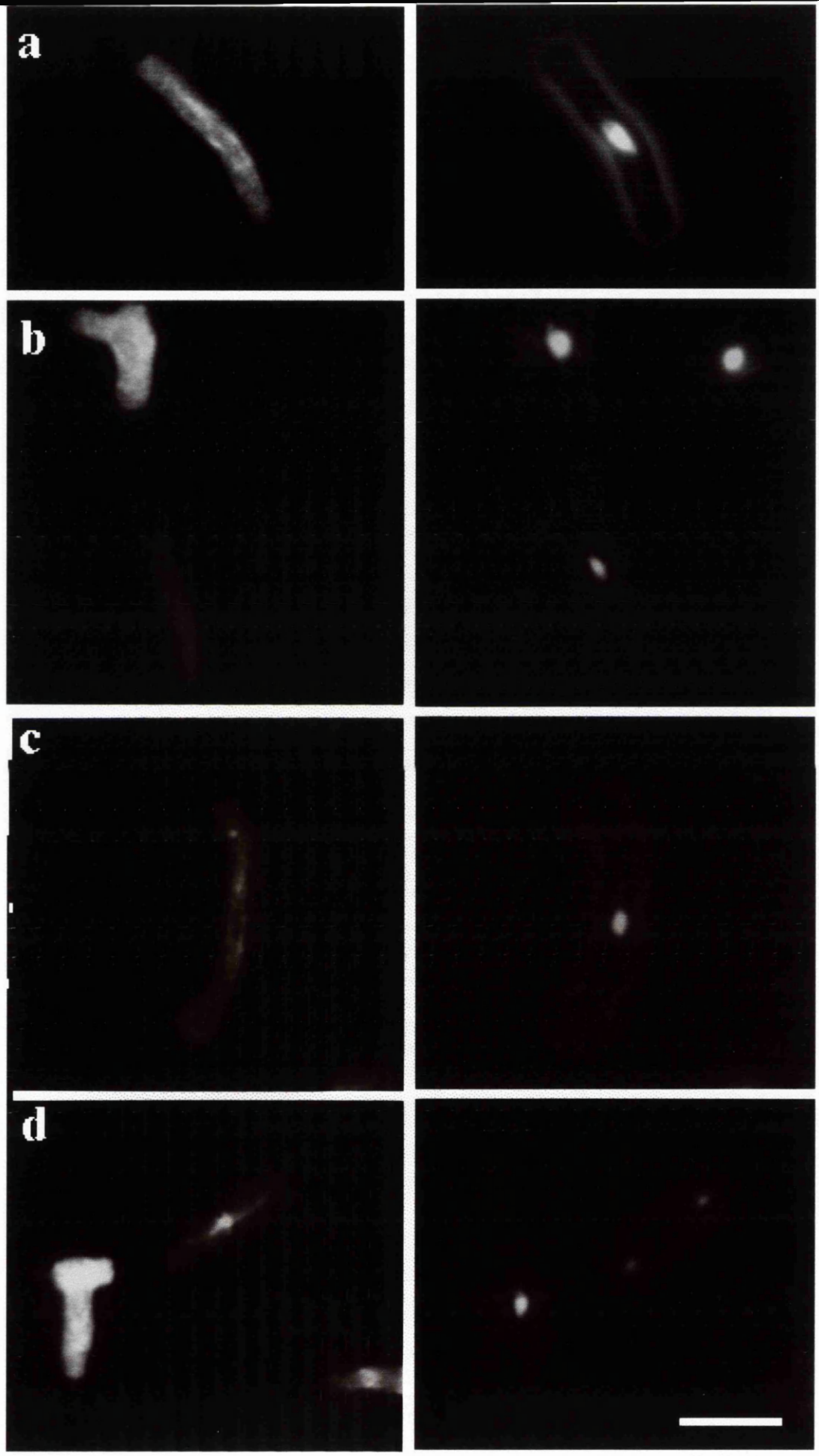
a
b
c
d

Figure 4.5 Anti-MAP2c staining immunofluorescence picture of wild type cells expressing MAP2c. Levels of MAP2c expression vary between cells (a). At low levels of MAP2c expression, filamnts can be distinguished, suggesting MAp2c binds to microtubules. There is no MAP2c expression in control cells (b). Bar 10 μm

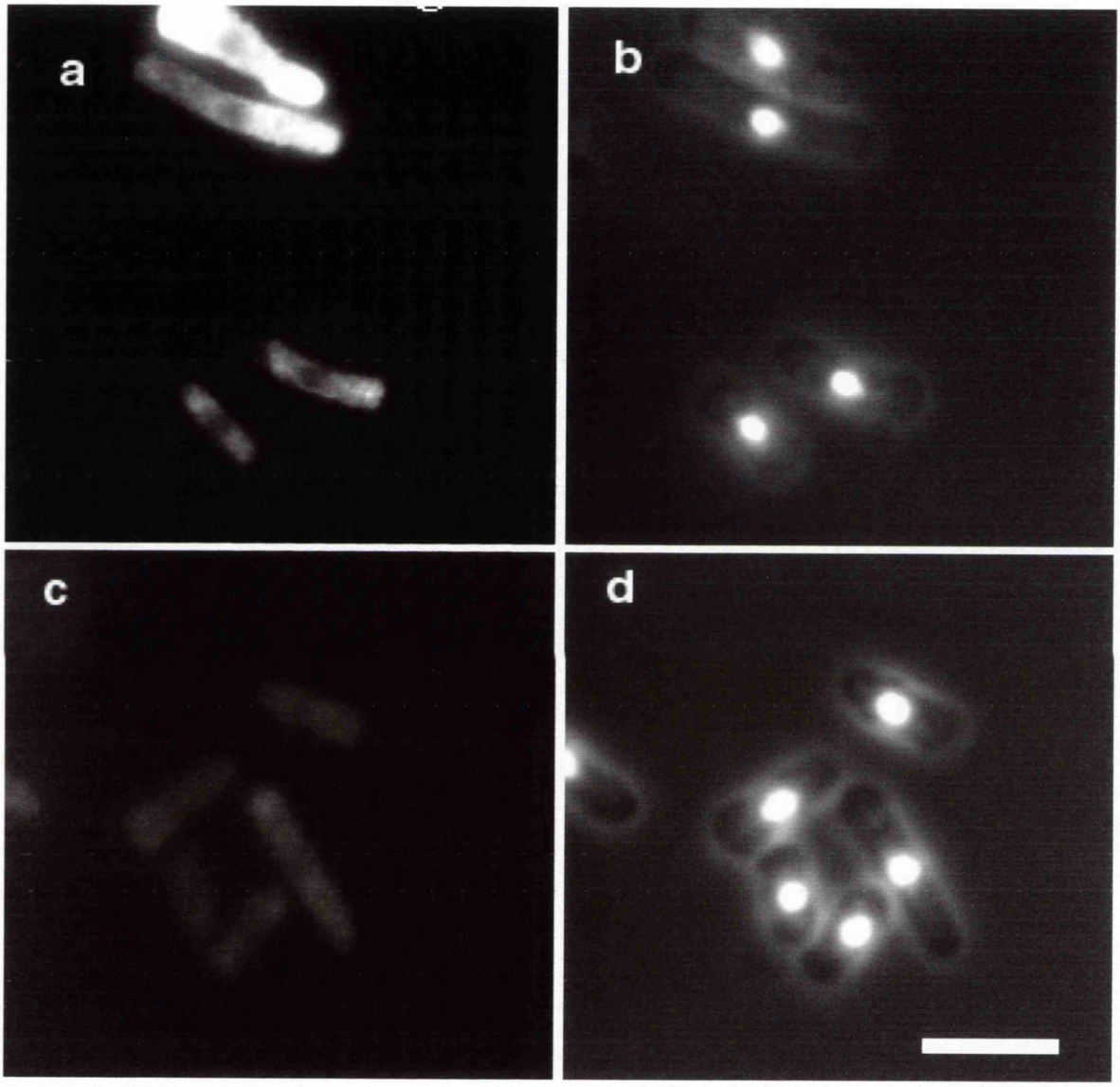
a
b
c
d

phenotype. However, in cells with lower levels of MAP2c, it appeared that MAP2c bound to microtubules as staining with the anti-MAP2c antibody showed the same 'filamentous' structure near the nucleus (Fig.4.5b). Fig. 4.5 c shows control cells, where no MAP2c is being expressed.

4.3.3 Effect of MAP4 on wild type fission yeast microtubules

MAP4 appeared to have a more potent effect on fission yeast microtubule organisation. Ectopic expression of MAP4 in fission yeast, as revealed by anti-tubulin immunofluorescence pictures, resulted in total depolymerisation of the interphase microtubules. Microtubule staining could be seen in the nucleus in some cells(Fig. 4.6 a). As with tau and MAP2c overexpressing cells, MAP4 expressing cells also showed a postmitotic tubulin staining ring at the cell centre. However, unlike tau and MAP2c expressing cells, these cells did not have microtubules emerging from the region of the tubulin staining ring (Fig.4.6b). Anti-MAP4 immunofluorescence, however, failed to show any evidence for the localisation of MAP4 to microtubules. Distribution of MAP4 was often assymetric and staining was more intense at one end of the cell than the other (Fig. 4.7). As with the other MAPs, MAP4 also appeared to vary in levels in different cells.

All three MAPs , when overexpressed in fission yeast, brought about a change in phenotype to varying extents. Both tau and MAP2c overexpression resulted in the occassional T-shaped cell, similar to the phenotype shown by fission yeast in the absence of the functional Tea1 protein. In a further effort to understand how microtubules and MAPs may influence cell morphology, tau and MAP2c were overexpressed in the *tea1* and *tea2* temperature-sensitive mutants. *tea1* and *tea2*

Figure 4.6 Microtubule and DAPI staining in wild type cells expressing MAP4. Cells are slihtly curved, and cytoplasmic microtubules appear totally depolymerised and tubulin levels are high. Some cells show tubulin staining of the nucleus (a). Dividing cells show a late mitotic tubulin staining ring at the cell equator (b) but no microtubules are seen emerging from the region of the ring. Bar 10 μm

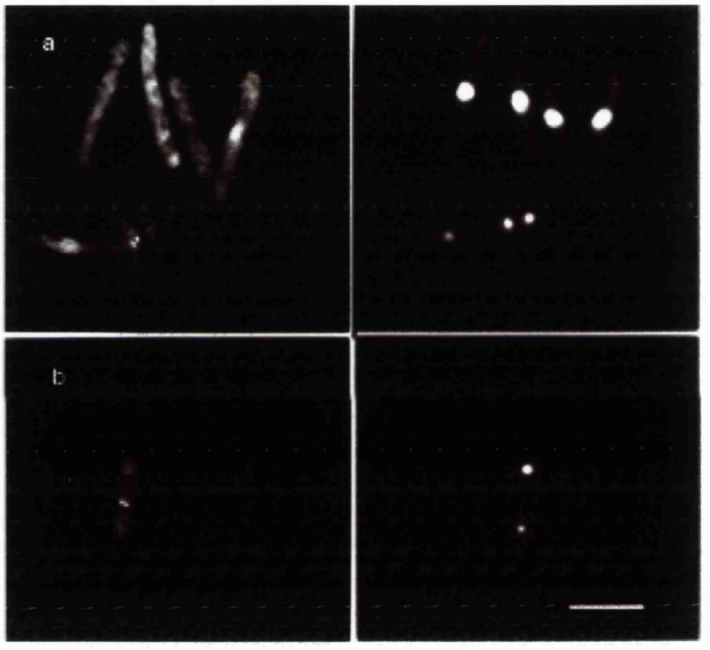
a
b

Figure 4.7 Anti-MAP4 and DAPI staining immunofluorescence picture of wild type cells expressing MAP4. MAP4 appears dispersed throughout the cell, with more intense staining at on end of the cell (a). Control cells (b) do not express MAP4. Bar 10μm

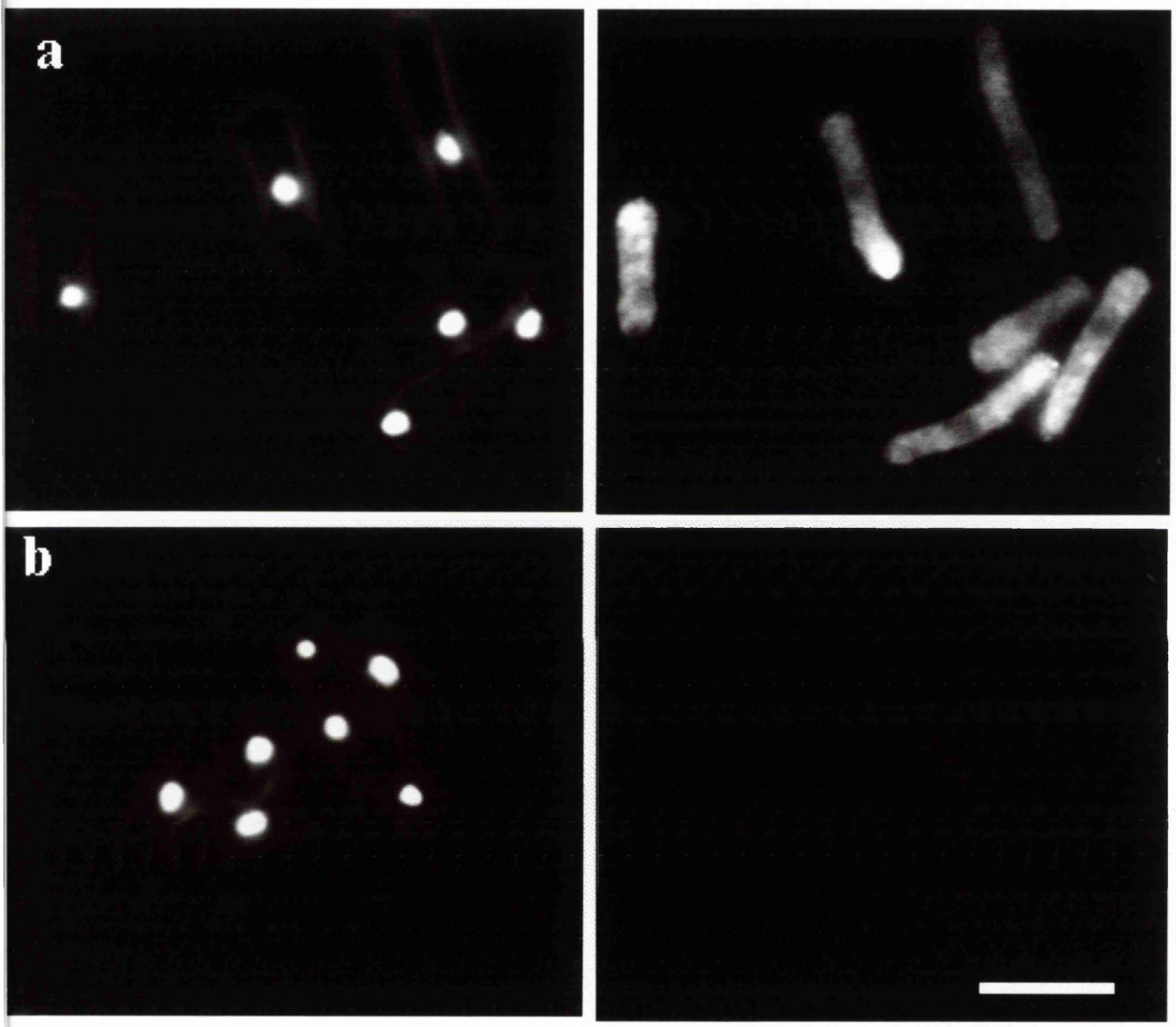
a
b

generally show a T-phenotype at 36^{0}C i.e. around 10% of the cells are T-shaped to varying degrees, whilst 90% appeared bent (Mata and Nurse, 1997; Verde et al., 1995).

4.3.4 Effect of tau and MAP2c on *tea1* cells

Control *tea1* cells not expressing any MAP show microtubules that appear to extend along both axes of the cell (Fig. 4.8 a). In bent cells the microtubules traverse across the length of the cell, but do not quite reach the tips (Fig. 4.8b). The nucleus in these cells appear to be centrally located at the point where the cell branches.

When *tea1* cells containing the plasmid pREP-tau or pREP-MAP2c were grown in the absence of thiamine for the first 30 hours at 36^{0}C, little difference was observed compared to the control cells. However, longer expression resulted in significant differences. Most tau-overexpressing cells were either bent (not shown) or had lost their T-shape and had expanded to produce a spherical 'bulbous' shape at one end (Fig. 4.9). In interphase cells, the microtubules appeared to traverse the cell, but were bundled and did not quite reach the cell tips (Fig. 4.9 a and b). Some cells were unable to form a normal spindle and showed a V-shaped tubulin staining pattern (Fig. 4.10 a) which is typical of mutants with a defective spindle pole body component or SPB-associated mitotic motor protein(Hagan and Yanagida, 1995). Others cells underwent nuclear division (fig.4.10 b,c), but showed a clear tubulin staining ring at the cell centre in late anaphase (Fig. 4.10 d, e, and f). Overall the effect of tau on phenotypic changes in the cells was weak.

Figure. 4.8 Microtubule and DAPI staining of control *tea1* cells containing the empty pREP1 plasmid. Cells appear T-shaped or bent and microtubules extend across both axes of the cell. Bar 10 μm

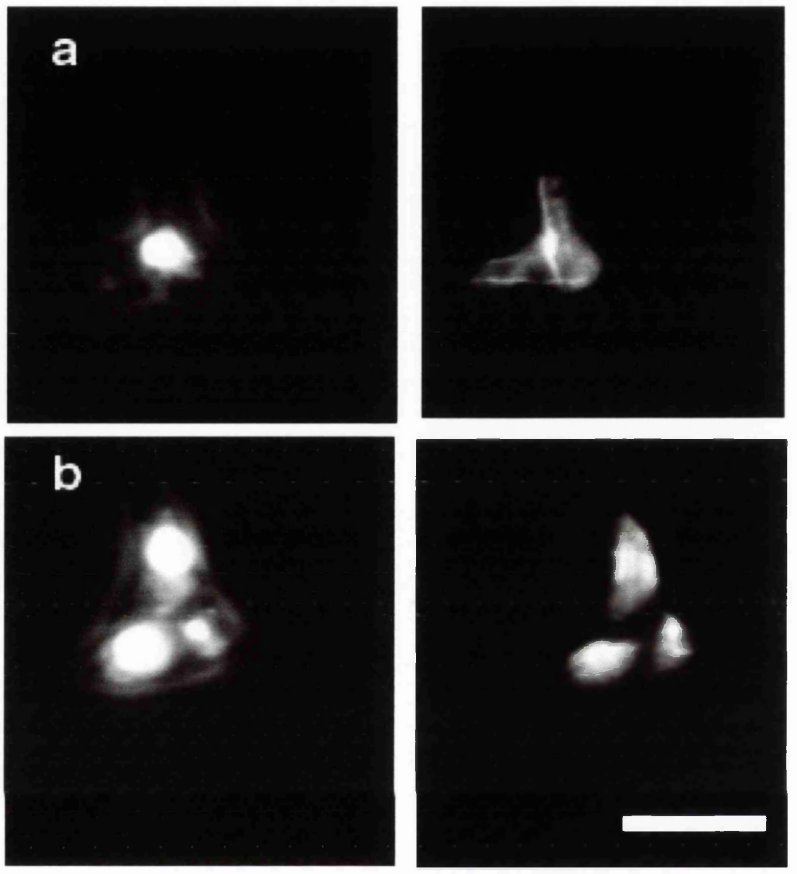
a
b

Figure 4.9 Microtubule and DAPI staining of tau expressing *tea1* cells. Cells appear bent and expanded at one end (a and b). Microtubules extend across the length of the cell, but there is no discernable tau-specific effect on microtubule arrangement. Bar 10μm

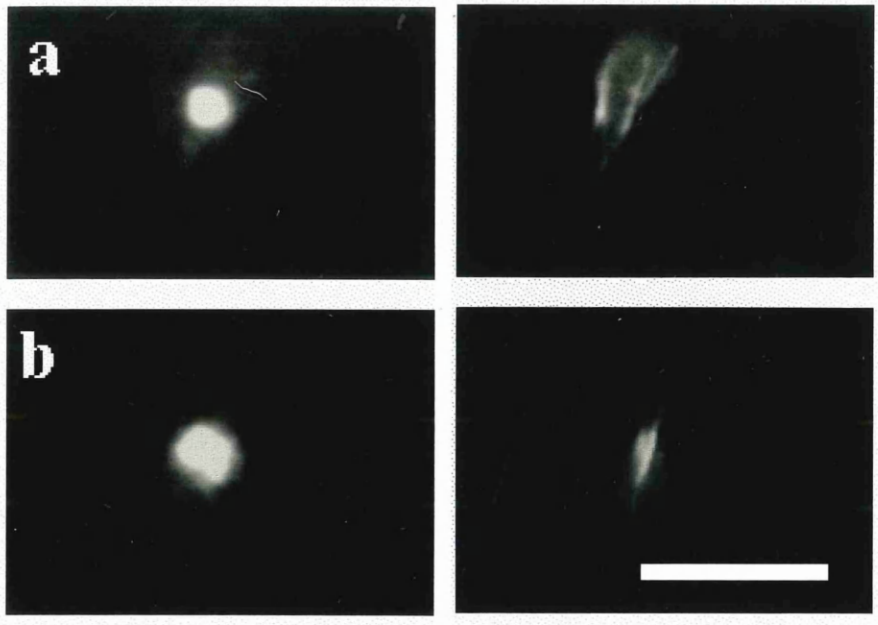
a
b

Figure 4.10 Microtubule and DAPI staining of tau-expressing *tea1* cells in various stages of cell division. A defective V-shaped spindle is seen in some cells (a). In others cell division appears to proceed normally in spite of the distorted cell phenotype (b,c,d,f). The spindle extends to traverse the length of the cell (b,c). In late anaphase and telophase, a tubulin staining ring appears at the cell equator (D,E and f). Bar 10μm

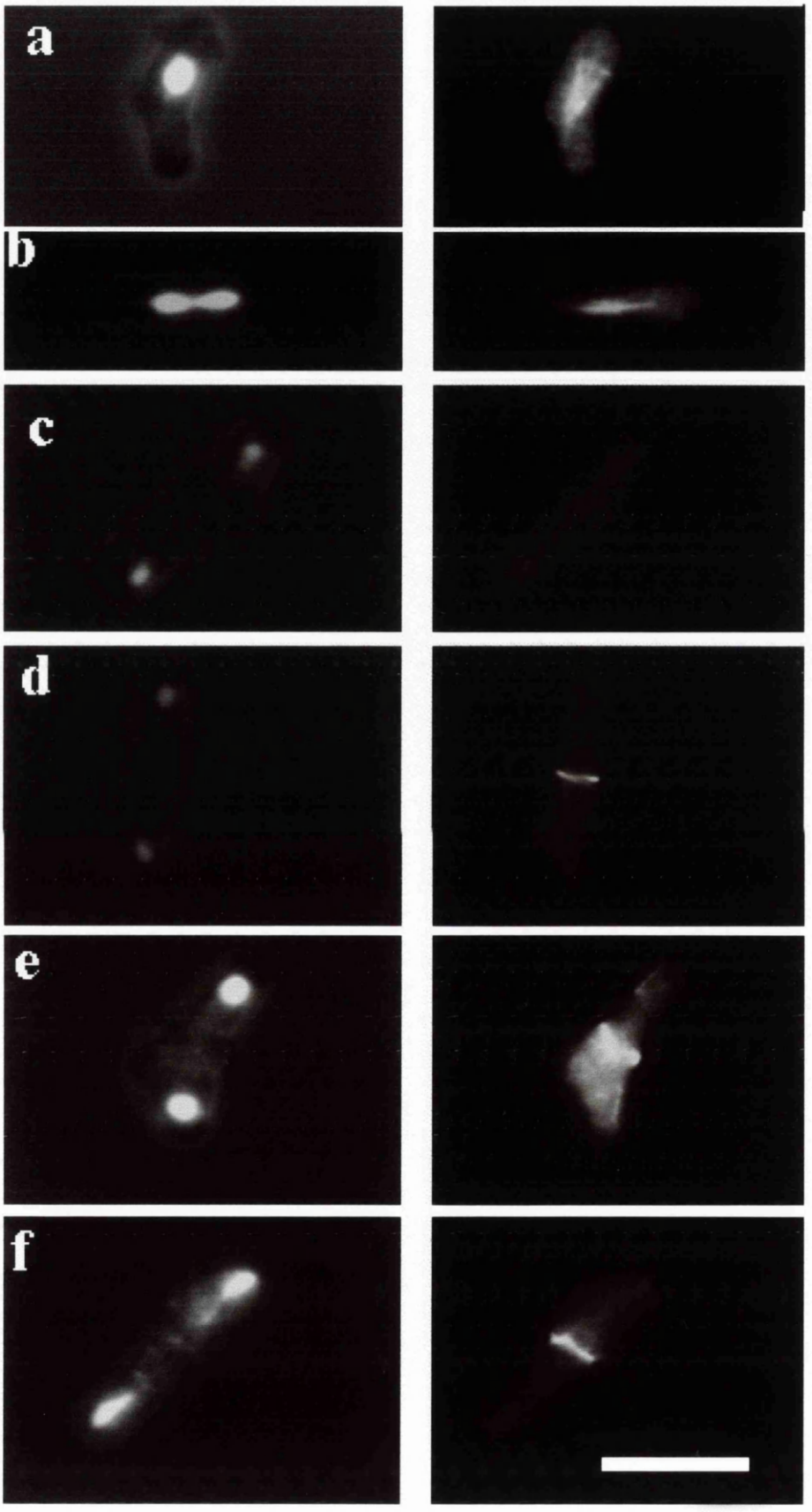
a
b
c
d
e
f

Figure 4.11 Anti-tau and DAPI staining of tau-expressing *tea1* cells, encompassing a range of phenotypes. Levels of tau expression vary amongst cells (a). In some cells expressing lower levels of tau, it appears to bind to microtubules in the region surrounding the nucleus(b). In other cells, tau is more uniformly dispersed throughout the cell. Where tau expression levels are very high, the cell fluoresces brightly and also appears to lose its shape totally (e). Figure 4.11 (f) shows control *tea1* cells where tau expression has not been detected. Bar 10μm

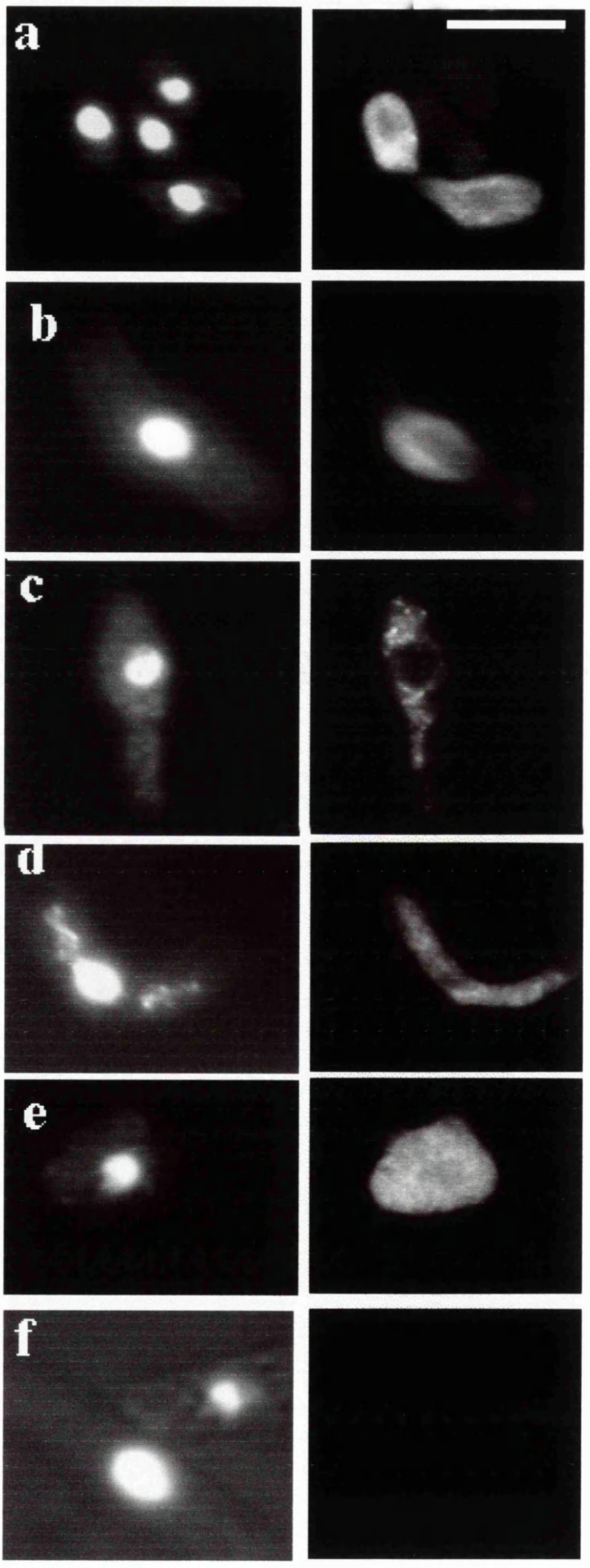
a
b
c
d
e
f

Immunofluorescence pictures of cells stained with the anti-tau antibody Tau-1 confirmed that tau was expressed in these cells (Fig. 4.11). Levels of tau varied between cells (Fig. 4.11 a), and its distribution varied within a given cell. In bent cells, or cells that were swollen in the centre, tau appeared to be localised to short microtubules around the nucleus, therefore it would appear that tau binds to microtubules in these cells (Fig. 4.11 b,c,d). In some cells, which appeared to have lost their shape, there were high levels of tau throughout the cell, so that cells appeared to glow brightly (Fig. 4.11 e). Staining of control cells with anti-tau antibody did not show any protein being expressed (Fig. 4.11f)

In contrast to tau, *tea1* cells overexpressing MAP2c at 36^0C, showed a dramatic effect at 35-40 hours. The cells appeared bigger and showed a range of phenotypes from slightly bent to hammer-shaped to bulbous to spherical. No actual T-shaped cells remained (Fig. 4.12). The nucleus, stained with DAPI, was positioned near the centre of the cell, or close to the bulbous end. As with wild type cells overexpressing MAP2c, *tea1* cell staining for tubulin revealed short microtubules that surrounded the nucleus (Fig. 4.12 a,b,c). Once again, as seen in all other MAP expressing cells, a late mitotic tubulin staining ring was seen in the cell centre (Fig. 4.12 c,d,and e). This ring appeared before the disappearance of the spindle, and was seen at right angles to the spindle in late anaphase (Fig. 4.12 c). Subsequently as the spindle disappeared (Fig. 4.12d) and the nuclei postioned themselves at the centre of the daughter cells, microtubules appeared to emanate from tubulin staining ring (fig. 4.12 e).

Figure 4.12 Microtubule and DAPI staining of *tea1* cells expressing MAP2c. Cells expand at one end so that phenotypes range from 'hockey stick' like appearance (d,e) to totally globular ends (a,b). The nucleus is located at the centre of the cell at interphase (b,a) and microtubules are short and surround the nucleus. In dividing cells, a tubulin staining ring ppears at the cell equator (c,d,e), crossing the spindle at late anaphase (c). As the nuclei return to the centre of the daughter cells , microtubules appear to emanate from the region of the tubulin staining ring (e). Bar 10 μm

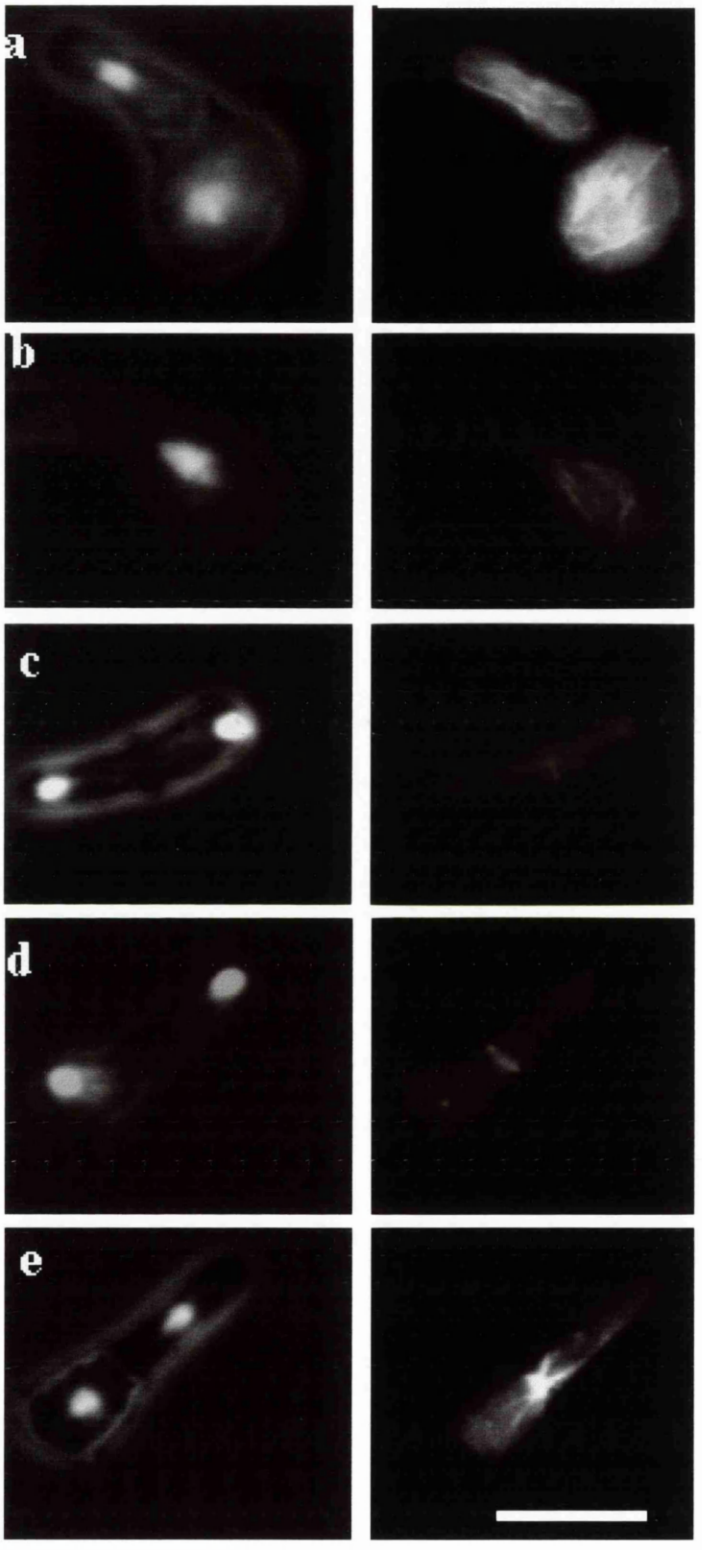
a
b
c
d
e

Figure 4.13 Anti-MAP2 and DAPI staining of *tea1* cells expressing MAP2c. Expression of MAP2c varies amongst cells (a,b,c,d and e). MAP2c is distributed throughout the cell, but this distribution appears asymmetric (c,d). At low levels of MAP2c expression, MAP2c appears to bind to microtubules near the nucleus(a,b). Control *tea1* cells did not stain with anti-MAP2 (e). Bar 10μm

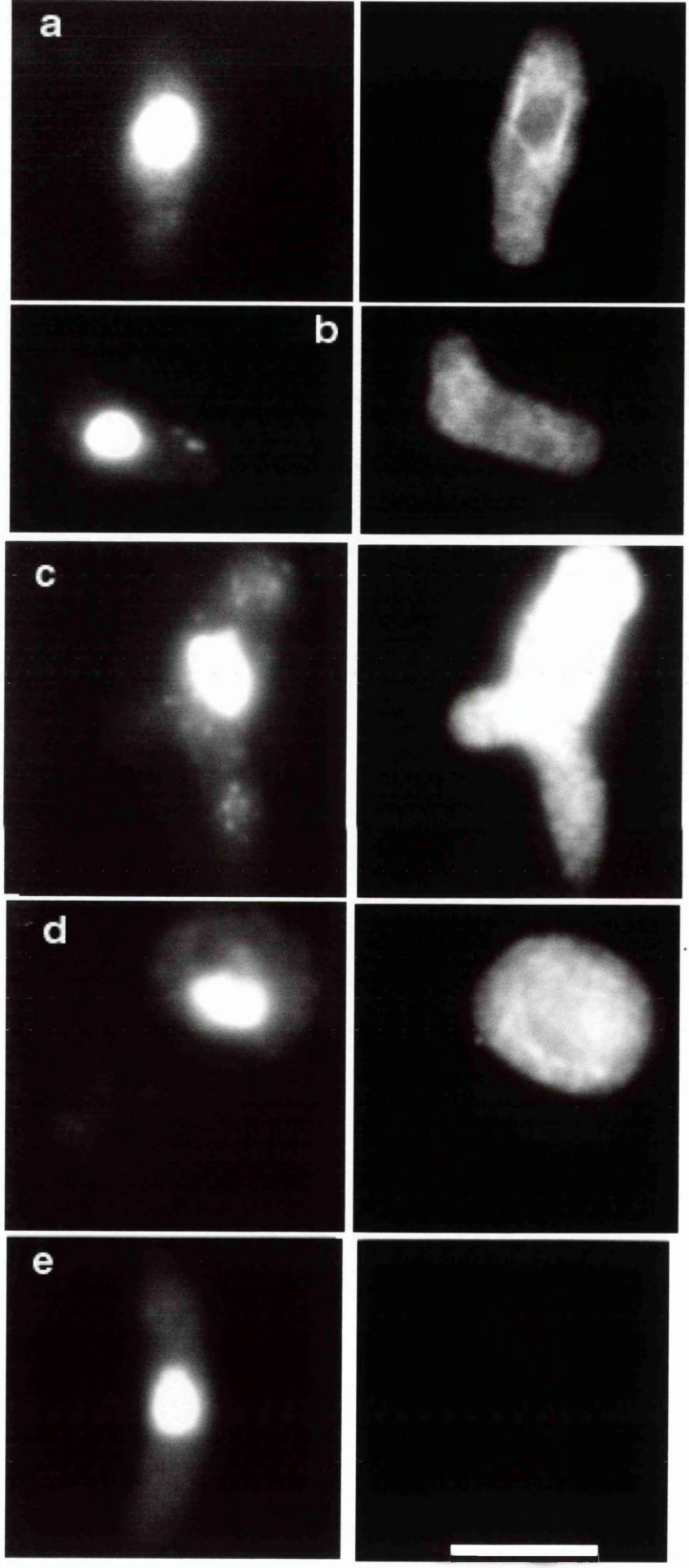
a
b
c
d
e

Immunofluorescence staining with anti-MAP2c revealed that the levels of MAP2c expression varied between cells. A microtubule-like pattern of staining could be distinguished near the nucleus in cells expressing lower levels of MAP2c, so it appears that MAP2c binds to microtubules (Fig. 4.13 a and b). In branched or bulbous cells, MAP2c distribution appeared polarised towards one of the branches (Fig. 4.13 c) or in the bulbous head (4.13 d).

4.3.5 Effect of tau and MAP2c on *tea2* cells

Temperature sensitive *tea2* cells, containing the empty pREP1 vector, showed mainly short microtubules when grown at 36^0C for 35 hours, although the occassional microtubule traversed the cell (Fig. 4.14). The cells were morphologically bent or T-shaped.

Tea2 cells overexpressing tau at 36^0C for 35 hours mostly remain morphologically similar to the control cells (Fig. 4.15, Fig.4.16), but approximately 1% of the cells show 'giant' tea cells (Fig.4.15). Microtubules appear localised near the nucleus, and were short, almost totally depolymerised. (Fig. 4.15 a, b). In dividing cells, microtubules that emanate from the MTOC at the cell equator were longer, but appeared to form a meshwork as they approached the nucleus (Fig.4.15 c). The levels of tau varied amongst different cells, but the localisation of tau appeared to be polarised. (Fig.4.16). In T-shaped cells, tau appeared to be more concentrated on one 'arm' of the cell (Fig. 4.16 a, c), whereas in bent cells, it was clearly more concentrated at one end (Fig. 4.16 b, d, e,f).

Figure 4.14 Microtubule and DAPI staining of *tea2* cells containing the empty pREP1 vector. Cells appear bent or T-shaped, with short microtubules along the longitudinal axis of the cell. Bar 10 μm

Figure 4.15 Microtubule and DAPI staining of *tea2* cells expressing tau. Although the cells appear to maintain their *tea* phenotype, some cells appear larger. Microtubules are localised near the nucleus and appear very short. Individing cells, microtubules emanating from the cell equator are longer compared to interphase microtubules, but appear as a meshwork. Bar 10 μm

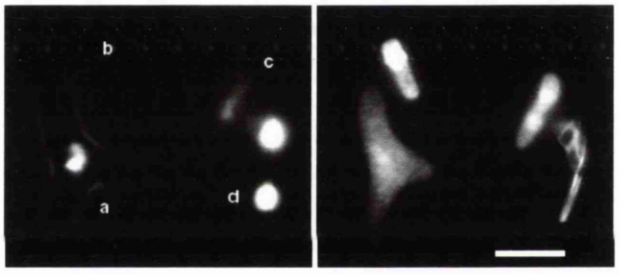
b
c
a
d

Figure 4.16 Anti-tau and DAPI staining of *tea2* cells expressing tau. Tau expression levels vary amongst cells. Although low levels of tau are seen throughout the cell, tau appears to localise more strongly to one region, either one end of a bent cell, or one of the branches of a T-shaped cell. Low levels of tau expresasion show that tau binds to microtubules. Bar 10μm

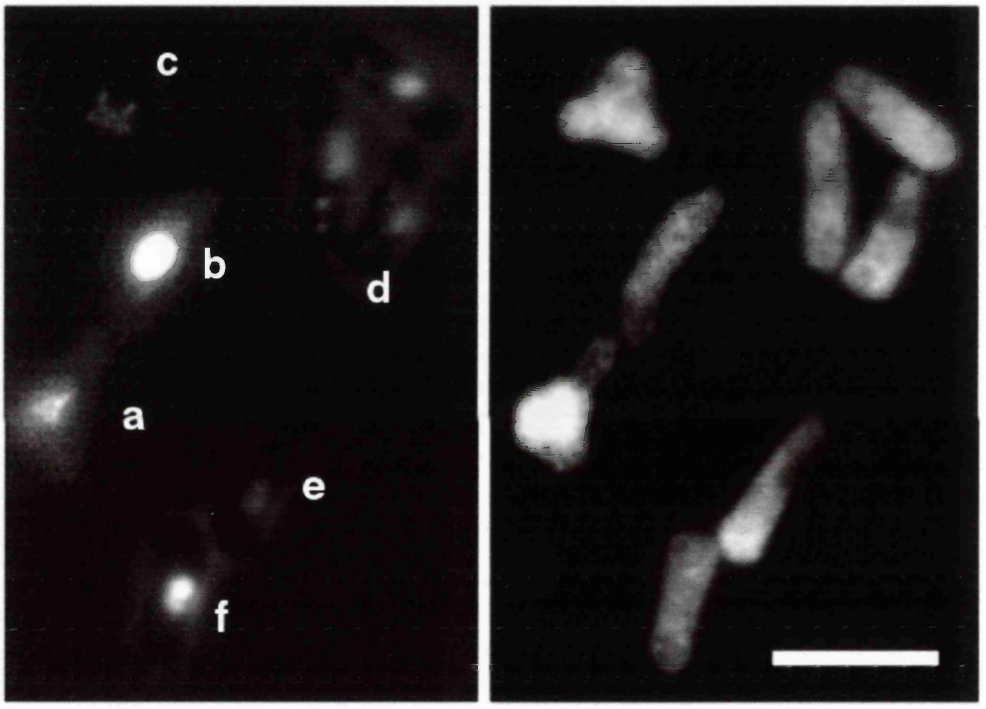
c
b
d
a
e
f

Figure 4.17 Microtubule and DAPI staining of MAP2c expressing *tea2* cells. Cells appear larger compared to the control cells, and misshapen. One end of the cell appears expanded to form a globular shape. In most cells, microtubules appear almost totally depolymerised, with high levels of tubulin in the cell. Tubulin localisation appears polarised in some cells. In Other cells, microtubules are intact but located near the nucleus at one end of the cell. Bar 10μm

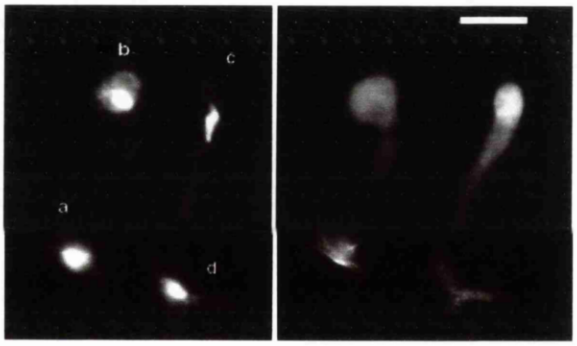
b
c
a
d

Figure 4.18 Anti-MAP2c and DAPI staining of *tea2* cells expressing MAP2c. Expression levels of MAP2c vary amongst cells, and appears highest in cells that have lost their shape totally and become spherical. Distribution of MAP2c appears polarised, and localised to the expanded globular end of the cell. The nucleus also appears to be located to the globular end of the cell. Bar 10μm

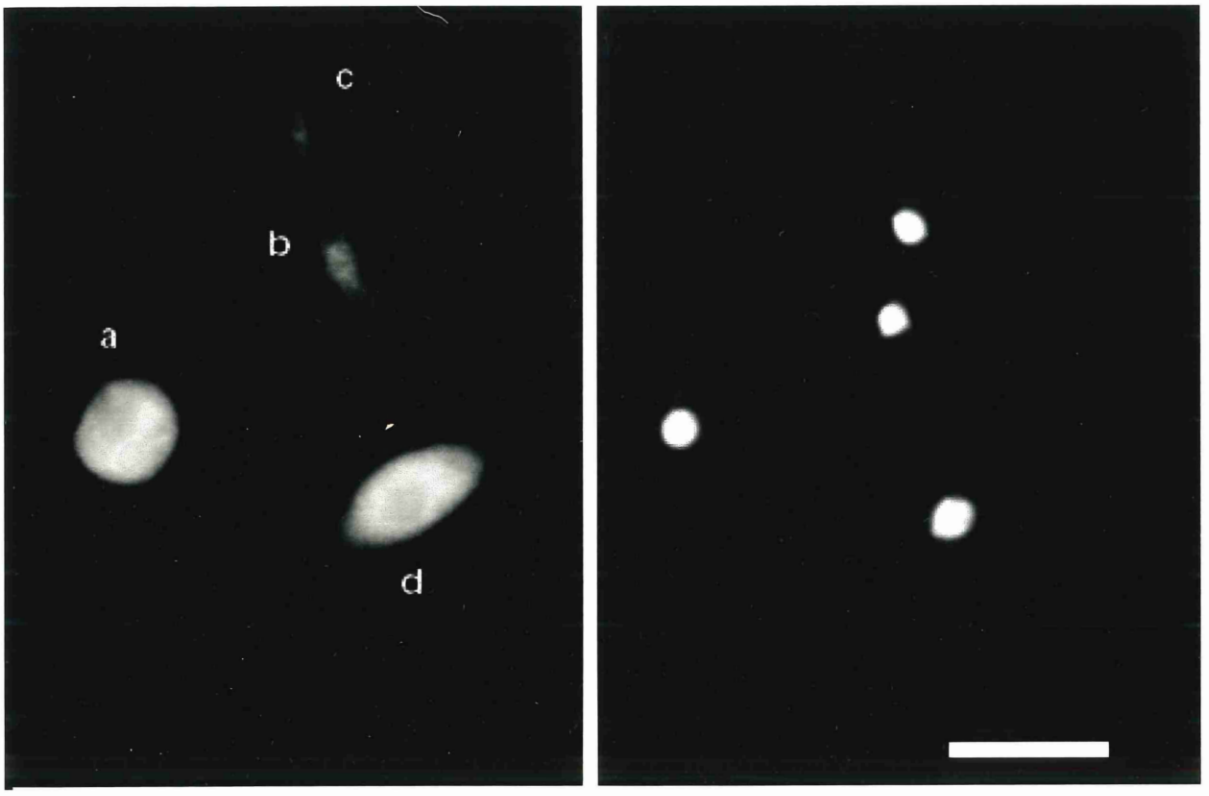
c
b
a
d

Overexpression of MAP2c in *tea2* cells grown at 36^0C for 35 hours results in dramatic morphological changes to the cells (fig. 4.17). Some bent cells appeared grossly swollen at one end. (Fig. 4.17 a). Other T-shaped cells appeared more like catapults (Fig. 4.17b). Some cells exhibited slightly swollen T-shapes (Fig. 4.17c) , while others were long and bent, giving a worm-like appearance (fig.4.17d). In most cells, microtubules appear almost totally depolymerised, and the brightness of some cells at one end (fig. 4.17d) suggest that there is polarised localisation of tubulin in the cells. In a few cells (fig. 4.17c) microtubules are intact, although abnormal in distribution. The levels of MAP2c, as seen by immunofluorescence after staining with ant-MAP2c polyclonal antibody, vary between cells, but appear mainly around the nucleus of the cell.

4.4 Discussion

The MAPs tau, MAP2c and MAP4 all belong to the family of type II MAPs (Bulinski, 1994; Goedert et al., 1994; Matus, 1994). They have in common three or more imperfect repeats of an 18 amino-acid sequence at their C-terminus, with proline rich regions flanking these repeats, an ability to bind microtubules via the region containing these repeats, heat stability, and several sites that could be the potential targets of various kinases (reviewed by (Mandelkow, 1995)). However, the fact that there are so many mammalian MAPs with apparently similar functions, leads to the question why there should be such redundancy of function. The fact that they are tissue-specific, developmentally regulated and specifically localised within cells where they are expressed, indicates that despite their similarities, MAPs might have

specific, distinct roles. Many different approaches have been used to elucidate the functions of these MAPs. Anti-sense oligonucleotides have revealed that tau is necessary for axon formation while MAP2c is required for minor meurite formation (Caceres and Kosik, 1990; Caceres et al., 1992). Expression of MAP2 and tau in insect cell lines such as Sf9 resulted in long processes being formed, thereby indicating that MAP2 and tau influence cell morphology. Expression of these MAPs in mammalian non-neuronal cells has revealed that all MAPs stabilise microtubules into the formation of bundles (Bulinski, 1994; Goedert et al., 1994; Matus, 1994). Barlow *et. al.* (1994) compared tau and MAP4 by overexpression in CHO cells, and concluded that the MAPs have differing roles *in vivo* as although both stabilise microtubules, only tau produces bundles (Barlow et al., 1994). However all three MAP functions do not appear to have been compared in one system in order to elucidate their similarities and disparities in function. Therefore we attempted to compare the effects of overexpression of all three MAPs.

As detailed in the previous chapter, fission yeast is an ideal organism in which to compare the effects of the overexpression of the three MAPs. It has no reported MAPs that may interfere with the functions of mammalian MAPs. However, it was possible that the mammalian MAPs would be unable to bind to fission yeast microtubules despite the approximately 70% homology to mammalian tubulins (Yanagida, 1987) . The chicken βII tubulin isoform contains the sequences YQQYQDATADEQG and GEFEEEGEE, which have been shown to interact with MAP2 (Cross et al., 1991) (Luduena, 1993). The corresponding sequences in fission yeast, YQQYQEAGIDEGD and DEDYEIEEEare similar enough so that it is reasonable for MAPs to bind these sequences too (Yanagida, 1987).

All of the experiments reported here are based on the expression of the vector pREP1 (Maundrell, 1993). Since it is not possible to standardise plasmid copy number, the level of expression of a heterologously expressed protein varies considerably from cell to cell (Tournier et al., 1996), and this report confirms this observation. This complicates the analysis since cells expressing all three MAPs examined were heterogenous with regards to phenotype.

Overexpression of tau in fission yeast did not have a significant effect in most cells, both in terms of morphology and in terms of microtubule organisation, compared to the +thiamine controls. However, in a minority of cells, the microtubules appeared as thick bundles running the length of the cells but displaced towards the cell periphery. This is similar to the effects of tau on microtubules in non-neuronal cells (Baas et al., 1994; Barlow et al., 1994; Goedert et al., 1994; Preuss et al., 1997). One way of explaining the bundling effect of tau on microtubules is by the 'jaws' model of tau-microtubule interaction (Mandelkow, 1995; Mandelkow, 1995). In this model, it is not the repeats of 18 amino acid motif at the C-terminal end, but the regions flanking the repeats, the 'targetting' domain, that position the MAP on the microtubule surface and cause tight binding. By themselves, the repeats do not bind tightly to microtubules or add to their stability. However, once positioned on the microtubule, the repeat sequences appear to promote microtubule assembly (Mandelkow, 1995; Preuss et al., 1997). Preuss *et. al.* (1997) suggest that bundling occurs due to high activity of microtubule assembly in a restricted space, so that the microtubules become aligned in a liquid-crystalline manner. Tau, with its microtubule stabilising properties, is responsible for increasing the levels of *de novo* assembly, and could also

modulate surface charge to allow microtubules to be packed together. Tau could also act as a physical spacer.

A small proportion of tau cells are T-shaped, or branched, or long or multiseptate, phenotypes observed when fission yeast microtubules are destabilised by mutations in the β tubulin gene *nda3* (Hiraoka et al., 1984) or following treatment with TBZ (Toda et al., 1983; Umeneso et al., 1983) (Sawin and Nurse, 1998). Thus high levels of tau expression appear to destabilise rather than stabilise fission yeast microtubules. However, since microtubule bundles have also been observed in tau-expressing fission yeast cells, it could be the lack of dynamic microtubules, either due to bundling or destabilisation, that leads to the obseved phenotypes. Fission yeast cells extend at their tips due to the action of the polarity-determining Tea1 protein, which is maintained at the cell poles by microtubules (Mata and Nurse, 1997). It is possible that microtubule stabilisation by tau could affect the localisation of Tea1p at the tip of the microtubules, leading to branching. As the cell passes the G2/M boundary, microtubules depolymerise and Tea1 is displaced from the cell tips. Stabilisation of microtubules would mean that Tea1 is 'frozen' in position where it continues to signal to the cell to carry on growing, leading to long cells.

As the majority of cells overexpressing tau appear normal, it appears that tau does not have a potent effect on fission yeast. Immunofluorescence pictures of fission yeast using an anti-tau antibody show that tau binds to microtubules. The lack of resulting phenotype might argue against the existence of endogenous fission yeast MAPs which, it could be argued, would be displaced by competition by tau for microtubule binding sites. It might also be argued that fission yeast microtubules are not as

dynamic as mammalian microtubules, and therefore relatively insensitive to the stabilising effects of the foreign MAP.

Compared to tau, MAP2c had a greater effect on fisssion yeast microtubules. In the previous chapter, it was seen that the majority of MAP2c overexpressing cells underwent significant morphological changes. Cells were generally long or bulbous, with occasional tea-shaped or bent cells. These changes appear to reflect changes in the organisation of the microtubule cytoskeleton. As seen by indirect immunofluorescence microscopy, microtubules in MAP2c-overexpressing fission yeast cells were short and extended on either side of outside the nucleus. This observation appears contradictory to reports that MAP2c stabilises and bundles microtubules both *in vivo* and *in vitro,* in insect and mammalian cells (Chen et al., 1992; Gamblin et al., 1996; Umeyama et al., 1993). On the contrary, it argues that MAP2c depolymerises fission east microtubules. Interestingly, short microtubules due to the overexpression of MAP2 has been reported in PLC cell lines (Matus, 1994).]. Why microtubules do not completely depolymerise is not known but similar short microtubule fragments around the nucleus are seen following treatment of cells with TBZ (Sawin and Nurse, 1998). The depolymerising effect of MAP2c is further confirmed by the increased background staining of tubulin in MAP2c expressing cells, presumably reflecting the rise in the pool of soluble tubulin dimers. In the experiments reported here MAP2c expression levels varied greatly between the cells. Cells expressing the highest levels of MAP2c were brightly fluorescent, preventing direct observation of microtubules. In cells expressing lower levels of MAP2c however it was clear that MAP2c bound to microtubules. Umeyama *et. al* (1993) also reported that biotin-labeled tubulin were incorporated into the distal ends of

microtubule bundles in fibroblasts overexpressing mouse MAP2c. In the fission yeast system too, the dynamics of microtubules in the presence of MAP2c appears to be regulated at the microtubule ends, although with an increase in subunit disassociation rates. An alternative explanation might be that MAP2c binds to tubulin dimers, shifting the intracellular equilibrium betwwen polymer and subunit to favour depolymerisation. Although such hypotheses might explain why microtubule depolymerisation fails to go to completion, it is contrary to what we understand about the interactions of MAP2c with microtubules both *in vivo* and *in vitro* (Gamblin et al., 1996).

In the previous chapter, it was shown by western blotting that MAP2c undergoes partial proteolysis in fission yeast, possibly due to the presence of its PEST sequence. This could result in MAP2 fragments having altered affinity with microtubule ends. MAP2 binding can be regulated by phosphorylation (Matus, 1994). MAP2 is a substrate for a wide variety of kinases, such as mitogen-activated kinases, cyclic-AMP dependant kinases, calcium-calmodulin-dependant kinases, and MARKs (MAP/microtubule affinity regulating kinases) (Matus, 1994) (Drewes et al., 1997). Most of these kinases have homologues in *S. pombe* that should be able to act on MAP2c. For example, the catalytic domain of MARK1 has 50% homology with the *S. pombe* gene *kin1* (Drewes et al., 1997) [Levin, 1990 #124. Both tau and MAP2c were expressed in *kin1*+ deleted cells (results not shown), but did not show any change in phenotype compared to the +thiamine controls. Phosphorylation of MAP2c by kin1p may therefore indeed play a part in the distinct phenotypic effectt of MAP2c on fission yeast cells. The different morphologies such as bulbous -shaped and T-

shaped cells could be due to erroneously placed marker proteins for cell growth such as *tea1*, due to the short microtubules.

Overexpression of MAP4 on fission yeast also has a dramatic and unexpected effect on *S. pombe*. The interphase microtubules appear to be depolymerised, and some cells contain spindles, indicating that MAP4 pushes the cell towards the M-phase. This is contrary to our understanding of the role of MAP4 as a protein that stabilises microtubules (Bulinski, 1994) (Olson et al., 1995). Immunofluorescence microscopy of cells expressing MAP4 stained with anti-MAP4 antibody showed that MAP4 was dispersed throughout the cell. MAP4 has been shown to regulate the depolymerisation of microtubules at the onset of M-phase in mammalian cell lines such as Hela cells and CHO cells when it is phosphorylated by the cdc2 kinase (Ookata et al., 1995; OOkata et al., 1997; Ookata et al., 1993). It is possible that the fission yeast cdc2 kinase phosphorylates MAP4, leading to microtubule depolymerisation. However, this event would be expected as a result of the cell approaching mitosis, rather than an essential step that leads the cell to mitosis. These results might reveal a more active role role for MAP4 in bringing about the role of mitosis. Alternatively, the part of the MAP4 fragment that is missing in this plasmid may contain the cdc2 phosphorylation site and therefore inactivated by cdc2 kinase during mitosis, and this may be a signal for the onset of mitosis and depolymerisation of microtubules. Overexpression of MAP4 with this portion missing may accelerate the cell into mitosis, overriding other checkpoints. Further experiments are required, with different regions of MAP4 being expressed to confirm whether this is true. If it is so, it would indicate a novel function for MAP4, whose role has not been totally clear from previous studies.

All three MAPs tau, MAP2c and MAP4 effect *S. pombe* morphology in various ways and to varying degrees. Overexpression of both tau and MAP2c results in a few t-shaped cells, similar to the tea-shaped cells resulting from the lack of the *tea1* gene in *S. pombe*. Both tau and MAP2c were therefore overexpressed in *tea1* temperature-sensitive mutants to study how each affect the morphology of *tea* cells, and in the process, get a better idea of how cell morphology in cells may be affected by MAPs and microtubules.

The *tea1* gene is required for the fission yeast cell to maintain growth in a longitudinal manner, with the two tips precisely opposing each other (Mata and Nurse, 1997; Verde et al., 1995). Tea1p acts as a tightly localised end marker, and appears to rely on microtubules for maintainence at the cell tips(Mata and Nurse, 1997). In the absence of the functional *tea1* protein, the cells do not grow with the tips precisely opposite. Instead the tip centres are at an angle, and the size of this angle determines whether the cells are slightly bent or whether an extra tip is generated to produce a T-shaped cell (Mata and Nurse, 1997).

Overexpression of tau did not have a markedly different effect on *tea1* cells compared to the controls. Most cells were bent or had various degrees of T-shapes. However, a small percentage of cells did appear to have completely lost polarity, whilst others displayed a spherical end. In these cases, tau appeared to be concentrated in the regions that had lost their shape, as seen by anti-tau immunofluorescence staining. As in wild type cells, the microtubules appeared to be bundled by tau, as seen by the relative thickness of the fibres. However, cell division appeared to continue. In some

cells, the spindle appeared to be unipolar and V-shaped, suggesting tau may somehow affect the migration of the spindle pole bodies in *tea1* cells. Although nucleolar localisation of tau has been reported in CG neuroblastoma cell lines (Thurston et al., 1997), anti-tau antibodies did not show the presence of tau in the nucleus in fission yeast.

Overexpression of MAP2c in *tea1* cells results in a greater change in morphology. Although many cells appeared similar to the control, many cells were larger, and had become spherical. Other large cells had a bulbous end. Cells appeared to divide normally. Microtubules in interphase cells were short and surrounded the nucleus, as in wild type cells overexpressing MAP2c. MAP2c also appeared to bind to microtubules, and the phenotypic variations could, once again, be explained by the variations of the level of MAP2c in different cells. Although MAP2c appeared to be distributed throughout the cell, in some cells, the anti-MAP2c staining was more intense at one pole. In bulbous shaped cells, MAP2c appeared to be present almost entirely in the spherical head.

In both tau and MAP2c overexpression in *tea1* cells, the effect the MAPs had on microtubules was not significantly different from the effect the MAPs had on microtubules in wild type cells. However, the resulting morphological change in was far greater in the absence of a functioning Tea1 protein. This could mean that there are other proteins that play a part in dictating fission yeast morphology along with the Tea1p, and that these proteins are also dependant on the microtubule organisation for their localisation and/or function. The function of such proteins could either overlap, or be close linked to that of the tea1 protein. For example, fission yeast mutants such

as *ban3.2* and *ban4.81* are bent, and *orb* mutants of fission yeast are spherical. The products of these genes therefore appear to be connected to fission yeast morphology, and the change in microtubule organisation due to the MAPs could directly affect their function. Alternatively, the MAPs themselves, irrespective of their effect on the microtubule organisation, could affect cell morphology by blocking/replacing/inactivating the proteins that direct cell morphology. For example, deletion of the gene *mal3* results in branched and bent cells in fission yeast, and also result in short microtubules around the nucleus, similar to the effects of MAP2c overexpression (Beinhauer et al., 1997). It is possible that MAP2c physically blocks the interaction of Mal3p with microtubules, resulting in a phenotype similar to the *mal3* deletion, and this is more potent in *tea1* cells as Tea1p is also involved in directing cell growth at the correct location. Overexpression of the MAPs, especially MAPs tagged with the green fluorescent protein, in other morphological mutants, will reveal more about how *S. pombe* morphology is regulated by microtubules and possible microtubule associated proteins.

The role of Tea2p in microtubule polarity is not clear, although it clearly has a role as its absence results in bent and T-shaped cells, as well as short microtubules (Verde et al., 1995). Recently Tea2p has been identified as a kinesin (Hayles and Nurse, personal communication) and it is therefore likely that Tea2p is the motor that transports Tea1 to the cell tips. Both tau and MAP2c appear to exacerbate the effects of the lack of a functional Tea2p on the cell, particularly MAP2c. Kinesin and tau or MAP2 have been reported to compete for almost the same binding domains located at the carboxy-terminal side of α- and amino-terminal site of β-tubulin in neuronal cells (Hagiwara, 1994). Furthermore, the projection of tau and MAP2 was shown to inhibit

the binding of kinesin by steric hindrance, with MAP2 showing a more potent effect (Hagiwara, 1994; Heins et al., 1991).

Tau overexpression in *tea2* cells result in the microtubules becoming even shorter than the controls. However, tau does not bring about any significant changes in phenotype. The tea2p is not absent at 36^0C, merely non-functional. It is possible that the interaction of tau to Tea2p changes its structure in a way that encourages further microtubule depolymerisation.

The presence of MAP2c in the absence of a functional tea2p results in a dramatic change/loss of shape in fission yeast cells. The effects of MAP2c overexpression on *tea2* cells, may be similar to that proposed for tau, above. Alternatively, MAP2c may interfere with mechanisms that co-opearate with tea2p to regulate cell morphology. Overexpression of a small GTP-binding protein Rho2 leads to aberrantly shaped fission yeast cells (Hirata et al., 1998), similar to those seen when MAP2c is overexpressed in *tea2*. A GTP-binding protein of the rho family is also essential in establishing a polarised site for budding in *S. cerevisiae* (reviewed by (Mata and Nurse, 1998)). Rho1 in fission yeast has been shown to target the enzyme 1,3--glucan syntase, involeved in cell wall biosynthesis, while rho1 could be linked to protein kinase C. MAP2c and tau are also substrates for protein kinase C (Matus, 1994), and therefore large amount of MAP2c, produced due to overexpression, may interfere and block signalling pathways that direct cell morphology and growth.

The one common effect of all three MAPs was to stabilise a late mitotic tubulin ring at the centre of the fission yeast cell. This effect was seen in wild type, *tea1* and *tea2*

cells following MAP expression, but was rarely seen in control cells. Pichova *et. al* (1995) had reported an equatorial tubulin ring at anaphase and telophase, which colocalised with an actin contractile ring, suggesting that they may control the plane of cell division cooperatively (Pichova et al., 1995). MAP2c has been reported to be an efficient actin gelling protein which organises actin filaments into organised arrays (Cunningham et al., 1997). Tau has also been reported to interact with the neural plasma membrane with its N-terminal domain in its role in establishing neural polarity (Brandt, 1995). The observations in *S. pombe* that all three MAPs stabilise the equatorial tubulin ring in late mitosis suggests that one of the functions of type II MAPs may be to mediate interactions between actin and microtubules to direct cell polarity or cell division.

5. Effect of the MAPs tau, MAP2c and MAP4 on Organelle distribution in fission yeast

5.1 Introduction

Eucaryotic cells employ a strategy of division of labour amongst organelles, as compartmentalization provides the advantage of allowing enzymes to operate more efficiently, and separating competing reactions. Compartmentalization, however, requires developing specific processes to ensure correct targetting and delivery of enzymes and substrates to the proper organelles. Coordination of the roles and spatial distribution of different organelles is therefore essential for the survival of the cell, and every membrane-bound organelle has a characteristic copy number, size and position which reflects its function in the cell type.

Mitochondrial distribution depend on the energy requirements within the cell. Mitochondria are generally stiff and cylindrical shaped but they are mobile and plastic and can even fuse with each other and then separate. They contain their own DNA which generally code for some mitochondrial proteins, such as ATP synthase and cytochrome c (Bereiter-Hahn, 1990), although the majority of proteins for ATP synthesis in the mitochondria are transcribed in the nucleus. Mitochondria are abundant in energy-dependant cells such as muscle cells, where they are interwoven with the myofibrils that generate mechanical force. They provide the energy needed for sperm movement by being arranged tightly wrapped around the flagella. In ion-transporting epithelial cells, they are found interspersed within the substantial folds of

the plasma membrane, across which a high flux of ions is pumped. Mitochondria are packed together in longitudinal arrays in the inner segments of retinal rods and cones, where they provide the energy for the phototransduction process (reviewed by (Warren and Wickner, 1996)). In the budding yeast *S. cerevisiae*, mitochondria have been observed, using flourescent dyes, as tubular organelles aligned in radial arrays that converge at the bud neck (Simon et al., 1995). Studies of mitochondrial distribution in avtin and myosin mutants of budding yeast reveal that mitochondrial motility in this organism is actin-dependant (Simon et al., 1995). However, chemicals that disrupt microtubule function do not appear to affect mitochondrial distribution or the movement of mitochondria into the neck of the budding yeast (Jacobs et al., 1988).

Mitochondria in living fission yeast cells have been studied by staining the organelle with the fluorescent dye DASPMI (dimethylaminostyrylmethylpyridinium) as it cannot be easily observed by simple phase-contrast microscopy. Robinow and Hyams (1989) have described mitochondria in fission yeast as generally stretched over the full length of the cell, and arranged approximately parallel to each other in what appears to be an inherently organised pattern (Robinow and Hyams, 1989). Cell division results in disarray and fragmentation of the mitochondria, which subsequently fuse to restore the long snaky pattern in the daughter cells (Robinow and Hyams, 1989). Mitochondrial distribution in wild type fission yeast cells have also been described by Yaffe et. al (1996) as extended tubules or tubular networks extending the length of the cell. Using a number of *S. pombe* temperature-sensitive or cold-sensitive mutants such as *ban-5* and *nda2* and *nda3*, which result in a disrupted microtubule cytoskeleton, to study mitochondrial distribution , it has been shown that

mitochondrial distribution in fission yeast cells is regulated by microtubule organisation (Yaffe et al., 1996).

Organelles of the central membrane system in eucaryotes, the endoplasmic reticulum (ER), the golgi apparatus, endosomes and lysosomes/vacuoles, exhibit defined shapes and occupy stable positions within the cytoplasm. These organelles have specific roles in modifying proteins for their cellular functions and are therefore tightly regulated as part of the two major pathways through which protein trafficking takes place in the cell: the secretory pathway and the endocytic pathway.

The ER represents the entry point for newly synthesized proteins destined for the secretory pathway. The newly synthesized proteins are selectively incorporated into transport vesicles budding off from the ER. Transport from the ER to the Golgi is mediated by a pre-Golgi intermediate compartment (IC), first identified when viral envelope proteins were found to accumulate in morphologically distinct structure distributed throughout the cytoplasm when viral infected cells were incubated at 15^0C. (Hong, 1998). ER to golgi trafficking has been visualised in mammalian tissue culture cells using the temperature-sensitive vesicular stomatitis viral G protein (VSVG) tagged with green fluorescent protein (GFP) (Presley et al., 1997). Proteins and lipids enter the *cis*-Golgi, and transit along towards the *trans*-Golgi network (TGN). The secretory material in the TGN is progressively released through the formation of secretory granules, vesicles, or via other mechanisms, consuming the other organelle (Mironov et al., 1997). Some of the golgi membrane follow a pathway back to the ER, resulting in conservation of machinery required for the forward secretory pathway (Pelham, 1991). This may be an inherent of proteins in the Golgi,

as Golgi -resident chimeras containing the temperature-sensitive lumenal domain of VSVG were found to redistribute themselves back to the ER on shifting the temperature, although VSVG itself did not recycle back (Lippincott-Schwartz, 1998). The third destination for material from the Golgi is the lysosome in higher eucaryotes or vacuoles in lower eucaryotes (Scott and Klionsky, 1998). The vacuole is the main degradative compartment in the yeast cell.

The endocytic pathway can be divided into two stages: early and late. In the early stages molecules are internalised from the plasma membrane. The internalised molecules are delivered to the endosomes and then to the lysosome/vacuole in the late stages (Wendland et al., 1998). A large number of membrane proteins are known to be internalised from the plasma membrane and are transported through distinct endocytic compartments to the vacuole, where they are degraded. Some common examples are the Ste2p, which mediates endocytosis of its ligand, the mating pheromone α-factor, and transporters such as the amino acid and uracil permeases (Wendland et al., 1998).

A number of sorting/targetting components are present in the vesicles to direct the vesicle to the correct pathway (Lippincott-Schwartz, 1998; Scott and Klionsky, 1998; Wendland et al., 1998). Vesicle docking takes place when soluble NSF attachment protein (SNAP) receptors on a vesicle membrane (v-SNAREs) bind to SNAP receptor proteins on the target membranes (t-SNAREs). As t-SNAREs have been known to interact with several v-SNAREs from different populations of transport vesicles, however, other proteins could provide specificity required for a vesicle to dock and fuse with the correct organelle (Gotte and von Mollard, 1998). Adaptor proteins in

membrane coat proteins have been shown to direct organelle selection (Odorizzi et al., 1998). Clathrin, the first coat protein to be identified, assembles with two distinct but closely related adaptor protein (AP) complexes which either direct the vesicle to the Golgi for sorting (AP1), or for endocytosis at the plasma membrane (AP2) (Odorizzi et al., 1998). A third adaptor protein complex, AP3, appears to direct protein transport to the yeast in vacuoles(Odorizzi et al., 1998). The secretory and endocytic pathways are connected as the proteins that govern the steps of late endocytosis generally overlap with the vacuolar protein sorting (vps) gene products, which are required for the delivery of biosynthetic traffic from the golgi to the vacuole (Wang et al., 1996) (Wendland et al., 1998).

As the main degradative component of the cell, the vacuole is involved in both the endocytic and secretory pathways. Metabolic enzymes as well as proliferated organelles that are no longer required are targeted to the vacuole for degradation and recycling in order to maintain cellular balance and allow the cell to survive starvation (Takeshige et al., 1992). Many *S.cerevisiae* mutants have been isolated and used to study vacuolar targetting and sorting pathways. A number of vacuolar protein sorting (*vps*) mutations reveal that Class D vacuolar proteins are required for sorting vacuole proteins from the Golgi and mutations in these proteins result in missorting to the plasma membrane (Raymond et al., 1992). Class E VPs gene products are required for normal endosomal function, and any mutation in this class of proteins results in accumulation of biosynthetic and endocytic traffic destined for the vacuole(Raymond et al., 1992). Traffic from the golgi to the vacuole is important as the golgi not only provides material for degradation, but also the hydrolases necessary for vacuole function. There are at least two routes from the Golgi to the vacuole: the 'CPY'

pathway, which involves transit through the endosomal/pre-vacuolar compartment (PVC), and the recently identified 'ALP' pathway, which bypasses the PVC, but follows compartments which have not yet been identified (Conubear and Stevens, 1998). Both t-SNARES and rabs, the low molecular weight GTP-binding proteins, play a role in CPY pathway. The t-SNARe Pep12p was the first endosomal t-SNARE to be identified and its major role is in biosynthetic traffic from the late Golgi to the vacuole. In *pep12* mutants, the carboxypeptidaseY (CPY) vacuolar hydrolase was missorted into the secretory pathway and secreted into the periplasmic space (Wendland et al., 1998). *S. cerevisiae* mutants have also been used to study the degradation of organelles. There have been reports that the budding yeast *yme1* mutant has elevated rates of migration of nuclear DNA to the nucleus, and these rates are suppressed in strains in mutations in vacuolar hydrolases(Scott and Klionsky, 1998) (Campbell et al., 1994). The *yme1* mutants are also more susceptible to mitochondrial degradation and the mitochondria are found in close proximity to the vacuoles, indicating that the Yme1p may be involved in signals for mitochondrial degradation (Scott and Klionsky, 1998). Uptake of proteins for vacuolar degradation may take place by two mechanisms, and the uptake of the regulatory enzyme for gluconeogenesis, Fructose-1,6-biphosphatase (FBPase) has been studied to elucidate these mechanisms. The presence of FBPase at the site of vacuolar membrane invagination suggested a microautophagic means of entry (Chiang et al., 1996). Vacuoloar import and degradation (*vid*) mutants have also been isolated which are defective in FBPase degradation, and these mutants show the involvement of a vesicle-mediated pathway as the second mechanism for vacuolar uptake (Huang and Chiang, 1997). It has also been observed in *S. cerevisiae* by electron microscopy that in response to nutrient deprivation, double-membrane autophagosomes surrounf bulk

regions of cytosol including mitochondria and ribosomes as well as enzymes. These membranes fuse at the vacuoles, delivering a single-membrane autophagic body into the vacuole lumen, where the autophagic bodies are digested (Takashige et al., 1992). Two genes essential for autophagocytosis in *S. cerevisiae*, AUT2 and AUT7, code for proteins that attach to microtubules, suggesting that microtubules are involved in the delivery of autophagic vesicles to the vacuole (Lang et al., 1998).

The vacuole has been less extensively studies in the fission yeast *S. pombe*. Phase-contrast photomicrographs of living cells initially revealed groups of little vacuoles containing granules that had an affinity for neutral red, called volutin granules (Robinow and Hyams, 1989). Three different kinds of vacuoles were seen by electron microscopy, depending on their method of fixation: many empty vacuoles of irregular shape in permanganate fixed cells, or a round, ovoid or angle-cornered, solidly dense material surrounded by a clear membrane, occassionally including granular matter or whorls of membranes in glutaldehyde-formaldehyde fixation, or numerous vacuoles with dark contents scattered all over the cytoplasm in low-power electron micrographs. However comparison with light micrographs of fission yeast stained with acidified toluidine blue revealed that the differences were due to preparation of the samples but the images were of the same thing, i.e. vacuoles containing volutin granules (Robinow and Hyams, 1989). Recent studies of the functions of vacuoles in the fission yeast showed that vacuole fusion and fission, as in budding yeast, is regulated by the mitogen activated protein (MAP) kinase pathway in response to osmotic stress (Bone et al., 1998). Vacuole fusion and fusion therefore appear to function as homeostatic mechanism that restore the concentration of the cytosol (Bone et al., 1998). Mechanisms required for protein sorting to the vacuole, and vacuole

morphology, has not been as extensively studied in fission yeast as in the budding yeast. Recently, however, the fission yeast *vps34+* gene has been cloned, and its product, which is 43% homologous in amino acid sequence to the *S. cerevisiae* Vps34 protein, shows phosphotidylinositol 3-kinase activity (Takegawa et al., 1995). Mutant fission yeast *vps34* strains showed enlarged vacuoles (Takegawa et al., 1995). It is possible that Vps34p in fission yeast is a member of a family of PI 3-kinases whose primary role is to facilitate vesicle-mediated protein sorting (Takegawa et al., 1995).

Organelles therefore play vital roles in the cell, and the control of their movement and positioning is as important as their biochemical functions for the cell. The interaction of organelles with microtubules is therefore important for efficient membrane trafficking because it maintains the organelles in defined relative positions, as well as supporting directed movement of tubules and vesicles between compartments. Several studies support this observation. In the absence of microtubules, transport from the Golgi apparatus to endosomes and/or lysosomes is greatly reduced (Scheel et al., 1990). Microtubule inhibitors such as nocodazole also inhibit transport of material from early to late endosomes (Gruenberg et al., 1989). The fact that the movement of organelles are both directional and linear suggests a role for microtubule-based motors, and this has been confirmed using both *in vivo* and *in vitro* approaches (Rickard and Kreis, 1996).

Many differentiated cells, such as epithelial cells and neurons, have polarised structures which are essential for their function. In the neuron, for example, there is no protein synthesis in the axon, and all proteins required for the axon, and for the synaptic termini, must be transported down the axon. As proteins are generally

transported as complexes in membraneous organelles, organelle transport in the axon is fundamentally important for neuronal morphogenesis and function. The axon was therefore used as a model for early studies of organelle transport. It was shown that various types of membraneous organelles were transported anterogradely, whereas multivesicular bodies and endosomes are transported retrogradely, although the opposite also occurs at different velocities. Mitochondria are transported in both directions (Hirokawa, 1996) (Grafstein and Forman, 1980). Studies using light and electron microscopy combined with biochemical analyses have revealed that microtubule motor protein ATPases, kinesin and dynein, are involved in organelle transport. Various studies involving antisense primers, blocking antibodies, transfection of various kinesin cDNA with point mutations , have revealed that kinesin is responsible for the microtubule plus-end directed transport of membranous organelles, which is important for neurite outgrowth of neurons, and in microtubule plus-end directed lysosome transport in various types of cells (Hirokawa, 1998). Proteins of the kinesin superfamily that have been identified as involved in organelle transport are the KHC, Unc104/KIF1, KIF3/$KRP_{85/95}$, KIF4 and Klp67A families (with N-terminal motor domains), the KIF2 family (middle motor domain), and the KIFC2/C3 family (C-terminal motor domain) (Hirokawa, 1998). Dynein, on the other hand, is involved in retrograde organelle transport, as it moves along a microtubule from the plus to the minus end. Experiments to follow the viral glycoprotein VSVg tagged with green fluorescent protein (VSVG-GFP) have conclusively shown the role of microtubules and microtubule motors in organelles transport. It was seen that the protein gets exported from the ER to pre-golgi structures, which then translocate towards the golgi along microtubules by using the microtubule minus-end-directed motor complex of dynein/dynactin (Presley et al., 1997).

For organelles to move by motors, membranes must establish contact with microtubules. Membrane proteins can act as receptors, e.g. Kinectin, a membrane protein of the ER, has been identified as a putative kinesin receptor(Toyoshima et al., 1992). Similar organelle specific proteins that act as receptors could be a way of regulating organelle movement and positioning. Other non-motor, microtubule binding proteins are also involved in docking of organelles before movement, and in specifying their stable cytoplasmic location. These molecules, which act as 'mediators' have been termed cytoplasmic linker proteins, or CLIPs (Pierre et al., 1992; Rickard and Kreis, 1991; Scheel and Kreis, 1991). CLIPs have been isolated in vitro by assaying for cytosolic proteins (in extracts immunodepleted for kinesin and dynein) for which organelles are dependant in order to bind to microtubules. These studies revealed that there were specific CLIPs for different organelles, and one of them, CLIP-170, was identified as a binding factor. It has been extensively characterised, and it is confirmed that CLIP-170 associates with endosomal membranes (Rickard and Kreis, 1996) (Pierre et al., 1992; Rickard and Kreis, 1991; Scheel and Kreis, 1991).

As microtubules appear to be essential for organelle function, any change in microtubule dynamics should have an impact on organelle dynamics. In this chapter, we investigate whether overexpression of the mammalian MAPs have an effect on organelle distribution in the fission yeast *S. pombe.*

5.2 Methods

To stain mitochondria, 1x 10^5 cells/ml were incubated with mitotracker (100μg/ml) for 15-45 minutes at 30 ^{0} C, with constant shaking to prevent the cells from becoming anoxic. The cells were then fixed on slides and observed under a rhodamine filter using a confocal fluorescence microscope.

Vacuoles were stained using FM4--64 (1ng/ml) (Vida and Emr, 1995) added to 1x 10^5 cells/ml and incubated for 30 minutes at 30 ^{0} C, with constant shaking. The dye was then washed out using 1X PEMS, and the cells fixed and observed under the fluorescence microscope as above.

5.3 Results

5.3.1 MAP2c and MAP4 but not tau affect mitochondrial distribution in fission yeast

Figure 5.1 Mitochondrial localisation is affected by the overexpression of MAP2c but not tau . Cells were stained with the dye mitotracker, which localises to mitochondria, after the expression of tau (ii) and MAP2c A, (iii) due to growth of fission yeast in the absence of thiamine for 27 hours. The control cells , containing pREP1 without any MAP gene (I), shows a continuous string of mitochondria just within the cell

membrane. A similar pattern is seen in tau expressing cells. MAP2c show mitochondrial aggregation at the two poles. Bar 10 μm

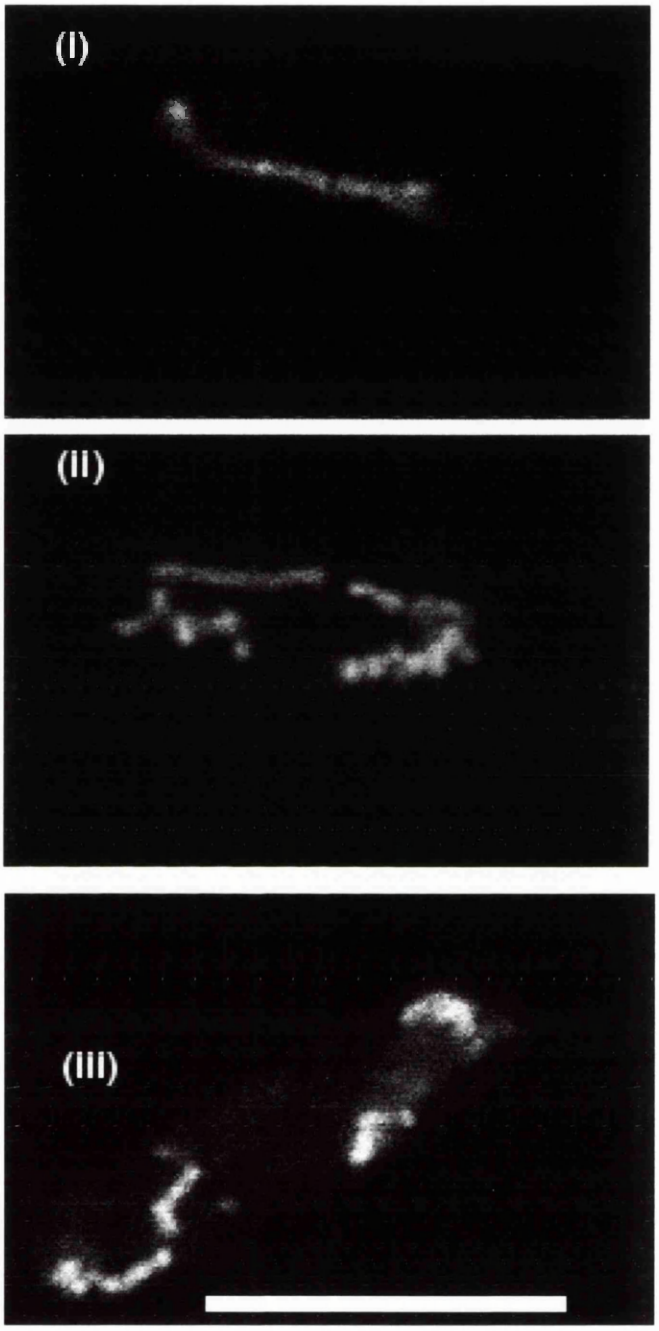
(I)
(II)
(III)

Figure 5.2 Overexpression of MAP4 causes mitochondrial aggregation in fission yeast. Control cells (I), containing pREP1 only, showed a continuous string of mitochondria upon staining with mitotracker. However, there were very few mitochondria present in cells expressing MAP4 (ii), and when present, they mitochondria were aggregated at the poles.

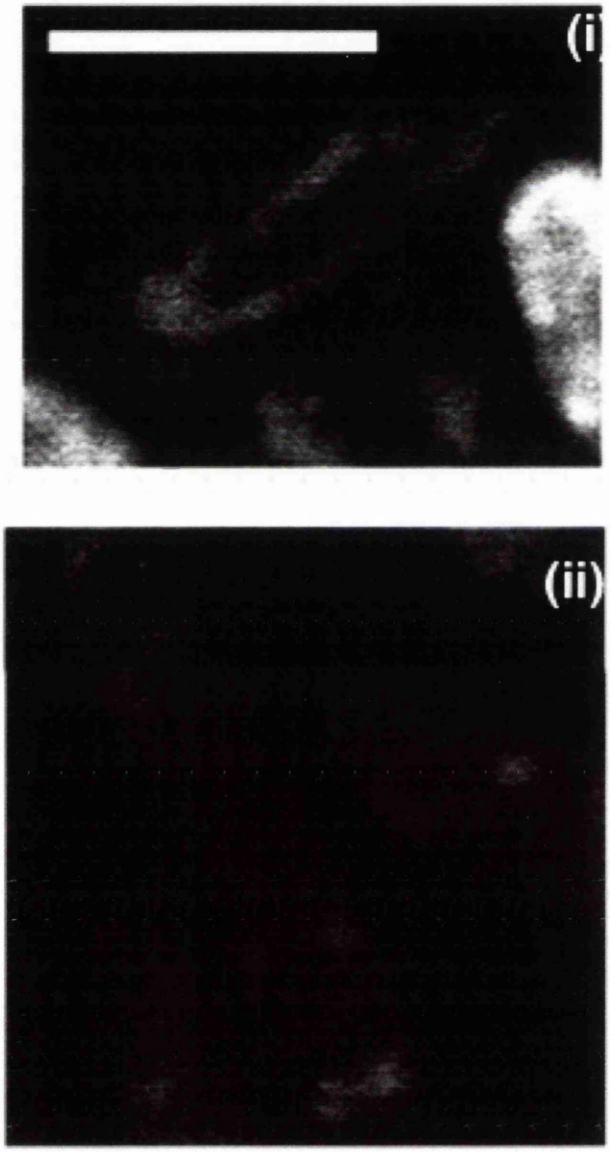
(i)
(ii)

In order to study whether overexpression of the MAPs tau, MAP2c and MAP4 have any effect on mitochondrial disribution in fission yeast, cells transformed with the plasmid pREP1 alone, pREP-tau, pREP-MAP2c, and pREP-MAP4 were grown in the absence of thiamine for 27 hours and stained with the mitochondrion-labelling dye, mitotracker. Figure 5.1 i and ii and iii show mitotracker staining of control cells and cells expressing tau and MAP2c respectively. In control *S. pombe* cells the mitochondria are distributed as extended tubules along the length of the cell. Cells expressing tau show a more complete formation of this tubule. MAP2c clearly interrupts the extended tubular formation of mitochindrial distribution, so that mitochondria now appear aggregated in discrete patches across the cell.

Figure 5.2 i and ii show mitotracker-stained cells that contain pREP1 only, and mitotracker-stained cells expressing MAP4, respectively. MAP4 expressing cells show disruptions in the tubular pattern that is seen in the control cells..

5.3.2 Tau, MAP2c and MAP4 have no obvious effect on vacuole distribution in fission yeast

Vacuole distribution in fission yeast was studied by staining cells containing pREP1, pREP1-tau, pREP1-MAP2c , and pREP1-MAP4, grown in the absence of thiamine for 27 hours, with the dye FM4-64. Figures 5.3. i, ii and iii show vacuole staining by FM4-64 in *S. pombe* cells expressing no MAP, tau, and MAP2c respectively. In all the figures, there were 20-30 FM4-64 staining bodies varying in diameter from 0.1-1μm distributed in an apparently random manner throughout the cell. There was no

Figure 5.3.Vacuole localisation is not affected by overexpression of tau and MAP2c in fission yeast. Fission yeast cells expressing tau (ii) and MAP2c (iii) were stained with the vacuole specific dye, FM4-64. There did not appear to be any difference in vacuole localisation compared to the control cells not expressing any MAP (I). Bar 3μm

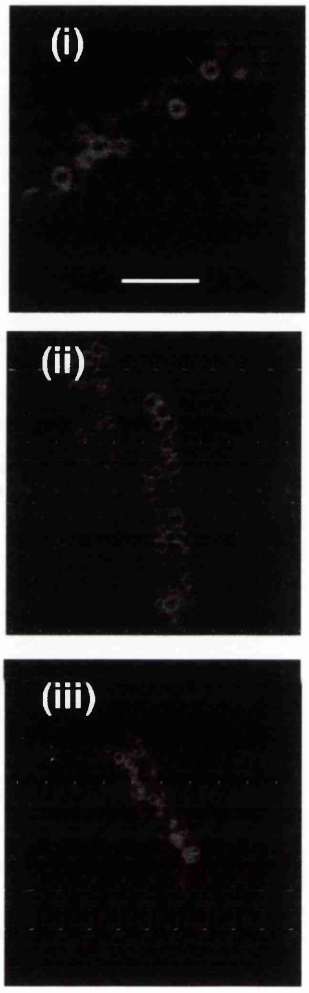
(i)
(ii)
(iii)

Figure 5.4 Overexpression of MAP4 does not affect vacuole localisation in fission yeast. Staining of fission yeast cells with the vacuole specific dye FM4-64 did not reveal any differences in vacuole patternm in cells expressing MAP4 (ii) compared to wild typecells not expressing MAP4(i). Bar 10μm

discernible differences is vacuole distribution between the controls and the MAP-expressing cells. Figures 5.4. i and ii show vacoule distribution in control cells and cells expressing MAP4 respectively. There does not appear to be any discernible difference from these figures due to the presence of MAP4.

5.3.3 Tau, MAP2c and MAP4 overexpression results in smaller vacuole size in fission yeast

As discussed in the sub-section 5.3.2, vacuole distribution appears unaffected by the overexpression of MAPs. However, as vacuoles are reported to fragment when microtubules depolymerise in fission yeast(Guthrie and Wickner, 1988), vacuole diameters of FM4-64 stained cells expressing the MAPs tau and MAP2c were measured. Figure 5.5 a, b and c show that tau , MAP2c and MAP4 appear to reduce the average vacuole size 38% , 18% and 34% respectively. However as the vacuole diameters are over a wide range, only tau appears to show a significant difference in vacuole diameter.

5.5 Overexpression of tau , MAP2c and MAP4 lead to smaller vacuole size in fission yeast. Measurement of vacuole size (as a percentage of total cell size) for at least 10 randomly chosen vacuoles in cells expressing tau, MAP2c, MAP4 and control wild type cells reveal that tau leads to a 38% reduction in vacuole size, while MAP2c leads to an 18% reduction in vacuole size and MAP4 reduces vacuole size by 38%. Error bars show standard deviation.

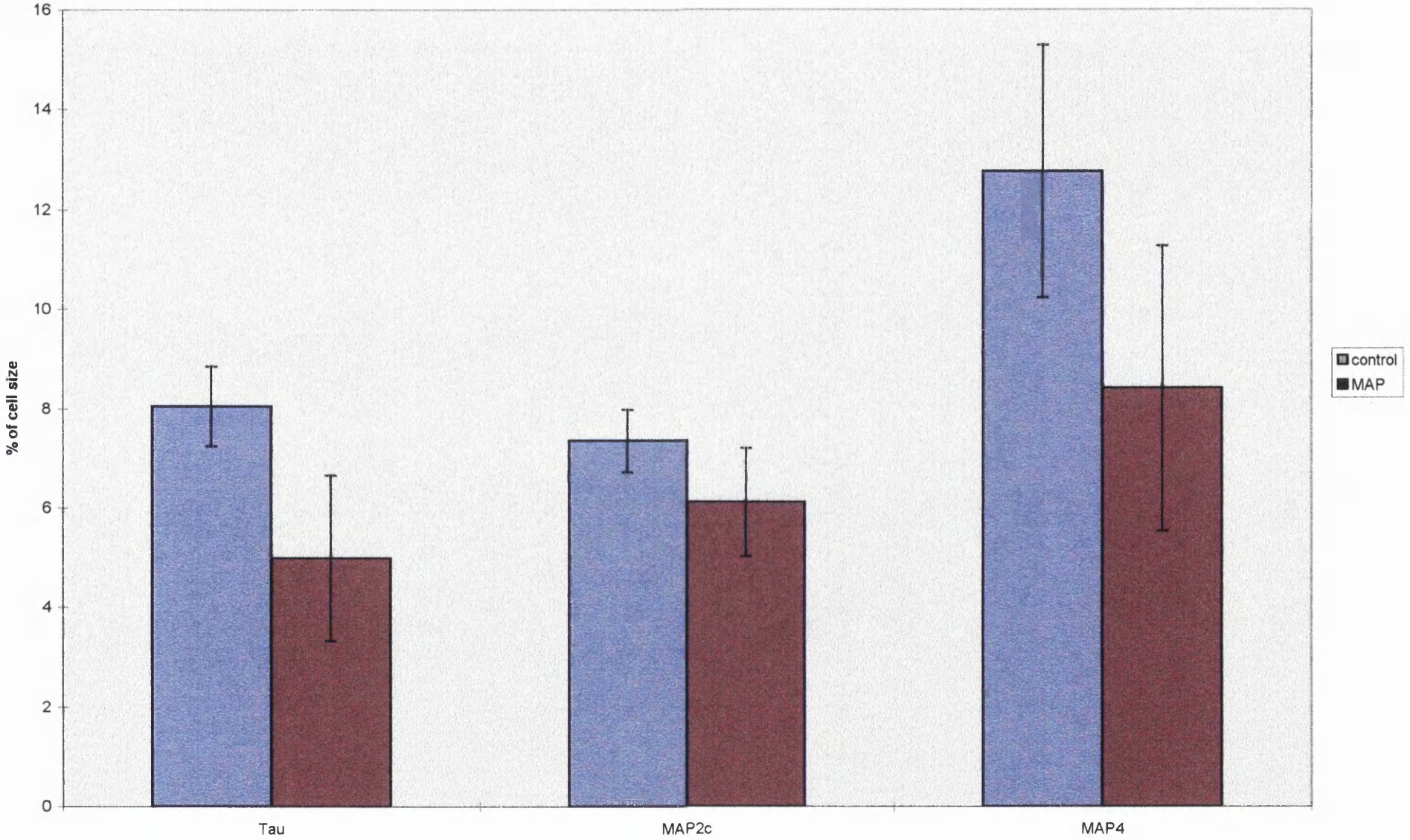
16
14
12
10
8
6
4
2
0
% of cell size
Tau
MAP2c
MAP4
control
MAP

5.4 Discussion

Several reports show that organelle traffic is closely linked to microtubules in various organisms and systems (Hirokawa, 1998; Hirokawa, 1996) (Rickard and Kreis, 1996) (Cole and Lippincott-Schwartz, 1995). Mitochondria are amongst those organelles that have been studied and closely linked to microtubules. Mitochondria travel along microtubules in living vertebrate neuronal axons. (Morris, 1995). Mitochondria were shown to be associated with a plus-end directed microtubule motor protein in *Drosophila* (Pereira et al., 1997) Treatment of cultures animal cells with chemical agents that depolymerise microtubules often lead to altered mitochondrial distribution(Yaffe et al., 1996). However, evidence relating mitochondria and microtubules have not been so clear-cut in unicellular organisms. In the budding yeast *Saccharomyces cerevisiae*, neither mutations nor chemicals that disrupt microtubules appear to affect mitochondrial distribution or movement. (Huffaker et al., 1988). Mitochondrial distribution similarly affected in *Aspergillus* β-tubulin mutants(Oakley and Reinhart, 1985). However, Yaffe et al (1997) showed that microtubules mediate mitochondrial distribution in fission yeast, and that microtubule disruption in *nda2* and *ban5* mutants show aggregation of mitochondria, and assymetrical distribution of the organelle in daughter cells (*nda2* codes for α1 tubulin (Yanagida, 1987) and *ban5* has been revealed as an allele of *atb2*, which codes for α2 tubulin (Yaffe et al., 1996)). The aggregation shown is similar to that seen in Fig. 5.2b and 5.3b respectively. It is therefore likely that the partial depolymerisation of microtubules that occurs MAP2c and MAP4 expression (Chapter 4) directly results in uneven distribution of mitochondria. However (Hagiwara, 1994) have shown that kinesin and dynein can

directly compete with MAP2 binding to microtubules. Considering the overexpression of the MAPs, another possible explanation therefore is that the motors could not bind to the microtubules in the presence of MAP2c and MAP4, resulting in non-transport and therefore aggregation of mitochondria. It is not clear, however, how mitochondria are transported in fission yeast. In vertebrate neurons, it is transported bidirectionally (Morris, 1995). An isozyme of kinesin has been localised to mitochondria in neuronal cells (Nangaku et al., 1994). However, to date, 6 kinesins have been identified in *S. pombe* (Hagan and Yanagida, 1990; Pidoux et al., 1996) but there have been no reports of mitochondrial localisation of any of the kinesins.

Membrane traffic is maintained in eucaryotic cells by balancing the secretory and endocytotic mechanisms. However, the secretory pathway has been more extensively characterised than the endocytotic pathway in yeast and other organisms. Lysosome movement in macrophages have been reported to be kinesin- and therefore microtubule- dependant (Hollenbeck and Swanson, 1990). There have been no reports about vacuole movement and the cytoskeleton in fission yeast. Results from this chapter show that vacuole positioning do not seem in the least affected by the overexpression of tau, MAP2c and MAP4. As these MAPs result in the disruption of the microtubule cytoskeleton, it would appear that vacuole positioning in fission yeast is not microtubule dependant. In the budding yeast *S. cerevisiae* actin and myosin appear to direct vacuole movement during cell division (Hill et al., 1996), and a similar mechanism may be present in *S. pombe*. Alternatively, vacuole movement could be microtubule based as well, but tightly regulated. Movement of endocytic cargo from the endosome to the lysosome requires retrograde transport, usually by dynein (Gruenberg et al., 1989). Assays of chick embryo fibroblasts have revealed

activators for dynein in microtubule-based vesicle transport (Schroer and Sheetz, 1991). Similar activators may exist in yeast, which may block the effects of the MAPs.

Although vacuole positioning is not affected by overexpression of MAPs, tau does appear to lead to a reduction in vacuole size, as seen in figure 5.4. In the budding yeast, microtubules appear to be involved in vacuole morphology, and disruption of microtubules by nocodazole and benzimadoles result in vacuole fragmentation in *S. cerevisiae* (Guthrie and Wickner, 1988). In the fission yeast, however, microtubule disruption due to overexpression of MAP2c or MAP4 (Chapter 4) does not appear to significantly reduce vacuole diameter. On the other hand, although tau overexpression does not result in microtubule depolymerisation in fission yeast, and in fact stabilises and bundles microtubules in most cells, tau overexpression appears to lead to a reduction in vacuole diameter. In mammalian cells as well as budding yeast, autophagic vesicles fuse with pre-lysosomes/vacuoles to form degradative lysosomes (Dunn, 1990; Lawrence and Brown, 1992). Two microtubule associated proteins in budding yeast, Aut2p and Aut7p, are reported to be essential for delivery of autophagic vesicles to the vacuole (Lang et al., 1998). It is possible that similar microtubule-based proteins are required for transporting endocytic vesicles to the vacuole in fission yeast. The high levels of tau could interfere with such proteins, resulting in accumulation of vesicles in the cytoplasm, rather than fusion with the vacuole. As a result the vacuoles could be smaller in diameter. The dye FM4-64 is also a marker for endocytic intermediates (Vida and Emr, 1995), and some of the smaller staining bodies seen could therefore be vesicles rather than the vacuole.

6. Isolation of Microtubule Stabilising Factors in the Fission Yeast S. pombe

6.1 Introduction

Microtubules are essential for many important cellular processes. However, These are dynamic polymers and abruptly change from periods of rapid growth to periods of rapid shrinkage. Growth or shrinkage takes place due to the association or disassociation of the tubulin heterodimers(Mitchison and Kirchner, 1984). The dynamic properties of microtubules are regulated by proteins binding to them. Microtubule Associated Proteins (MAPs) stabilise microtubules and prevent shrinkage possibly by acting as a 'hinge' that binds across protofilaments and therefore prevent them from 'peeling' apart (Downing and Nogales, 1998) (Joshi, 1998). MAPs have been discovered and isolated from most vertebrates. Goedert et. al(Goedert et al., 1996) have reported the first invertebrate MAP, PTL-1, with tau-like repeats and properties, from *Caenorhabditis elegans*. A MAP-like protein, MHP-1, was also isolated from *S. cerevisiae* by expression cloning using antibodies specific for the *Drosophila* 205K MAP (Irminger-finger et al., 1996).

S. pombe microtubules, like those of *S. cerevisiae*, are composed of 2 α- and one β-tubulin. The α tubulins of fission yeast are both 76% homologous to porcine α tubulin, whilst the β-tubulin is 75% and 73% homologous to chicken and budding yeast β-tubulins, respectively (Yanagida, 1987). MAPs such as tau and MAP2 have been reported to bind to the C-terminal domains of β-tubulin in vertebrates (Padilla et al., 1993). In chicken, the β_{II} tubulin sequences YQQYQDATADEQG and

GEFEEEGEE have been known to intereact with MAP2. The fission yeast β tubulin has similar sequences in its C-teminal region (YQQYQEAGIDEGD and DEDYEIEEE). In chapter 3 and 4, we have shown that the MAPs tau, MAP2 and MAP4 can bind and affect fission yeast microtubules. It is therefore likely that *S. pombe* has endogenous MAP(s) which regulate its dynamics. However there have been no reported MAPs in *S. pombe* so far.

Conventional methods of isolating *S. pombe* MAPs, such as heat-stabilised and taxol-stabilised microtubules, have been unfruitful (J.S. Hyams, personal communication). Neither has attempts at PCR-cloning of the *S.pombe* genome using primers based on the conserved 18-repeat domain of MAPs revealed a fission yeast MAP. In Chapter 3, we have shown that the MAPs tau and MAP2 rescue *S. pombe* from combined sensitivity to the cold and effects of thiabendazole. We have therefore used this assay in an attempt to isolate tubulin stabilising factors or MAPs in *S. pombe*.

6.2 Methods

A *S. pombe* CDNA library in pREP3X containing 300,000 - 600,000 clones from log phase 972h- *S. pombe* was kindly supplied by Dr. C. Norbury (ICRF, Oxford). The cDNAs are oriented and can be expressed in *S. pombe* using the thiamine repressible *nmt* promoter.

Leu⁻1.32h⁻ cells were grown to a density of 1.8 x 10^7 cells per ml (late log phase), and a total of 3 x 10^8 cells were transformed by electroporation with 100ng cDNA/ 5x 10^7 cells. Half the transformed cells were plated in MM+thiamine (8μg/ml) + TBZ

(10μg/ml), and the other half was plated in the same medium without thiamine. Untransformed cells were also plated in MM+/- thiamine as controls. Cells were then grown at 20^0C for 12 days.The transformants were tested for TBZ sensitivity by plating them in MM+T medium and MM-T medium in the presence of 0, 10, 20, 40 g/ml TBZ, at 29^0C and 36^0C.

Plasmids were isolated from transformants using methods described in Chapter 2. The plasmids were then re-transformed into E.coli, and isolated by Qiagen Miniprep method. The the cDNA were sequenced using a sequencing primer based on the *nmt* region, ATGTGCAGCGAAACTAAAAACC.

6.3 Results

6.3.1 The Fission yeast cDNA library rescued 10 colonies from sensitivity to a combination of cold and Thiabendazole

The *leu-1.32h-* strain is sensitive to 10μg/ml TBZ at 20^0C, and this sensitivity only disappears when mammalian MAPs and MAP2c are expressed (Chapter 3). Since the cDNA library is in the thiamine-repressible pREP3X vector, in the absence of thiamine, all the genes should express. However, the transformed cells should not survive unless a gene from the library that affects microtubule stability, such as a MAP, is expressed by the transformant. Only 10 colonies survived from the 1.5 X 10^8 cells plated in medium without thiamine, and none in the control plates (presence of thiamine which represes the library expression). These 10 colonies were called Lres 1-8.

6.3.2 Effect of the Lres colonies on fission yeast sensitivity to thiabendazole at higher temperatures

Only 8 of the 10 colonies rescued continued to show TBZ resistance at 20°C when replated. These 8 colonies were then grown in MM containing 10, 20 and 40μg/ml TBZ at 29^0C and 36^0C to check their resistance to the drug at higher temperatures. Figure 6.1 a shows that at 36^0C, Lres 1, 3, 4, 5 and 12 show resistance to TBZ at concentrations as high as 40μg/ml. However, this is not the case at 29^0C, where only Lres 5 showed resistance at 40μg/ml TBZ. (Figure 6.1b). All Lres plasmid containing cells, but not the control cells, showed resistance to 20μg/ml TBZ at 20^0C.(Figure 6.1c)

6.3.3 Sequencing of the cDNA clones revealed a ribosomal protein and the αchain of fatty acid synthetase

Lres 1, 2 and 8 were sequenced and the sequence compared for homology in genbank. Lres 2 did not show any significant ORF, as there was a large seqeuce of T's, it could be a poly-A tail of a protein.

Lres 1 showed almost total homology to L19, a 60s ribosomal protein in *S. cerevisiae* (78% identity), *Arabidopsis thaliana* (77% identity), *Drosophila melanogaster* (64% identity), human (58%).

Lres 8 was revealed as part of the α- subunit of fatty acid synthetase enzyme in fission yeast. This is coded for by the gene *lsd1*, mutants of which show a defect in nuclear division, resulting in daughter cells of dramatically different sizes (Lsd = Large and small daughter).

A.

	0μg/ml TBZ	10μg/ml TBZ	20μg/ml TBZ	40μg/ml TBZ
Lres1	+	+	+	+
Lres2	+	+	+	-
Lres3	+	+	+	+
Lres4	+	+	+	+
Lres5	+	+	+	+
Lres6	+	+	+	-
Lres7	+	+	+	-
Lres 12	+	+	+	+
control	+	+	+	-

B.

	0μg/ml TBZ	10μg/ml TBZ	20μg/ml TBZ	40μg/ml TBZ
Lres1	+	+	+	-
Lres2	+	+	+	-
Lres3	+	+	+	-
Lres4	+	+	+	-
Lres5	+	+	+	+
Lres6	+	+	+	-
Lres7	+	+	+	-
Lres 12	+	+	+	-
control	+	+	+	-

C.

	0μg/ml TBZ	10μg/ml TBZ	20μg/ml TBZ	40μg/ml TBZ
Lres1	+	+	+	-
Lres2	+	+	+	-
Lres3	+	+	+	-
Lres4	+	+	+	-
Lres5	+	+	+	-
Lres6	+	+	+	-
Lres7	+	+	+	-
Lres 12	+	+	+	-
control	+	+	-	-

Figure 6.1 Effect of Lres clones on TBZ sensitivity of fission yeast at 36^0C (A), 29^0C (B) and 20^0C (C). Cells containing the 8 Lres clones were grown at 36^0C, 29^0C and 20^0C in MM containing 0, 10. 20 and 40μg/ml thiabendazole (TBZ). Growth of cells is indicated by +, and - symbolises lack of growth of cells. At 36^0C, five clones, Lres 1,3,4 , 5 and 12 showed resistance to 40g/ml TBZ, which is lethal to control cells. At 29^0C, only Lres5 showed resistance to 40g/ml TBZ. At 20^0C, all eight clones rescued the TBZ sensitivity of control cells to 20μg/ml TBZ.

6.4 Discussion

The cold/TBZ assay was used to select transformants containing sequences from a *S. pombe* cDNA library that might identify possible genes for microtubule stabilising factors.. The rationale was that such genes would stabilise microtubules, possibly by the same mechanism as tau does, and therefore the cell would not be vulnerable to the microtubule depolymerising effects of the cold and TBZ.

Previous attempts to isolate *S. pombe* MAPs had included purifying tubulin by cycles of *in vitro* assembly. This method did not succeed due to the difficulties in purifying tubulin from fission yeast. Efforts were also made to utilise the heat stability, one of the features of MAPs, to isolate such a protein from boiled protein extracts from *S. pombe.* Immunoblotting such extracts with antibodies against known MAPs provided no bands at all. It is possible that the *S. pombe* MAP, like the *Drosophila* 205K MAP or the *S. cerevisiae* MAP MHP-1, is not immunologically related to the mammalian MAPs, but is similar to them in terms of an extensive acidic N-teminal region and a short acidic C-terminal region preceeded by a basic region that contains the MT-binding domain. This could also explain why, if a *S. pombe* MAP does exist, could not be isolated by PCR of the *S. pombe* genome. The PCR primers, based on the conserved 18-repeat sequence of the MT-binding domains of the MAPs tau, PTL1 from nematodes, and MHP-1 from S. cerevisiae, would be too degenerate to produce anything of significance.

The sequences of two of the genes that rescued *S. pombe* sensitivity to the combined effects of cold and TBZ were L19, a 60s ribosomal protein, and the α- subunit of fatty acid CoA synthetase. On the face of it, neither of these proteins are known to have any direct connections with microtubules.

Lres 1 bears 74% identity over a 44 amino-acid sequence overlap with the *S. cerevisiae* YL19 gene (also known as L23, YL14, RP33 or RP15L), which codes for the 60S ribosomal protein (Song et al., 1995). This is related to the mammalian L19 family of ribosomal proteins. Ribosomal proteins assemble co-operatively with ribosomal RNAs to form a ribosome which then carries out translation. Synthesis of ribosomal proteins is mainly regulated at the level of transcription of their genes. The function of the ribosomal protein L19 is not known, but there is a suggestion that is associated in the 60 S with the small rRNAs to participate in the binding of amino-acyl tRNA to ribosomes. It is unclear how L19 could stabilise TBZ-depolymerised microtubules in *S. pombe*. One possibility is that it plays a role in the synthesis of either tubulin or a tubulin stabilising factor or a TBZ-neutralising factor.

Lres8 is identical to the *lsd+* gene of fission yeast, which codes for the fatty acid synthetase α subunit, an enzyme that catalyses the synthesis of saturated long chain fatty acids from acetyl CoA, malonyl CoA and NADPH. Deletion of this gene results in dramatically different sizes of nuclei in daughter cells, one very large and one very small, due to aberrant nuclear elongation and division (Saitoh et al., 1996). In budding yeast, the fatty acid synthase complex consists of two types of polypeptide chains, and has the subunit composition of α6β6 (Wakil et al., 1983). In fission yeast, since an *lsd* phenotype is produced in the presence of Cerulenin, an anti-biotic that

inhibits β-ketoacyl Acyl Carrier Protein (ACP) synthetase, *lsd+* could code for this particular chain of the α-component of the fatty acid synthase complex. Saitoh et. al (1996) have shown that the *lsd+* mutant is recued by palmitate, i.e. fatty acid is required for correct cell and nuclear division. Sister chromatids are correctly separated in cells defective in this gene, indicating normal kinetochore and spindle functions. However there is an asymmetric division of non-chromosomal nuclear material. Stewart and Yaffe (Stewart and Yaffe, 1991) have shown that in budding yeast, unsaturated fatty acids are essential for mitochondrial movement and inheritance. Yaffe et. al. (1997) have shown that in fission yeast, microtubules mediate mitochondrial movement. Fatty acids could therefore play an intermediary role in organelle distribution through microtubules. Alternatively levels of fatty acid could act as 'signals' for proteins binding to microtubules further downstream. Another possibility is that fatty acids control the composition and therefore effective function of the nuclear envelope in fission yeast, thereby blocking TBZ entry into the nucleus.

Sequencing of the other genes that rescue TBZ/cold sensitivity of fission yeast could reveal not only possible MAPs,but also more about the relationships of different proteins to microtubules.

7. Summary and Future Directions

The fission yeast *S. pombe* was used as a unique *in vivo* system for the heterologous expression of the mammalian microtubule associated proteins (MAPs) tau, MAP2c and MAP4. The three MAPs had in common a homologous microtubule-binding repeat region but unique N-terminal regions (Mandelkow, 1995), and the aim of this project was to compare the distinct roles of the three MAPs, as well as to further define the role of fission yeast microtubules.

My studies showed that each of the MAPs had a distinct effect on cell growth, morphology, cold and drug sensitivity, cell progress into mitosis, and microtubule organisation and organelle distribution. Tau had the weakest effect, both in wild type cells as well as *tea1* and *tea2* temperature sensitive mutants. Where an effect was seen tau appeared to cause microtubule bundling. This is consistent with reports in other systems, where tau expression has been reported to cause microtubule bundling (Baas et al., 1991; Brandt and Lee, 1994; Chen et al., 1992; Hanemaaijer and Ginzburg, 1991; Hirokawa et al., 1996; Lee and Rook, 1992). Tau has also been shown to stabilise microtubules in insect Sf9 cells to the drug nocodazole, but not to the cold (Baas et al., 1994). Axonal microtubules in cultured sympathetic neurons, however, are cold stable (Baas et al., 1994). In fission yeast, tau appeared to rescue cells from a combination of cold and sensitivity to thiabendazole (TBZ), a microtubule depolymerising drug.. MAP2c, however, had a much stronger effect both in terms of morphology as well as microtubule organisation. In wild type as well as *tea1* and *tea2* cells, overexpression of MAP2c led to short, partially depolymerised microtubules. This is contrary to reports in other systems where MAP2c has been

reported to stabilise and bundle microtubules (Chen et al., 1992; Umeyama et al., 1993). MAP2c also appeared to be sensitive to proteases in *S. pombe*, possibly due to the presence of the PEST sequence. MAP2c appeared to rescue the sensitivity of fission yeast to a combination of cold and the microtubule depolymerising drug thiabendazole (TBZ), suggesting it might have a stabilising effect on microtubules under those conditions. MAP2c also appeared to slow down cell entry to mitosis, which is consistent with the long cells that were seen when MAP2c was expressed. MAP4 had the most dramatic effect on fission yeast microtubule organisation. Interphase microtubules were completely depolymerised, and in some cells spindles could be seen. Western blotting revealed that the size of MAP4 expressed in *S. pombe* was 125kD which corresponded to its molecular weight according to its amino acid composition, but was much lower than the 220KD band normally seen by gel electrophoresis (Bulinski, 1994). Part of MAP4 could have been rearranged during cloning as MAP4 is a large (5kb) fragment in a large pREP1 (7kb) vector, and the fragments produced by restriction digest could have beeen too large to be reveal the rearrangements. Restriction digests using other, more frquently cutting enzymes will reveal if, and which part, of MAP4 is missing.

The effect of all three MAPs overexpressed in *S. pombe* was heterogenous, and this was likely to be th result of the widely varying levels of MAPs in the different cells. Therefore integration of the MAPs into the *S. pombe* genome, possibly by using a pRIP vector, would reveal a more accurate picture of the distinct effects of each of the MAPs as the levels of the MAPs in different cells would then be constant.

The MAPs expressed in this study also varied in their microtubule binding domains. The tau isoform expressed was htau40, the largest isoform with four repats of the microtubule binding sequence, and the 54 amino-acid N-terminal insert. The MAP4 isoform expressed was also the largest MAP4 isoform with five repeats in the C-terminal domain. MAP2c, however, had a three-repeat C-terminal domain. Expression of three-repeat tau and four-repeat MAP4 will reveal if the differences in the effects of the three MAPs could be due to the number of homologous microtubule bnding repeats in the C-terminal domain.

All three MAPs, tau, MAP2cand MAP4, are regulated by phosphorylation (Bulinski, 1994; Goedert et al., 1994; Matus, 1994), and differential phosphorylation of the MAPs in *S.pombe* could also be a reason for their different effects. Further phosphorylation studies could reveal more about the distinct roles of each of the MAPs.

The observation that tau and MAP2c could rescue the combined sensitivity of fission yeast to the cold and TBZ was used in an attempt to isolate possible MAPs in fission yeast using the *S. pombe* cDNA library in pREP. Eight clones were isolated, of which two were sequenced and identified as a homologue of the ribosomal protein L19 and *lsd+*, which codes for the fatty acid synthetase α-subunit. It is unclear how eitherof these proteins function to stabilise microtubules, and further studies will reveal more about the regulation of microtubule function in the cell.

Bibliography

Adachi, Y., Toda, T., Niwa, O., and Yanagida, M. (1986). Differential expression of essential and non-essential alpha-tubulin genes in Schizosaccharomyces pombe. Molecular and Cellular Biology *6*, 2168-2178.

Aiwaza, H., Emori, Y., Mori, A., Mirofushi, H., Sakai, H., and Suzuki, K. (1991). Functional analysis of the domain structure of the microtubule associated protein 4 (MAPU). Journal of Biological Chemistry *266*, 9841-9846.

Aiwaza, H., Murofushi, H., Kotani, S., Hisanaga, S.-I., Hirokawa, N., and Sakai, H. (1987). Limited chymotryptic digestion of bovine adrenal 190000 Mr microtubule-associated protein and preparation of a 27000Mr fragment which stimulates microtubule assembly. Journal of Biological Chemistry *262*, 3782-3787.

Alfa, C., Fantes, P., Hyams, J., and McLeod, M. (1993). Experiments with Fission yeast: a laboratory manual: Cold Spring Harbour Laboratory, Cold Spring Harbour, new York).

Audebert, S., Koulakoff, A., Berwald-Netter, Y., Gros, F., Denoulet, P., and Edde, B. (1994). Developmental Regulation of polyglutamylated alpha tubulin and beta tubulin in mouse-brain neurons. Journal of Cell Science *107*, 2313-2322.

Ayscough, K., Hajibagheri, N. M. A., Watson, R., and Warren, G. (1993). Stacking of Golgi cisternae in *Schizosaccharomyces pombe* requires intact microtubules. Journal of Cell Science *106*, 1227-1237.

Baas, P., Pienkowski, T., and Kosik, K. (1991). Processes Induced by Tau Expression in Sf9 Cells Have an Axon-like microtubule Organisation. The Journal of Cell Biology *115*, 1333-1344.

Baas, P. W., Pienkowski, T. P., Cimbainik, K. A., Toyama, K., Bakalis, S., Ahmad, F., and Kosik, K. (1994). Tau confers drug stability but not cold stability to microtubules in living cells. Journal of Cell Science *107*, 135-143.

Barlow, S., Gonzalez-garay, M. L., West, R. R., Olmsted, J. B., and Cabral, F. (1994). Stable Expression of Heterologous Microtubule-associated Proteins (MAPs) in Chinese Hamster Ovary Cells: Evidence for Differing Roles of MAPs in Microtubule Organisation. The Journal of Cell Biology *126*, 1017-1029.

Basi, G., Schmid, E., and Maundrell, K. (1993). TATA box mutations in the Schizosaccharomyces pombe nmt1 promoter affect transcription efficiency but not the transcription start point or thiamine repressibility. gene *123*, 131-136.

Bassell, G. J., Singer, R. H., and Kosik, K. S. (1994). Association of poly(a) messenger RNA with microtubules in cultured neurons. Neuron *12*, 571-582.

Beinhauer, J. D., Hagan, I. M., Hegemann, J. H., and Fleig, U. (1997). Mal3, the fission yeast Homologue of the human APC-interacting protein EB-1 is required for microtubule integrity and maintenance of Cell form. Journal of Cell Biology *139*, 717-728.

Belmont, L., and Mitchison, T. J. (1996). Identification of a protein that Interacts with Tubulin Dimers and Increases the Catastrophe Rate of Microtubules. Cell *84*, 623-631.

Bereiter-Hahn, J. (1990). Behaviour of mitochondria in the living cell. Int. Rev. Cytol. *122*, 1-63.

Berlin, V., Styles, C. A., and Fink, G. R. (1990). BIK1, a protein required for Microtubule Function during mating and mitosis in *Saccharomyces cerevisiae*, colocalises with Tubulin. Journal of Cell Biology *111*, 2573-2586.

Binder, L. I., Frankfurter, A., Kim, H., Caceres, A., Payne, M. R., and Rebhun, L. I. (1984). Heterogeneity of microtubule associated protein 2 during rat brain development. Proc Natl Acad Sci USA *81*, 5613-5617.

Binder, L. I., Frankfurter, A., and Rebhun, L. I. (1985). The distribution of tau in the mammalian central nervous system. Journal of Cell Biology *101*, 1371-1378.

Bolivar, F., Rodriguez, R. L., Greene, P. J., Betlach, M. C., Heyneker, H. L., Boyer, H. W., Crosa, J. H., and Falkow, S. (1977). Construction and characterisation of new cloning vehicles II: a multipurpose cloning system. Gene *2*, 95.

Bone, N., Millar, J. B., Toda, T., and Armstrong, J. (1998). Regulated vacuole and fusion and fission in Schizosaccharomyces pombe : an osmotic response dependant on MAP kinase. Current Biology *8*, 135-144.

Brady, S. T., Lasek, R., and Allen, R. D. (1982). Science *218*, 1129-1131.

Brandt, R., Leger, Jocelyne and Lee, Gloria (1995). Interaction of tau with the neural plasma membrane mediated by Tau's Amino-terminal Projection Domain. The Journal of Cell Biology *131*, 1327-1340.

Brandt, R., and Lee, G. (1993). Functional Organisation of microtubule-associated protein tau: identification of regions which affect microtubule growth, nucleation and bundle formation in vitro. Journal of Biological Chemistry *268*, 3414-3419.

Brandt, R., and Lee, G. (1994). Orientation, assembly and stability of microtubule bundles induced by a fragment of tau protein. Cell Motility and the Cytoskeleton *28*, 143-154.

Brandt, R., Lee, G., Teplow, D. B., Shalloway, D., and Abdelghany, M. (1994). Differential effect of phosphorylation and substrate modulation on tau's ability to

promote microtubule growth and nucleation. Journal of Biological Chemistry *269*, 11776-11782.

Broker, M., Ragg, H., and Karges, H. E. (1987). Expression of human antithrombin III in *Saccharomyces cerevisiae* and *Schizosaccharomyces pombe*. Biochim. Biophys. Acta *908*, 203-213.

Bulinski, J. C. (1994). MAP4. In Microtubules, J. S. Hyams and C. Lloyd, eds., pp. 167-182.

Bulinski, J. C., and Borisy, G. G. (1979). Self-assembly of HeLa tubulin and the identification of HeLa microtubule-associated proteins. Proc. Natl. Acad. Sci. USA *76*, 293-297.

Burns, R., and Surridge, C. (1994). Tubulin: Conservation and Structure. In Microtbules, J. S. a. L. Hyams, C., ed.: Wiley-Liss, Inc.), pp. 3-31.

Butner, K. A., and Kirchner, M. W. (1991). Tau protein binds to microtubules through a flexible array of distributed weak sites. Journal of Cell Biology *115*, 717-730.

Byers, B., and Goetsch, L. (1975). Behaviour of spindles and spindle plaques in the cell cycle and conjugation of *Saccharomyces cerevisiae*. Journal of Bacteriology *124*, 511-523.

Caceres, A., and Kosik, K. (1990). Inhibition of neurite polarity by tau antisense oligonucleotides in primary cerebellar neurons. Nature *343*, 461-463.

Caceres, A., Mautino, J., and Kosik, K. S. (1992). Suppression of MAP2 in cultures cerebellar macroneurons inhibits minor neurite formation. neuron *9*, 607-618.

Campbell, C. L., Tanaka, N., White, K. H., and Thorsness, P. E. (1994). Mitochondrial morphological and functional defects in yeast caused by *yme1* are suppressed by a mutation of a 26S protease subunit homologue. Molecular Biology of the Cell *5*, 899-905.

Caplow (1992). Microtubule Dynamics. Current Opinion in Cell Biology *4*, 58-65.

Caplow, M., and Shanks, J. (1996). Evidence that a single monolayer tubulin-GTP cap is both necessary and sufficient to stabilise microtubules. Molecular Biology of the Cell *7*, 663-675.

Carminati, J., and Stearns, T. (1997). Microtubules orient the Mitotic Spindle in Yeast through Dynein-dependant Interactions with the Cell Cortex. The Journal of Cell Biology *138*, 629-641.

Chapin, S. J., and Bulinski, J. C. (1991). Non-neuronal 210 kD microtubule associated protein 4 (MAP4) contains a domain homologous to the microtubule binding domains of neuronal MAP2 and tau. Journal of Cell Science *98*, 27-36.

Chapin, S. j., Lue, C.-M., Yu, M. T., and Bulinski, J. C. (1995). Differential expression of alternatively spliced forms of MAp4: a repertoire of structurally different microtubule-binding domains. Biochemistry *34*, 2289-2301.

Chen, J., Kanai, Y., Cowan, N., and Hirokawa, N. (1992). Differential functions of MAP2, MAP2c and tau on the organisation of microtubules in the cells. Molecular Biology of the Cell *3*, 259a.

Chen, J., Kanai, Y., Cowan, N. J., and Hirokawa, N. (1992). Projection domains of MAP2 and tau determine spacings between microtubules in dendrites and axons. Nature *360*, 674-677.

Chiang, H. L., Schekman, R., and Hamamoto, S. (1996). Selective uptake of cytosolic, peroxisomal, and plasma membrane proteins into the yeast lysosome for degradation. Journal of Biological Chemistry *271*, 9934-9941.

Chretien, D., Fuller, S. D., and Karsenti, E. (1995). Structure of growing microtubule ends: two dimensional sheets close into tubes at variable rates. Journal of Cell Biology *129*, 1311-1328.

Cole, N. B., and Lippincott-Schwartz, j. (1995). Organisation of organelles and membrane traffic by microtubules. Current Opinion in Cell Biology *7*, 55-64.

Conubear, E., and Stevens, T. H. (1998). Multiple sorting pathways between the late golgi and vacuoles in yeast. Biochim Biophys Acta *1404*, 211-230.

Cravchik, A., Reddy, D., and Matus, A. (1994). Identification of a novel microtubule-binding domain in a Microtubule Associated Protein-1a. Journal of Cell Science *107*, 661-672.

Cross, D., Dominguez, J., Maccioni, R. B., and Avila, J. (1991). MAP-1 and MAP-2 Binding Sites at the C-terminus of beta-tubulin. Studies with Synthetic tubulin peptides. Biochemistry *30*, 4362-4366.

Cross, D., Farias, G., Dominguez, J., Avila, J., and Maccioni, R. B. (1994). Carboxy terminal sequences of the beta-tubulin involvd in hte interaction of HMW-MAPs. Studies using site-specific antibodies. Molecular and Cellular Biochemistry *132*, 81-90.

Crowther, R. A., Olesen, O. F., Jakes, R., and Goedert, M. (1992). The Microtubule Binding Repeats of Tau Protein assemble into filaments like those found in Alzheimer's Disease. FEBS Lett *309*, 199-202.

Cunningham, C. C., Leclerc, N., Flanagan, L. A., Lu, M., Janmey, P. A., and Kosik, K. S. (1997). Microtubule associated protein 2c reorganises both microtubules and microfilaments into distinct cytological structures in an actin-binding protein-280-deficient melanoma cell line. Journal of Cell Biology *136*, 845-857.

Davis, A., Sage, C. R., Wilson, L., and Farrell, K. (1993). Purification and Biochemical Characterisation of Tubulin from the Budding Yeast *Saccharomyces cerevisaiae*. Biochemistry *32*, 8823-8835.

DeBrabander, M., Bulinski, J. C., Geuens, G., DeMey, J., and Borisy, G. G. (1981). Ultrastructural immunochemical localisation of the 210K microtubule associated protein in cultured cells of primates. Journal of Cell Biology *91*, 438-445.

Ding, R., Mcdonald, K. L., and McIntosh, J. R. (1993). Three-dimensional Reconstruction and Analysis of Mitotic Spindles from the Yeast Schizosaccharomyces pombe. The Journal of Cell Biology *120*, 141-151.

Ding, R., West, R. R., Morphew, M., and McIntosh, J. R. (1997). The spindle pole body of Schizosaccharomyces pombe enters and leaves the nuclear envelope as the cell cycle proceeds. Molecular Biology of the Cell *8*, 1461-1479.

Dinsmore, J. H., and Solomon, F. (1991). Inhibition of MAp2 expression affects both morphological and cell division phenotypes of neuronal differentiation. Cell *64*, 817-826.

Doll, T., Meichsner, M., Riederer, B. M., Honneger, P., and Matus, A. (1993). An isoform of microtubule associated protein 2 (MAP2) containing four repeats of the tubulin-binding motif. Journal of Cell Science *106*, 633-640.

Doshi, P., Bossie, C. A., Doonan, J. H., May, G. S., and Morris, N. R. (1991). Two alpha-tubulin genes of Aspergillus nidulans encode divergent proteins. Mol. Gen. Genetics *225*, 129-141.

Downing, K., and Nogales, E. (1998). Tubulin and Microtubule Structure. Current Opinion in Cell Biology *10*, 16-22.

Drechsel, D. N., and Kirschner, M. W. (1994). The minimum GTP cap required to stabilise microtubules. Current Biology *4*, 1053-1061.

Drewes, G., Ebneth, A., Preuss, U., Mandelkow, E.-M., and Mandelkow, E. (1997). MARK, a novel family of protein kinases that phosphorylate microtubule-associated proteins and trigger microtubule disruption. Cell *89*, 297-308.

Drewes, G., Lichtenberg-Krag, B., Doring, F., Mandelkow, E.-M., Biernat, J., Goris, J., Doree, M., and Mandelkow, E. (1992). Mitogen activated protein (MAP) kinase transforms tau protein into an Alzheimer-like state. EMBO Journal *11*, 2131-2138.

Dunn, W. J. (1990). Studies on the mechanisms of autophagy: maturation of the autophagic vacuole. Journal of Cell Biology *110*, 1935-1945.

Edson, K., Weisshaar, B., and Matus, A. (1993). Actin depolymerisation induces process formation in MAP2-transfected non-neuronal cells. Development *117*, 689-700.

Endow, S. A., Kang, S. J., Satterwhite, L. L., Rose, M. D., Skeen, V. P., and Salmon, E. D. (1994). Yeast Kar3p is a minus-end microtubule motor protein that destabilises microtubules preferentially at the minus end. EMBO Journal *13*, 2708-2713.

Esch, F. S., Kiem, P. S., Beattie, R. W., Blacher, R. W., Culwell, A. R., Oltersdorf, T., McClure, D., and Ward, P. J. (1990). Cleavage of amyloid beta peptide during constitutive processing of its precursor. Science *248*, 1122-1124.

Fankhauser, C., Marks, J., Reymond, A., and Simanis, V. (1993). The S. pombe cdc16 gene is required both for maintenance of p34 cdc2 kinase activity and regulation of septum formation - a link between mitosis and cytokinesis. EMBO Journal *12*, 2697-2704.

Fantes, P. (1989). Cell Cycle Controls. In Molecular Biology of the Fission yeast, A. Nasim, P. Young and B. F. Johnson, eds. (San Diego: Academic Press).

Faruki, S., and Karsenti, E. (1994). Purification of Microtubule Proteins From Xenopus Egg Extracts: Identification of a 230 K MAP4-like Protein. Cell Motility and the Cytoskeleton *28*, 108-118.

Feiguin, F., Ferreira, A., Kosik, K., and Caceres, A. (1994). Kinesin-mediated organelle translocation revealed by specific cellular manipulations. Journal of Cell Biology *127*, 1021-1039.

Ferralli, J., Doll, T., and Matus, A. (1994). Sequence analysis of MAP2 function in living cells. Journal of Cell Science *107*, 3115-3125.

Forsburg, S. L. (1993). Comparison of Schizosaccharomyces pombe expression systems. Nucleic acid research *21*, 2955-2956.

Fraser, A., and James, C. (1998). Fermenting debate: do yeast undergo apoptosis. Trends in Cell Biology *8*, 219-221.

Friedrich, P., and Aszodi, A. (1991). MAP2: a sensitive cross-linker and adjustable spacer in dendritic architecture. FEBS Lett *295*, 5-9.

Frinczek, B., Marx, A., Mandelkow, E.-M., Murphy, D. B., and Mandelkow, E. (1993). Dynamics of Microtubules from Erythrocyte Marginal Bands. Molecular Biology of the Cell *4*, 323-335.

Gamblin, C. T., Nachmanoff, K., Halpain, S., and Williams, R. J. (1996). Recombinant Microtubule Associated protein 2c reduces the dynamic instability of individual microtubules. Biochemistry *35*, 12576-12586.

Gard, D. L., and Kirchner, M. W. (1987). A microtubule associated protein from *Xenopus* eggs that specifically promoted assembly at the plus ends. Journal of Cell Biology *105*, 2203-2215.

Garner, C. C., Brugg, B., and Matus, A. (1988). A 70-kilodalton microtubule-associated protein (MAP2c), related to MAP2. Journal of Neurochemistry *50*, 609-615.

Garner, C. C., and Matus, A. (1988). Different forms of microtubule-associated protein 2 are encoded by separate mRNA transcripts. Journal of Cell Biology *106*, 779-783.

Garner, C. C., Tucker, R. P., and Matus, A. (1988). Selective localisation of messenger RNA for cytoskeletal protein MAP2 in dendrites. Nature *336*, 674-677.

Garner, C. G., and matus, a. (1988). Different forms of Microtubule-associated Protein 2 are encoded by separate mRNA Transcripts. The Journal of Cell Biology *106*, 779-783.

Goedert, M., Spillantini, M.G., Jakes, R., Rutherford, D., and Crowther, R.A. (1989). Multiple Isoforms of Human Microtubule -Associated Protein Tau: Sequences and Localization in Neurofibrillary Tangles of Alzheimer's Disease. Neuron *3*, 519-526.

Goedert, M., Baur, C. P., Ahringer, J., Jakes, R., Hasegawa, M., Spillantini, M. G., Smith, M. J., and Hill, F. (1996). PTL-1, a microtubule-associated protein with tau-like repeats from the nematode Caenorhabditis elegans. Journal of Cell Science *109*, 2661-2672.

Goedert, M., Jakes, R., Spillantini, M. G., and Crowther, R. A. (1994). Tau Protein and Alzheimer's Disease. In Microtubules, J. S. Hyams and C. Lloyd, eds., pp. 183-200.

Goedert, M., Spillantini, M. G., and Crowther, R. A. (1992). Cloning of a big tau microtubule- associated protein characteristic of the peripheral nervous system. Proc. Natl. Acad. Sci. USA *89*, 1983-1987.

Goedert, M. a. J., Ross (1990). Expression of separate isoforms of human tau protein: correlation with the tau pattern in brain and effects on tubulin polymerisation. The EMBO Journal *9*, 4225-4230.

Goldstein, L. S. B., Laymon, R. A., and McIntosh, J. R. (1986). A microtubule associated protein in *Drosophila melanogaster:* Identification, characterisation and isolation of coding sequences. Journal of Cell Biology *102*, 2076-2087.

Goode, B. L., and Feinstein, S. C. (1994). Identification of a novel microtubule binding and assembly domain in the developmentally regulated inter-repeat region of tau. Journal of Cell Biology *124*, 769-782.

Gotte, M., and von Mollard, G. F. (1998). A new beat for the SNARE drum. Trends in Cell Biology *8*, 215-218.

Grafstein, B., and Forman, D. S. (1980). Intracellular transport in neurons. Physiological Review *60*, 1167.

Greenberg, S. G., and Davies, P. (1990). A preparation of Alzheimer paired helical filaments that displays distinct tau proteins by polyacrylamide gel electrophoresis. Proc. Natl. Acad. Sci. USA *87*, 5827-5831.

Gruenberg, J., Griffiths, G., and Howell, K. (1989). Characterisation of the early endosome and putative endocytic carrier vesicles in vivo and with an assay of vesicle fusion in vitro. Journal of Cell Biology *108*, 1301-1316.

Gustke, N., Trinczek, B., Biernat, J., Mandelkow, E.-M., and Mandelkow, E. (1994). Domains of tau protein and interactions with microtubules. Biochemistry *33*, 9511-9522.

Guthrie, B. A., and Wickner, W. (1988). Yeast vacuoles fragment when microtubules are disrupted. The Journal of Cell Biology *107*, 115-120.

Haas, C., Koo, E. H., Teplow, D. B., and Selkoe, D. J. (1994). Polarised secretion of beta amyloid precursor protein and amyloiud beta peptide in MDCK cells. Proc Natl. Acad. Sci. USA *91*, 1564-1568.

Hagan, I. (1998). Fission Yeast Microtubule cytoskeleton. Journal of Cell Science *111*, 1603-1612.

Hagan, I., and Hyams, J. S. (1996). Forces acting on the fission Yeast Anaphase Spindle. Cell Motility and the Cytoskeleton *34*, 69-75.

Hagan, I., and Yanagida, M. (1997). Evidence for a cell cycle specific, spindle pole body mediated, nuclear positioning in the fission yeast *Schizosaccharomyces pombe*. Journal of Cell Science *110*, 1851-1866.

Hagan, I., and Yanagida, M. (1995). The product of the spindle formation gene *sad1+* associates with the fission yeast spindle pole body and is essential for viability. Journal of Cell Biology *129*, 1033-1047.

Hagan, I. M., and Hyams, J. S. (1988). The use of cell division mutants to investigate the control of microtubule distribution in the fission yeast Schozosaccharomyses pombe. Journal of Cell Science *89*, 343-357.

Hagan, I. M., and Yanagida, M. (1990). Novel potential mitotic motor protein encoded by the fission yeast *cut7+* gene. Nature *347*, 563-566.

Hagiwara, H., Yorifuji, H., Sato-Yoshitake, R., Hirokawa, N. (1994). Competition between Motor Molecules and Fibrous Microtubule Associated proteins in Binding to Microtubules. The Journal of Biological Chemistry *269*, 3581-3589.

Hanemaaijer, R., and Ginzburg, I. (1991). Involvement of mature tau isoforms in the stabilisation of neurites in PC12 cells. J. Neuroscience Research *30*, 163-171.

Heald, R., Tournebize, R., Blank, T., Sandaltzopoulos, R., and Becker, P. (1996). Self-organisation of microtubules into bipolar spindles around artificial chromosomes In Xenopus egg extracts. Nature *382*, 420-425.

Heins, S., Song, Y.-H., Wille, H., Mandelkow, E., and Mandelkow, E.-M. (1991). Effect of MAP2, MAP2c and tau on kinesin-dependant microtubule motility. Journal of Cell Science *Supplement 14*, 121-124.

Hill, K. L., Catlett, N. L., and Weismann, L. S. (1996). Actin and myosin function in directed vacuole movement during cell division in Saccharomyces cerevisiae. Journal of Cell Biology *135*, 1535-1549.

Hiraoka, Y., Toda, T., and Yanagida, M. (1984). The NDA3 gene of fission yeast encodes beta tubulin: a cold sensitive nda3 mutation reversibly blocks spindle formation and chromosome movement in mitosis. Cell *39*, 349-358.

Hirata, D., Nakano, K., Fukui, M., Takenaka, H., Miyakawa, T., and Mabuchi, I. (1998). Genes that cause aberrant cell morphology by overexpression in fission yeast: a role of a small GTP-binding protein Rho2 in cell morphogenesis. Journal of Cell Science *111*, 149-159.

Hirokawa, N. (1982). Journal of Cell Biology *94*, 129-142.

Hirokawa, N. (1998). Kinesin and Dynein Superfamily Proteins and the Mechanism of Organelle Transport. Science *279*, 519-526.

Hirokawa, N. (1996). Organelle transport along microtubules - the role of KIFs. Trends in Cell Biology *6*, 135 - 141.

Hirokawa, N., Funakoshi, T., Sato-Harada, R., and Kanai, Y. (1996). Selective Stabilisation of Tau in Axons and Microtubule-associated protein 2C in Cell Bodies and Dendrites Contributes to polarised localisation of Cytoskeletal Proteins in Mature Neurons. The Journal of Cell Biology *132*, 667-679.

Hoenger, A., and Milligan, R. A. (1996). Polarity of 2-D and 3-D maps of tubulin sheets and motor-decorated sheets. Journal of Molecular Biology *263*, 114-119.

Hollenbeck, P. J., and Swanson, J. A. (1990). Radial extension of macrophage tubular lysosomes supported by kinesin. Nature *346*, 864-866.

Hong, W. (1998). Protein transport from the Endoplasmic Reticulum to the Golgi Apparatus. Journal of Cell Science *111*, 2831-2839.

Horio, T., and Hotani, H. (1986). Visualisation of the Dynamic Instability of Individual Microtubules by Dark-Field Microscopy. Nature *321*, 605-607.

Horio, T., Uzawa, S., Jung, M. K., Oakley, B. R., Tanaka, K., and Yanagida, M. (1991). The fission yeast gamma tubulin is essential for mitosis and is localized at the microtubule organising centres. Journal of Cell Science *99*, 693-700.

Horio, T. a. O., Berl R. (1994). Human gamma-tubulin functions in fission yeast. The Journal of Cell Biology *126*, 1465-1473.

Huang, P.-H., and Chiang, H.-L. (1997). Identification of novel vesicles in the cytosol to vacuole degradation pathway. Journal of Cell Biology *136*, 803-810.

Huffaker, T. C., Thomas, J. H., and Botstein, D. (1988). Journal of Cell Biology *106*, 1997-2010.

Hyman, A., and Karsenti, E. (1996). Morphogenetic Properties of Microtubules and Mitotic Spindle Assembly. Cell *84*, 401-410.

Illenberger, S., Zheng-Fischhofer, Q., Preuss, U., Stamer, K., Baumann, K., Trinczek, B., Biernat, J., Godemann, R., Mandelkow, E.-M., and Mandelkow, E. (1998). The Endogenous and Cell Cycle dependent phosphorylation of tau protein in Living cells: Implications for Alzheimer's disease. Molecular Biology of the Cell *9*, 1495-1512.

Irminger-finger, I., Hurt, E., Roebuck, A., Collart, M. A., and Edelstein, S. J. (1996). MHP-1, an essential Gene in Saccharomyces cerevisiae Required for Microtubule Function. The Journal of Cell Biology *135*, 1323-1339.

Irminger-Finger, I., Laymon, R. A., and Goldstein, L. S. B. (1990). Analysis of the Primary sequence and Microtubule-binding Region of the *Drosophila* 205K MAP. Journal of Cell Biology *111*, 2563-2572.

Jacobs, C. W., Adams, A. E. M., Szaniszlo, P. J., and Pringle, J. R. (1988). Journal of Cell Biology *107*, 1409-1426.

Jakes, R., Novak, M., Davison, M., and Wischik, C. M. (1991). Identification of 3- and 4-repeat tau isoforms within the PHF in Alzheimer's Disease. EMBO Journal *10*, 2725-2729.

Johnson, K. A., and Borisy, G. G. (1977). Kinetic analysis of microtubule self-assembly in vitro. Journal of Molecular Biology *96*, 669-678.

Joshi, H. (1998). Microtubule Dynamics in Living Cells. Current Opinionin Cell Biology *10*, 35-44.

Joshi, H. C., Palacios, M. J., McNamara, L., and Cleveland, D. W. (1992). Gamma Tubulin is a Centrosomal Protein required for cell-cycle dependant microtubule nucleation. Nature *356*, 80-83.

Kalcheva, N., Albala, J. S., O'Guinn, K., Rubino, H., Garner, G., and Shafit-Zagardo, B. (1995). genomic structure of human microtubule associated protein 2 (MAP2) and characterisation of additional MAP2 isoforms. Proc. Natl. Acad. Sci. USA *92*, 10894-10898.

Kalcheva, N., Rockwood, J. M., Kress, Y., Steiner, A., and Shafit-Zagardo, B. (1998). Molecular and Functional Characteristics of MAp2a: Ability of MAP2a Versus

MAP2B to induce stable microtubules in COS cells. Cell Motility and the Cytoskeleton *40*, 272-285.

Kaufer, N. F., Simanis, V., and Nurse, P. (1985). Fission Yeast Schizosaccharomyces pombe correctly excises a mammalian RNA transcript intervening sequence. Nature *318*, 78-80.

Kilmartin, J. B., and Adams, A. E. M. (1984). Structural rearrangement of tubulin and actin during the cell cycle of the yeast *Saccharomyces*. Journal of Cell Biology *98*, 922-933.

Kindler, S., Schulz, B., Goedert, M., and Garner, C. C. (1991). Molecular structure of microtubule-associated protein 2b and 2c from rat brain. Journal of Biological Chemistry *265*, 19679-19684.

Kirschner, M. W., and Mitchison, T. (1986). Beyond Self-assembly : From Microtubules to Morphogenesis. Cell *45*, 329-342.

Kosik, K., and McConlogue, L. (1994). Microtubule-Associated Protein Function: Lessons from Expression in *Spodoptera frugiperda* cells. Cell Motility and the Cytoskeleton *28*, 195-198.

Kosik, K., Orecchio, L. D., Bakalis, S., and Neve, R. (1989). Developmentally regulated sequences of specific tau sequences. Neuron *2*, 1389-1397.

Kosik, K. S. (1994). The Alzheimer's Disease Sphinx: A riddle with plaques and tangles. The Journal of Cell Biology *127*, 1501-1504.

Lang, T., Schaeffeler, E., Bernreuther, D., Bredschneider, M., Wolf, D. H., and Thumm, M. (1998). Aut2p and Aut7p, two novel microtubule-associated proteins are essential for delivery of autophagic vesicles to the vacuole. The EMBO Journal *17*, 3597-3607.

Langkopf, A., Hammarback, J., Muller, R., Vallee, R., and Garner, C. (1992). Microtubule-associated proteins 1A and LC2: two proteins encoded in one messenger RNA. Journal of Biological Chemistry *267*, 16561-16566.

Lawrence, B. P., and Brown, W. J. (1992). Autophagic vacuoles rapidly fuse with pre-existing lysosomes in cultured hepatocytes. Journal of Cell Science *102*, 515-526.

Leclerc, N., Baas, P. W., Garner, C. C., and Kosik, K. S. (1996). Juvenile and mature MAP2 isoforms induce distinct patterns of process outgrowth. Molecular Biology of the Cell *7*, 443-455.

Lee, G., Neve, rachel L. and Kosik, Kenneth S. (1989). The Microtubule Binding Domain of Tau. Neuron *2*, 1615-1624.

Lee, G., and Rook, S. L. (1992). Expression of tau protein in non-neuronal cells: microtubule binding and stabilisation. Journal of Cell Science *102*, 227-237.

Lee, M. G. a. N., P. (1987). Complementation used to clone a human homologue of the fission yeast cell cycle control gene cdc2+. Nature *335*, 251-254.

Levin, D., and Bishop, J. M. (1990). A putative protein kinase gene (kin1+) is important for growth polarity in Schizosaccharomyces pombe. Proc. Natl. Acad. Sci. USA *87*, 8272-8276.

Li, Q., and Joshi, H. C. (1995). Journal of Cell Biology *130*, 1137-1147.

Lippincott-Schwartz, J. (1998). Cytoskeletal proteins and Golgi Dynamics. Current Opinion in Cell Biology *10*, 52-59.

Litman, P. J., Barg, L., Rindzooski, L., and Ginzburg, I. (1993). Subcellular localisation of tau mRNA in differentiating neuronal cell culture: implications for neuronal polarity. Neuron *10*, 627-638.

Luduena, R. F. (1993). Are Tubulin Isotypes Functionally Significant. Molecular Biology of the Cell *4*, 445-457.

Luduena, R. F., Banerji, Asok, Khan, Israr (1992). Tubulin Structure and Biochemistry. Current Opinion in Cell Biology *4*, 53-57.

Mandelkow, E., Song, Y.-H., Schweers, O., Marx, A., and Mandelkow, E.-M. (1995). On the Structure of Microtubules, Tau and Paired Helical Filaments. Neurobiology of Aging *16*, 347-354.

Mandelkow, E. a. M., Eva-Maria (1995). Microtubules and Microtubule-associated Proteins. Current Opinion in Cell Biology *7*, 72-81.

Mandelkow, E.-M., Biernat, J., Drewes, G., Gustke, N., Trinczek, B., and Mandelkow, E. (1995). Tau domains, Phosphorylation, and Interaction with Microtubules. Neurobiology of Aging *16*, 355-363.

Mandelkow, E.-M., Drewes, G., Biernat, J., Gustke, N., Van Lint, J., Vandenheede, J. R., and Mandelkow, E. (1992). Glycogen synthase kinase-3 and the Alzheimer-like state of microtubule associated protein tau. FEBS Lett. *314*, 315-321.

Mann, S. S., and Hammarback, J. A. (1994). Molecular Characterisation of light chain -3, a microtubule binding subunit of MAP1a and MAP1b. Journal of Biological Chemistry *269*, 11492-11497.

Marks, J., Hagan, I. M., and Hyams, J. S. (1986). Growth Polarity and Cytokinesis in Fission Yeast: the Role of the Cytoskeleton. Journal of Cell Science *5*, 229-241.

Mata, J., and Nurse, P. (1998). Discovering the poles in yeast. Trends in Cell Biology *8*, 163-167.

Mata, J., and Nurse, P. (1997). tea1 and the microtubular cytoskeleton are important for generating global spatial order within the fission yeast cell. Cell *89*, 939-949.

Matus, A. (1994). MAP2. In Microtubules, J. S. Hyams and C. Lloyd, eds., pp. 155-166.

Matus, A. (1994). Stiff microtubules and neuronal morphology. Trends in Neurological Sciences *17*, 19-22.

Maundrell, K. (1990). nmt1 of Fission Yeast. The Journal of Biological Chemistry *265*, 10857-10864.

Maundrell, K. (1993). Thiamine- repressible expression vectors pREP and pRIP for fission yeast. Gene *123*, 127-130.

McNally, F. J., and Vale, R. D. (1993). Cell *75*, 419-429.

McNally, F. J., and Vale, R. D. (1993). Identification of Katanin, an ATPase that severs and disassembles stable microtubules. Cell *75*, 419-430.

Merdes, A., Ramyar, K., Vechio, J. D., and Cleveland, D. W. (1996). A complex NuMA and cytoplasmic dynein is essential for mitotic spindle assembly. Cell *87*, 447-458.

Mironov, A. A., Weidman, P., and Luini, A. (1997). Variations on the Intracellular Transport Theme: Maturing Cisternae and Trafficking Tubules. Journal of Cell Biology *138*, 481-484.

Mitchinson, J. M., and Nurse, P. (1985). Growth in cell length in the fission yeast *Schizosaccharomyces pombe*. Journal of Cell Science *75*, 357-376.

Mitchison, T., and Kirchner, M. (1984). dynamic Instability of Microtubule Growth. Nature *312*, 237-242.

Moreno, S., Klar, A., and Nurse, P. (1991). Molecular genetic analysis of fission yeast *Schizosaccharomyces pombe*. Methods Enzymol. *194*, 795-823.

Morishima-Kawashima, M., Hasegawa, M., Takio, K., Suzuki, M., Yoshida, H., Watanabe, A., Titani, K., and Ihara, Y. (1995). Hyperphosphorylation of tau in PHF. Neurobiology of Aging *16*, 365-380.

Morris, R. L. a. H., P.J. (1995). Axonal Transport of Mitochondria along microtubules and F-actin in living vertebrate Neurons. The Journal of Cell Biology *131*, 1315-1326.

Nangaku, M., Sato-Yoshitake, R., Okada, Y., Noda, Y., Takemura, R., Yamazaki, H., and Hirokawa, N. (1994). Cell *79*, 1209-1220.

Nare, B., Lubega, G., Prichard, R. K., and Georges, E. (1996). p-Azidosalicyl-5-amino-6-phenoxybenzimidazole Photolabels the N-terminal 63-103 Amino Acids of Haemonchus contortus beta tubulin-1. The Journal of Biological Chemistry *271*, 8575-8581.

Nedelec, F. J., Surrey, T., Maggs, A. C., and Leibler, S. (1997). Self-organisation of microtubules and motors. Nature *389*, 305-308.

Neff, N., Thomas, J. H., Grisafi, P., and Botstein, D. (1983). Isolation of the beta tubulin gene from yeast and demonstration of its essential function. Cell *33*, 211-219.

Neve, R. L., Harris, P., Kosik, K. S., Kurnit, D. M., and Donlon, T. A. (1986). Identification of cDNA clones for the human microtubule-associated protein tau and chromosomal localisation of the genes for tau and microtubule-associated protein-2. Molecular Brain Research *1*, 271-280.

Nguyen, H.-L., Chari, S., Gruber, D., Lue, C.-m., Chapin, S. J., and Bulinski, J. C. (1997). Overexpression of full or partial length MAP4 stabilises microtubules and alters cell growth. Journal of Cell Science *110*, 281-294.

Oakley, B. R., Oakley, C. E., Yoon, Y., and Jung, M. K. (1990). Gamma tubulin is a component of the spindle pole body that is essential for microtubule function in Aspergillus nidulans. Cell *61*, 1289-1301.

Oakley, B. R., and Reinhart, J. E. (1985). Journal of Cell Biology *101*, 2392-2397.

Oakley, C. E., and Oakley, B. R. (1989). Identification of gamma tubulin, a new member of the Tubulin Superfamily by *mipA* gene of *Aspergillus nidulans*. Nature *338*, 662-664.

Odorizzi, G., Cowles, C. R., and Emr, S. D. (1998). The AP-3 Complex: a coat of many colours. Trends in Cell Biology *8*, 282-287.

Okabe, S., and Hirokawa, N. (1989). Rapid turnover of Microtubule Associated Protein 2 (MAP2) in the axon revealed by microinjection of biotinylated MAP2 into cultured neurons. Proc. NAtl. Acad. Sci. USA *86*, 4127-4131.

Okabe, S., and Hirokawa, N. (1989). Rapid turnover of microtubule associated protein MAP2 in the axon revealed by microinjection of biotinylated MAP2 into cultures neurons. Proc NAtl Acad Sci USA *86*, 4127-4131.

Olmsted, J. B. (1986). Microtubule Associated Proteins. Annual Review of Cell Biology *2*, 421-457.

Olson, K. R., McIntosh, J. R., and Olmsted, J. B. (1995). Analysis of MAP4 function in living cells using green fluorescent protein (GFP) chimeras. Journal of Cell Biology *130*, 639-650.

Ookata, K., Hisanaga, S.-i., Bulinski, J.-C., Murofushi, H., Aizawa, H., Itoh, T. J., Hotani, H., Okumura, E., Tachibana, K., and Kishimoto, T. (1995). Cyclin B Interaction with Microtubule -associated Protein 4 (MAP4) targets p34cdc2 kinase to microtubules and is a potential regulator of M-phase dynamics. The Journal of Cell Biology *128*, 849-862.

OOkata, K., Hisanaga, S.-I., Sugita, M., Okuyama, A., Murofushi, H., Kitazawa, H., Chari, S., Bulinski, J. C., and Kishimoto, T. (1997). MAP4 is the in Vivo Substrate for cdc2 kinase in HeLa Cells: Identification of an M-phase Specific and a Cell Cycle-Independent Phosphorylation Site in MAP4. Biochemistry *36*, 15873-15883.

Ookata, K. S., Hisanaga, S., Okumura, E., and Kishimoto, T. (1993). Association of p34cdc2/cyclin B complex with microtubules in starfish oocytes. Journal of Cell Science *105*, 873-881.

Padilla, R., Otin, C. L., Serrano, L., and Avila, J. (1993). Role of the carboxy terminal region of beta tubulin on microtubule dynamics through its interaction with the GTP phosphate binding protein. FEBS *325*, 173-176.

Page, B., and Snyder, M. (1993). Chromosome segregation in yeast. Annual Review of Microbiology *47*, 231-261.

Papandrikopoulou, A., Doll, T., Tucker, R. P., Garner, C. C., and Matus, A. (1989). Embryonic MAP2 lacks the cross-linking side-arm sequences and dendritic targeting signal of adult MAP2. Nature *340*, 650-652.

Paturele-Lafanechere, L., Manier, M., Trigault, N., Pirollet, F., Mazarguil, H., and Job, D. (1994). Accumulation of delta-2-tubulin, a major tubulin variant that cannot be tyrosinated in neuronal tissues and in stable microtubule assemblies. Journal of Cell Science *107*, 1529-1543.

Pelham, H. R. (1991). Recycling of proteins between the endoplasmic reticulum and Golgi complex. Current Opinion in Cell Biology *3*, 585-591.

Pereira, A. J., Dalby, B., Stewart, R. J., Doxsey, S. J., and Goldstein, L. S. B. (1997). Mitochondrial association of a plus-end directed microtubule motor expressed during mitosis in Drosophila. Journal of Cell Biology *136*, 1081-1090.

Pichova, A., Kohlwein, S. D., and Yamamoto, M. (1995). New Arrays of cytoplasmic microtubules in the fission yeast *Schizosaccharomyces pombe*. Protoplasma *188*, 252-257.

Pidoux, A. L., LeDizet, M., and Cande, W. Z. (1996). Fission yeast pkl1is a kinesin-related protein involved in mitotic spindle function. Molecular Biology of the Cell *10*, 1639-1655.

Pierre, P., Scheel, J., Rickard, J. E., and Kreis, T. e. (1992). CLIP-170 links endocytic vesicles to microtubules. Cell *70*, 887-900.

Presley, J. F., Cole, N. B., Schroer, T. A., Hirchberg, K., Zaal, K. J. M., and Lippincott-Schwartz, J. (1997). ER-to-Golgi transport visualised in living cells. Nature *389*, 81-85.

Preuss, U., Biernat, J., Mandelkow, E.-M., and Mandelkow, E. (1997). The 'jaws' model of tau-microtubule interaction examined in CHO cells. Journal of Cell Science *110*, 789-800.

Preuss, U., Doring, F., Illenberger, S., and Mandelkow, E.-M. (1995). Cell Cycle-dependent Phosphorylation and Microtubule Binding of Tau Protein Stably transfected into Chinese Hamster Ovary Cells. Molecular Biology of the Cell *6*, 1397-1410.

Pringle, J. R., and Hartwell, L. H. (1981). The *Saccharomyces cerevisiae* cell cycle. In Molecular Biology of the yeast Saccharomyces, J. N. Strathern, E. W. Jones and J. R. Broach, eds. (Cold Spring Harbour: Cold Spring Harbour laboratories).

Pryer, N. K., Walker, R. A., Skeen, V. P., Bourns, B. D., Soboeiro, M. F., and Salmon, E. D. (1992). Brain Microtubule-Associated Proteins Modulate Microtubule Dynamic Instability in Vitro. Journal Of Cell Science *103*, 965-976.

Raymond, C. K., Howald-Stevenson, I., Vater, C. A., and Stevens, T. H. (1992). Morphological classification of yeast vacuolar protein sorting mutants: evidence for a prevacuolar compartment in class E vps mutants. Molecular Biology of the Cell *3*, 1389-1402.

Rickard, J. E., and Kreis, T. E. (1991). Binding of pp170 to microtubules is regulated by phosphorylation. Journal of Biological Chemistry *266*, 17595-17605.

Rickard, J. E., and Kreis, T. E. (1996). CLIPs for organelle-microtubule interactions. Trends in Cell Biology *6*, 178-183.

Robinow, C. J., and Hyams, J. S. (1989). General Cytology of Fission Yeasts. In Molecular Biology of the Fission Yeast, A. Nasim, P. Young and B. F. Johnson, eds. (San Diego: Academic Press).

Rodinov, V. I., and Borisy, G. G. (1997). Microtubule treadmilling in vivo. science *275*, 215-218.

Roy, D., and Fantes, P. (1983). Benomyl-resistant mutants of Schizosaccharomyces pombe cold-sensitive for mitosis. Current Genetics *6*, 195-202.

Russell, P. (1989). Gene Cloning and Expression in Fission Yeast. In Molecular Biology of the Fission Yeast, A. Nasim, P. Young and B. F. Johnson, eds. (New York: Academic Press), pp. 243-271.

Sadot, E., Barg, J., Rasouly, D., Lazarovici, P., and Ginzburg, I. (1995). Short- and long-term mechanisms of tau regulation in PC12 cells. Journal of Cell Science *108*, 2857-2864.

Saitoh, S., Takahashi, K., Nabeshima, K., Yamashita, Y., Nakaseko, Y., Hirata, A., and Yanagida, M. (1996). Aberrant Mitosis in Fission yeast Mutants defective in Fatty Acid Synthatase and Acetyl CoA Carboxylase. The Journal of Cell Biology *134*, 949-961.

Sanchez, I., and Cohen, W. D. (1994). Localisation of Tau and Other Proteins of Isolated Marginal Bands. Cell Motility and the Cytoskeleton *27*, 350-360.

Saunders, W., Hornack, D., Lengyel, V., and Deng, C. (1997). The Saccharomyces cerevisiae Kinesin-related motor protein Kar3p Acts at pre-anaphase spindle poles to limit the number and length of microtubules. The journal of Cell Biology *137*, 417-431.

Sawin, K. E., and Nurse, P. (1998). Regulation of Cell Polarity by Microtubules in Fission Yeast. The Journal of Cell Biology *142*, 457-471.

Schatz, P. J., Pillus, L., Grisafi, P., Solomon, F., and Botstein, D. (1986). Genetically essential and non-essential alpha-tubulin genes specify functionally inter-changeable proteins. Molecular Cell Biology *6*, 3711-3721.

Scheel, J., and Kreis, T. E. (1991). Motor protein independant binding of endocytic carrier vesicles to microtubules *in vitro*. Journal of Biological Chemistry *266*, 18141-18148.

Scheel, J., Matteoni, R., Ludwig, T., Hoflack, B., and Kreis, T. E. (1990). Journal of Cell Science *96*, 711-720.

Schliwa, M. (1986). The Cytoskeleton : an Introductory Survey, Volume 13, M. Alfert, T. Beerman, L. Goldstein and K. R. Porter, eds. (Wien New York: Springer-Verlag).

Schroer, T. A., and Sheetz, M. P. (1991). Two Activators of Microtubule-based Vesicle Transport. The Journal of Cell Biology *115*, 1309-1318.

Scott, S. V., and Klionsky, D. J. (1998). Delivery of proteins and organelles to the vacuole from the cytoplasm. Current Opinion in Cell Biology *10*, 523-529.

Shiina, N., Gotoh, Y., Kubomura, N., Iwamatsu, A., and Nishida, E. (1994). Microtubule severing by elongation factor 1alpha. Science *266*, 282-285.

Shiina, N., Moriguchi, T., Ohta, E., Gotoh, Y., and Nishida, E. (1992). Regulation of a major microtubule associated protein by MPF and MAP kinase. EMBO Journal *11*, 3977-3984.

Shina, N., Gotoh, Y., Kubomura, N., Iwamatsu, A., and Nishida, E. (1994). Science *266*, 282-285.

Shuster, E. O., and Guthrie, C. (1990). Human U2 snRNA can function in pre-mRNA splicing in yeast. Nature *345*, 270-273.

Simon, V. R., Swayne, T. C., and Pon, L. A. (1995). Actin-dependant Mitochondrial Motility in Mitotic Yeast and Cell-Free Systems: Identification of a motor activity on the mitochondrial surface. The Journal of Cell Biology *130*, 345-354.

Song, J. M., Cheung, E., and Rabinowitz, J. C. (1995). Nucleotide sequence and Characterisation of the Saccharomyces cerevisiae RPL19 gene encoding a Homolog of the MAmmalian Ribosomal Protein L19. Yeast *11*, 383-389.

Stearns, T., Evans, L., and Kirchner, M. (1991). Gamma tubulin is a highly conserved Component of the Centrosome. Cell *65*, 825-836.

Stearns, T., and Kirchner, M. (1994). In vitro reconstitution of centrosome assembly and function: the central role of gamma tubulin. Cell *76*, 623-638.

Stewart, L., and Yaffe, M. (1991). A Role for Unsaturated Fatty Acids in Mitochondrial Movement and Inheritence. The Journal of Cell Biology *115*, 1249-1257.

Takashige, K., Baba, M., Tsuboi, S., Noda, T., and Ohsumi, Y. (1992). Autophagy in yeast demonstrated with proteinase-deficient mutants and conditions for its induction. Journal of Cell Biology *119*, 301-311.

Takegawa, K., DeWald, D. B., and Emr, S. D. (1995). Schizosaccharomyces pombe Vps34p, a phosphotidylinositol-specific PI 3-kinase essential for normal cell growth and vacuole morphology. Journal of Cell Science *108*, 3745-3756.

Takeshige, K., Baba, M., Tsuboi, S., Noda, T., and Ohsumi, Y. (1992). Autophagy in yeast demonstrated with proteinase deficient mutants and conditions for its induction. Journal of Cell Biology *119*, 301-311.

Thurston, V., Pena, P., Pestell, R., and Binder, L. (1997). Nucleolar localisation of the Microtubule associated Protein Tau in Neuroblastomas using Sense and Anti-sense transfection strategies. Cell Motility and the Cytoskeleton *38*, 100-110.

Toda, T., Umesuno, K., Hirata, A., and Yanagida, M. (1983). Cold-sensitive Nuclear Division Arrest Mutants of the Fission Yeast Schizosaccharomyces pombe. Journal of Molecular Biology *168*, 251-270.

Tournier, S., Leroy, D., Goubin, F., Ducommun, B., and Hyams, J. (1996). Heterologous Expression of the Human Cyclin-dependant Kinase Inhibitor p21cip1 in the Fission Yeast, Schizosaccharomyces pombe Reveals a Role for PCNA in the chk1+ Cell Cycle Checkpoint Pathway. Molecular Biology of the Cell *7*, 651-662.

Toyoshima, I., Yu, H., Stuer, E. R., and Sheetz, M. P. (1992). Kinectin, a major kinesin binding protein on ER. Journal of Cell Biology *118*, 1121-1131.

Tran, P. T., R.A., W., and Salmon, E. D. (1997). A metastable intermediate state of microtubule dynamic instability that differs significantly between plus and minus ends. The Journal of Cell Biology *138*, 105-117.

Trinczek, B., Biernat, J., Baumann, K., Mandelkow, E.-M., and Mandelkow, E. (1995). Domains of Tau protein, Differential Phosphorylation and Dynamic Instability of Microtubules. Molecular Biology of the Cell *6*, 1887-1902.

Tucker, J. (1992). The Microtubule Organising Centre. BioEssays *14*, 861-867.

Umeneso, K., Toda, T., Hayashi, S., and Yanagida, M. (1983). Two Cell Division Cycle Genes *NDA2* and *NDA3* of the Fission Yeast *Schizosaccharomyces pombe* Control Microtubular Organisation and Sensitivity to Anti-mitotic Benzimidazole Compounds. Journal of Molecular Bioogy *168*, 271-284.

Umeyama, T., Okabe, S., Kanai, Y., and Hirokawa, N. (1993). Dynamics of Microtubules bundled by Microtubule Associated Protein C(MAP2C). Journal of Cell Biology *120*, 451-465.

Vallee, R. B. (1980). Structure and Phosphorylation of Microtubule Associated Protein 2(MAP2). Proc Natl Acad Sci USA *77*, 3206-3210.

Vallee, R. B., Dibartolomeis, M. J., and Theurkauf, W. E. (1981). A protein kinase bound to the projection domain of MAP2 (microtubule associated protein 2). Journal of Cell Biology *90*, 568-576.

Vallen, E. A., Scherson, T. Y., Roberts, T., van Zee, K., and Rose, M. D. (1995). Assymetric mitotic segregation of the yeast spindle pole body. Cell *69*, 505-515.

Verde, F., Mata, J., and Nurse, P. (1995). Fission Yeast Cell Morphogenesis - Identification of New Genes and Analysis of their Role during the Cell Cycle. Journal of Cell Biology *131*, 1529-1538.

Vida, T. A., and Emr, S. D. (1995). A New Stain for Visualizing Vacuolar Membrane Dynamics and Endocytosis in Yeast. The Journal of Cell Biology *128*, 779-792.

Wade, R. H., and Hyman, A. A. (1997). Microtubule Structure and Dynamics. Current Opinion inCell Biology *9*, 12-17.

Wakil, S. J., Stoops, J. K., and Joshi, V. C. (1983). Fatty Acid Synthesis and its regulation. Annual Review of Biochemistry *52*, 537-579.

Wallis, K., Azhar, S., Rho, M., Lewis, S., Cowan, N., and Murphy, D. B. (1993). The mechanism of equilibrium binding of microtubule associated protein -2 to microtubules: binding is a multiphasic process and exhibits positive cooperativity. Journal of Biologocal Chemistry *268*, 15158-15167.

Wang, X. M., Peloquin, J. G., Zhai, Y., Bulinski, J. C., and Borisy, G. G. (1996). Removal of MAP4 from microtubules in vivo Produces No Observable Phenotype at the Cellular Level. The Journal of Cell Biology *132*, 345-357.

Wang, Y.-X., Zhao, H., Harding, T. M., Gomes de Mesquita, D. S., Woldringh, C. L., Klionsky, D. J., Munn, A. L., and Weisman, L. S. (1996). Multiple classes of Yeast Mutants are defective in vacuole partitioning yet target vacuole proteins correctly. Molecular Biology of the Cell *7*, 1375-1389.

Warren, G., and Wickner, W. (1996). Organelle Inheritance. Cell *84*, 395-400.

Watson, D. F., Hoffman, P. N., and Griffin, J. W. (1990). The cold stability of Microtubules increases during axonal maturation. Journal of Neuroscience *10*, 3344-3352.

Wendland, B., Emr, S. D., and Riezman, H. (1998). Protein traffic in the yeast endocytic and vacuolar protein sorting pathways. Current Opinion in Cell Biology *10*, 513-522.

West, R. R., Tenbarge, K. M., and Olmsted, J. B. (1991). A model for microtubule associated protein 4 structure: domains defined by comparisons of human, mouse and bovine sequences. Journal of Biological Chemistry *266*, 21886-21896.

Wordeman, L., and Cande, Z. W. (1987). Reactivation of spindle elongation in vitro is correlated with the phosphorylation of a 205 kD spindle associated protein. Cell *50*, 535-543.

Yaffe, M. P., Harata, D., Verde, F., Eddison, M., Toda, T., and Nurse, P. (1996). Microtubules mediate mitochondrial distribution in fission yeast. Proceedings of the National Academy of Sciences of the United States of America *93*, 11664-11668.

Yanagida, M. (1987). Yeast tubulin genes. Microbiological Sciences *4*, 115-117.

Yannisch-Perron, C., Vietra, J., and Messing, J. (1985). Improved M13 phage cloning vectors and host strains: nucleotide sequencing of the M13mp18 and pUC19 vectors. Gene *4*, 175.

Yeh, E., Skibbens, R. V., Cheng, J. W., Salmon, E. D., and Bloom, K. (1995). Spindle Dynamics and Cell Cycle Regulation of Dynein in the Budding Yeast *Saccharomyces cerevisiae*. Journal of Cell Biology *130*, 687-700.

Yoshida, T., Imanaka-Yoshida, K., Murofushi, H., Tanaka, J., Ito, H., and Inagaki, M. (1996). Microinjection of Intact MAP-4 and fragments Induces Changes of the Cytoskeleton in PtK2 cells. Cell Motility and the Cytoskeleton *33*, 252-262.

Zhang, D., and Nicklas, R. B. (1995). Chromosomes initiate spindle assembly upon experimental dissolution of the nuclear envelope in grasshopper spermatocytes. Journal of Cell Biology *131*, 1125-1131.

Zhao, Y., and Lieberman, H. B. (1995). Schizosaccharomyces pombe: A Model for Molecular Studies of Eucaryotic Genes. DNA and Cell Biology *14*.

Zheng, Y., Jung, M. K., and Oakley, B. R. (1991). Gamma Tubulin is present in Drosophila melanogater and Homo sapiens and is associated with the centrosome. Cell *65*, 817-823.